AD NUMBER

AD833953

NEW LIMITATION CHANGE

TO

Approved for public release, distribution unlimited

FROM

Distribution authorized to U.S. Gov't. agencies and their contractors; Critical Technology; JAN 1968. Other requests shall be referred to Space and Missile System Organization, Los Angeles, CA 92409.

AUTHORITY

SAMSO ltr, 28 Feb 1972

SAMSO TR 68 - 123

AD 668 656

Final Report

AN INVESTIGATION OF CARBON DEPOSITION IN CHARS. II

Eric Weger
Jere R. Brew
Ronald A. Servais

Washington University
St. Louis, Missouri 63130

January 1968

Prepared for

SPACE AND MISSILE SYSTEMS ORGANIZATION
AIR FORCE SYSTEMS COMMAND
Norton Air Force Base, California 92409

SAMSO TR 68 - 123

Final Report

AN INVESTIGATION OF CARBON DEPOSITION IN CHARS. II

Eric Weger
Jere R. Brew
Ronald A. Servais

Washington University
St. Louis, Missouri 63130

January 1968

Prepared for

SPACE AND MISSILE SYSTEMS ORGANIZATION
AIR FORCE SYSTEMS COMMAND
Norton Air Force Base, California 92409

FOREWORD

This report was prepared by Washington University under USAF Contract No. F04694-67-C-0013. It covers work conducted from 1 November 1966 to 31 October 1967 and was monitored by Captain Mercer. This report was submitted January 1968.

This document is subject to special export controls and each transmittal to foreign governments or foreign nationals may be made only with prior approval of Space and Missile Systems Organization. Information in this report is embargoed under the Department of State International Traffic in Arms Regulations. This report may be released to foreign governments by departments or agencies of the U. S. Government subject to approval of Space and Missile Systems Organization (SMSD) Los Angeles AFS, California, or higher authority within the Department of the Air Force. Private individuals or firms require a Department of State Export License.

This Technical Report has been reviewed and is approved.

Captain W. E. Mercer III, SMYSE
Air Force Systems Command
Norton Air Force Base, California 92409

ABSTRACT

The techniques for the investigation of char densification phenomena which had been developed under a previous contract (see BSD TR 66-385) were extended to include transpiration experiments with gases and gas mixtures typical of the decomposition products of phenolic resins. As before, the chars used in the experiments were produced by charring high performance carbon cloth phenolic composites in a plasma jet. Data on the structural characteristics and permeabilities of the chars, and the change occurring during transpiration, are presented. Comparisons of the experimental data with kinetic rate data from the literature are made. A simplified program for calculating the change in permeability of and pressure drop across a growing char is presented. The effort required to extend this program to more complex situations is discussed.

CONTENTS

TABLES

FIGURES

NOMENCLATURE

c	Kozeny constant, defined in equation 2.6
C_i	concentration of component i, moles L^{-3}
C'_i	number of sites of type i per unit mass, M^{-1}
C_f	active carbon site free of oxygen
C_o	active carbon site occupied by oxygen
C_2	constant defined by equation 10.5
C_4	constant defined by equation 10.6
f	mole fraction of carbon containing compound in gas stream
I.D.	inside diameter, L
K	permeability, L^2
K_i	reaction equilibrium constant
k	reaction rate constant
L	height of cylinder, L
M	mobility, dimensionless
M.W.	molecular weight, M/mole
n	number of capillaries per unit area, L^{-2}
n	number of free carbon sites
n_i	number of moles of given substance per unit time, moles/t
O.D.	outside diameter of the cylinder, L
P	pressure, M/Lt^2
Q	volumetric flow rate, L^3t^{-1}
R	universal gas constant, ML^2/t^2T mole

r	radius of cylinder, L
r_i	rate of formation of component i by reaction, moles $t^{-1} L^{-3}$
S	specific surface area, ratio of the area of the capillaries to the enclosing volume of the solid, L^{-1}
T	absolute temperature, T
t	time, t
V	volume, L^3
V_x	velocity in x direction in rectangular coordinate system, L/t
W	mass, M
x	distance in x direction
Y	radial distance through the char originating at the inside of the char, L
$\bar{\delta}$	average pore diameter, L
ε	porosity of porous material, dimensionless
μ	viscosity of the gas, M/Lt
ρ	density of the material, M/L^3

Subscripts

1	quantity evaluated at the inside surface of the cylinder
2	quantity evaluated at the outside surface of the cylinder
o	quantity evaluated at time zero

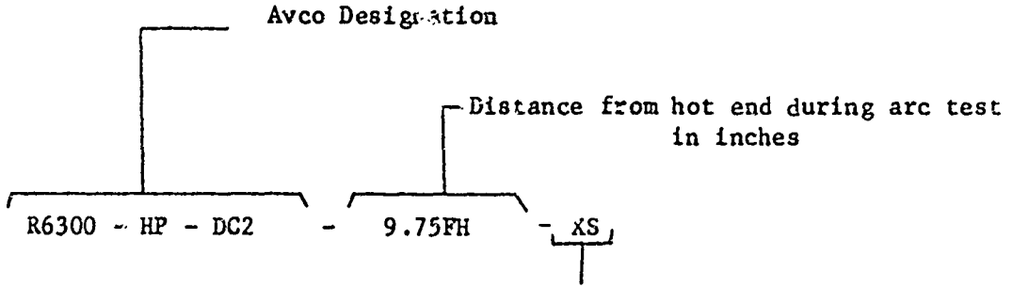

CROSS SECTION; inside 1/2, outside 1/2, middle 1/3;
if blank it represents entire cross section.

I

INTRODUCTION

The basic objective of the study described in this report was to provide reliable experimental data which is necessary for devising appropriate analytical expressions for predicting changes in permeability and pressure drop occurring in chars during reentry. More accurate expressions of this type are needed for incorporation into analyses describing transient heat shield behavior.

In order to satisfy the objective of the study, experimental data on the effect of the reactions which are typical of those occurring in the char (at least for a phenolic composite) were obtained. These consisted of permeability and pressure drop characteristics of chars as a function of time (time related to the reentry time scale). This data was correlated with the changes in the internal physical structure of the chars and will permit better extrapolation of the results of the present project to materials of a somewhat different nature.

Some initial results have been reported previously (Reference 1). In that report data were presented on the changes in permeability and structural characteristics which occur in typical ablative chars when carbon deposition is caused by the decomposition of methane in the char pores at typical re-entry temperatures. For purposes of comparison, data were also presented for the densification process as it takes place in commercial graphites and carbons.

The details of the apparatus and techniques developed for that part of the investigation will be found in the aforementioned report. Also, as an appendix in that report, an analysis was presented which permitted the prediction of the change of permeability as a function of both time and position in the porous medium while the dimensions of the pores were being changed by the deposition of carbon due to thermal decomposition of methane.

In the present investigation, the previous work has been extended to include carbon deposition and removal using acetylene, hydrogen, carbon monoxide, water, and methane for the test gases. These were used singly and in mixtures. The effects of actual pyrolysis gases, obtained from a phenolic resin, were also investigated. The chars used were produced from cylinders having the BSD designation of R6300-HP.

Carbon monoxide and hydrogen were found to have a negligible effect on the permeability of the chars. Both methane and acetylene decreased the permeability while water increased the permeability of the chars. The phenolic ablation products decreased the permeability. It was also noted that the chars could develop cracks from thermal stresses alone.

The use of the results obtained for predicting char phenomena during actual re-entry was considered. An analytical procedure was developed for the case of a growing char in which carbon deposition is occurring due to the cracking of methane.

II

BACKGROUND

2.1 DARCY'S LAW

Efforts to correlate the flow rate of a fluid through a porous material with the pressure drop across it have been made for more than a hundred years.

The experiments of Darcy (Reference 2) and later workers led to the development of a differential equation which has come to be known as "Darcy's law". For one dimensional flow this is

$$-\frac{dP}{dx} = \frac{\mu}{K} V_x \tag{2.1}$$

where

P = pressure
x = distance in x direction
K = permeability
μ = viscosity
V_x = gas velocity in x direction

Thus, Darcy's law states that the flow rate through a porous medium is proportional to the pressure graduent across the medium.

2.2 ANALYTICAL MODELS FOR PERMEABILITY

In order to describe the change in permeability with carbon deposition a mathematical model will be needed. There has been considerable work done in predicting permeability as a function of various structural parameters of porous media. Scheidegger (Reference 3) presents an excellent review of the models which have been used to represent porous structures.

The simplest model of a porous medium is that consisting of a bundle of straight capillaries. The flow, Q, through a capillary can be described by the Hagen-Poiseuille Law:

$$Q = \frac{-\pi \bar{\delta}^4}{128 \mu} \frac{dP}{dx} \tag{2.2}$$

where $\bar{\delta}$ is the diameter of the pores in the model.

By expressing this for the case where there are n capillaries per unit area and combining with Darcy's law, one obtains the following equation for the permeability:

$$K = \frac{n\pi \bar{\delta}^4}{128} \tag{2.3}$$

This equation can be put into various other forms. Letting the porosity ε be represented by

$$\varepsilon = \frac{1}{4} n\pi \bar{\delta}^4 \tag{2.4}$$

and the specific internal surface area of the porous matrix (the ratio of the area of the capillaries to the enclosing volume of the solid be given by

$$S = n\pi \bar{\delta} \tag{2.5}$$

one can substitute for n or $\bar{\delta}$ in terms of ε or S.

One of the most widely accepted theories for permeability was presented by Kozeny (Reference 4) in 1927. He represented a porous medium by channels of various cross-sections, but of definite length. Kozeny solved the Navier-Stokes equations (under certain assumptions) for the flow in channels and then substituted his results into Darcy's law to obtain the Kozeny equation:

$$K = \frac{c\varepsilon^3}{S^2} \tag{2.6}$$

where ε and S are defined as before and c is the Kozeny constant.

The Kozeny equation contains an important parameter in the surface area. For this reason it has been widely used in determining surface areas. For surface area determinations, the value of 1/5 for c is generally assumed.

2.3 KINETICS OF CARBON FORMATION AND REMOVAL

The most important parameters for predicting the effect on permeability due to carbon deposition or removal are the rates of the reactions of the gases flowing through the char. The flow model employed and the density of the deposits are of minor importance in the analysis compared to the kinetics of the reactions which occur.

2.3.1 Methane Decomposition

The kinetics of the decomposition of methane to carbon has been studied extensively. This reaction can be represented by

$$CH_{4(g)} \rightarrow C_{(S)} + 2H_{2(g)} \tag{2.7}$$

It is almost universally agreed that the reaction rate for carbon formation from methane gas can be represented by a first order reaction of the form

$$r_C = k_{CH_4} C_{CH_4} \tag{2.8}$$

Palmer and Cullis (Reference 5) have combined the experimental findings on the decomposition of methane to carbon of several authors in an Arrhenius

plot. The rate constant derived from this figure was used in the previous report (Reference 1). It is

$$r_c = 10^{(15.16 - \frac{2.28 \times 10^4}{T})} C_{CH_4} \qquad (2.9)$$

Several authors have noted that hydrogen inhibits the decomposition of methane in the temperature range of 1025 to 1500°K. However, Kevorkian, Heath, and Boudart (Reference 6) in the temperature range 1660 to 1965°K and Skinner and Ruehrwein (Reference 7) in the temperature range 1430 to 1790°K report no effect of hydrogen.

2.3.2 The Kinetics of Carbon Formation from Acetylene

Carbon formation from acetylene has been widely studied because of its appearance in reactions involving carbon formation. It has been postulated by Porter (Reference 8) in the acetylene theory of carbon formation that carbon is formed directly from acetylene.

At lower temperatures (below 900°K) polymerization is the principal reaction of acetylene. At higher temperatures the products are carbon, hydrogen, diacetylene, vinylacetylene, and sometimes methane (Reference 9 and 8). As a general rule the last three are formed in negligible quantities at the high temperatures.

Because of this, the reaction can be represented by

$$C_2H_2 \rightarrow 2C + H_2 \qquad (2.10)$$

for the temperature regions of interest in this investigation.

Most investigators agree that the kinetics of acetylene decomposition can be represented by a second order reaction of the form

$$-r_{C_2H_2} = k_{C_2H_2} C^2_{C_2H_2} \qquad (2.11)$$

However, there are some exceptions to this agreement. Kozlov and Knorre (Reference 9) found their data to be best represented by a first order homogeneous reaction rate and Silcocks (Reference 10) found his data to be best represented by a combination of a first order heterogeneous reaction with the surface in his reaction vessel and a second order homogeneous reaction.

2.3.3 Carbon from Carbon Monoxide

The reaction describing this carbon formation is known as the Boudouard reaction:

$$2\ CO \rightleftharpoons CO_2 + C \qquad (2.12)$$

Kassel (Reference 11) has studied the equilibrium of this reaction. He writes the reaction in the reverse direction so that the equilibrium constant is defined as

$$K_{eq} = \frac{P_{CO}^2}{P_{CO_2}}, \text{ atm} \qquad (2.13)$$

Table 1 lists the values he obtained for the equilibrium constant.

From the equilibrium data one can see that the reaction favors carbon formation only below 1000°K. Therefore, one might expect carbon to be formed at temperatures below 1000°K. However, this is not the case since the reaction rate becomes small at low temperatures. Gaydon and Wolfhard (Reference 12) report that below 1500°K the gas phase reaction does not occur. From the equilibrium data one can see that when the reaction does occur, the amount of carbon formation is negligible.

2.3.4 Reaction of Carbon with Hydrogen

The reaction of carbon with hydrogen is the reverse of the reactions thus far discussed; i.e., carbon is removed from the surface rather than being deposited.

Sanders (Reference 13) studied this reaction at temperatures from 1825 to 2550°K. He found that his experimental weight losses agreed with his calculations based on thermodynamic data for the hydrogen-graphite theoretical equilibrium composition, with acetylene the major reaction product. At lower temperatures methane is the major reaction product.

Table 2 gives the equilibrium constants obtained from thermodynamic data. From the table it can be seen that at 1800°K only methane and acetylene contribute measurably to the carbon weight loss, while at 2600°K only acetylene is significant.

The main point to note about the carbon-hydrogen reaction is that its equilibrium conversion is small for the temperature range discussed. It is not until temperatures in excess of 3000°K that the reaction of hydrogen with carbon becomes significant.

2.3.5 Reaction of Carbon with Steam

As with many heterogeneous reactions, the determination of the kinetics of the carbon-steam reaction poses many problems. Processes can be controlled by gas film diffusion, by pore diffusion, by the chemical reaction rate, and by combinations of these.

The rate of the carbon-steam reaction is often expressed as

$$r = \frac{k_4 P_{H_2O}}{1 + k_5 P_{H_2} + k_6 P_{H_2O}} \qquad (2.14)$$

According to Ergun and Mentser (Reference 14) the individual reactions forming the reaction sequence are a surface reaction:

$$H_2O + C_f \underset{k_7'}{\overset{k_7}{\rightleftharpoons}} H_2 + C_o \tag{2.15}$$

(where C_f and C_o refer to free and unoccupied active carbon sites respectively), followed by the gasification reaction:

$$C_o \xrightarrow{k_3} CO + nC_f \tag{2.16}$$

The carbon monoxide can also react to form carbon dioxide according to

$$CO + C_o \underset{k_8'}{\overset{k_8}{\rightleftharpoons}} CO_2 + C_f \tag{2.17}$$

This can be further complicated by the water-gas shift reaction:

$$CO + H_2O \underset{k_9'}{\overset{k_9}{\rightleftharpoons}} CO_2 + H_2 \tag{2.18}$$

Using the analysis of Ergun and Mentser in their review of the carbon-steam reaction, the rate of carbon removal can be expressed as

$$-\frac{dn_c}{dt} = \frac{K_4 k_3 C'_{ct} W}{K_4 + C_{H_2}/C_{H_2O}} \tag{2.19}$$

where $-\frac{dn_c}{dt}$ is the rate of carbon removal from the surface, atoms per second; W is the mass of the solid carbon; K_4 is the equilibrium constant for reaction (2.15); and $k_3C'_{ct}$ is the product of the rate constant for reaction (2.16) times the total number of active carbon sites. This expression is on a weight basis. However, a more applicable expression may be obtained by writing this in terms of the surface area, which is the actual governing parameter for the reaction rate, rather than the weight.

The surface area per unit volume may be expressed in terms of the permeability using the Kozeny equation to obtain

$$-\frac{dn_c}{dt} = \frac{K_4 V k'_3 C'_{ct}\sqrt{\frac{\epsilon^3}{5K}}}{K_4 + C_{H_2}/C_{H_2O}} \tag{2.20}$$

where V is the volume and k'_3 is the rate constant k_3 in terms of surface area.

Ergun and Mentser experimentally studied this reaction in the range 1275 to 1475°K and determined values for K_4 and $k_3 C'_{ct}$. Their value of K_4 should hold for other types of porous carbonaceous systems. The term $k'_3 C_{ct}$ will give the temperature dependence of $k'_3 C'_{ct}$.

In analyzing their results, Ergun and Mentser determined that the water-gas shift reaction was at equilibrium at 1475°K in their reaction vessel and reached equilibrium by the time the H_2O was 50% converted at lower temperatures. This fact can be used for determining the product distribution in the reaction zone.

2.3.6 Mixtures

The effect of hydrogen on the rate of carbon formation from methane was discussed in the section on methane. There is no information on the effect of hydrogen on the reactions of the other gases except for the reaction of water vapor with carbon. In this case the effect of hydrogen and of carbon monoxide can be taken into account with the water-gas shift equilibrium.

The only other interactions that might be expected are the interactions between the water vapor and the methane and acetylene. However, a literature search has uncovered no information on this subject.

2.4 DENSITY OF DEPOSITED CARBON

The density of the deposit is needed to determine the volume the deposited carbon will occupy in the pores. The density of deposited carbon formed by the decomposition of hydrocarbon gases has been studied by Brown and Watt (Reference 15). They found that the density of the deposited material is dependent on the temperature of deposition. The density varied from a minimum of 1.14 g/cm^3 at 1975°K to a maximum of 2.22 g/cm^3 at 2375°K. At temperatures from 2300 to 2400°K and higher, the density was essentially constant. Figure 1 shows the change in density with temperature of deposition.

III

EQUIPMENT

3.1 INDUCTION FURNACE

The induction furnace for heating the samples to temperatures characteristic of ablation is discussed in detail in Reference 1. The apparatus was capable of operating at temperatures up to 3000°K for indefinite periods of time. It was leakproof so that air could not enter the system and the gases being passed through the system could not escape. Provision was also made for accurate optical pyrometer temperature measurements despite deposition of opaque matter on the quartz containing walls.

The furnace without the radiation shield is shown in Figure 2. As indicated by the name, induction heating was used to achieve the necessary temperature levels. The power was supplied by a Lepel Model T25-3, 25 kilowatt generator with a frequency range from 180 kc to 450 kc.

The gases used in the experiments were introduced into the specimen cylinders through an inlet in the bottom of the furnace. A thin pyrolytic graphite tube was used to carry the gases from the bottom of the furnace to the hole in the bottom sample holders. The gases then flowed radially outward through the specimen and exited through the top of the furnace.

A Leeds and Northrup 8630-series optical pyrometer was used to measure the surface temperatures of the chars during the transpiration experiments. This was a single-adjustment, potentiometer-type of instrument. The sample was viewed through a quartz sight tube (1/4 inch O.D.) which was attached to the inside surface of the quartz cylinder about 1 1/2 inches below the level of the specimen. Part of the cooling gas was diverted to flow past the sight tube to keep the sight path clear. A mirror was placed on the bottom steel end plate to reflect the radiation coming through the sight tube at an angle more convenient for viewing with the pyrometer.

In order to obtain the high temperatures desired in the furnace, it was necessary to use a radiation shield. A pyrolytic graphite cylinder (1 1/2 inches high and approximately 1/4 inch thick) was used for this purpose. The graphite was oriented so that the direction of lowest conductivity was in the radial direction.

3.2 FURNACE MODIFICATION FOR WATER VAPOR

The gas inlet system to the furnace had to be modified to incorporate water vapor as the test gas. This was accomplished by injecting the water through a small nozzle into the primary test gas stream where the water was vaporized. The nozzle was made from a stainless steel Luer syringe 27 gauge needle. The primary gas stream was heated to approximately 120°C by

wrapping the gas line with electrical heating tape. A Variac was used to control the temperature of the tape. The liquid water flow was monitored with a rotameter. The water injection system is depicted in Figure 3.

3.3 FURNACE MODIFICATION FOR YARN

The yarn consisted of a phenolic resin impregnated in a carbon yarn which was then cured. The yarn was passed through the center of the char in the furnace where the phenolic resin was partially pyrolyzed. The system used for handling the yarn is shown in Figure 4. Prior to an experiment, the yarn was wound on the source spool and then threaded through the gas inlet to the furnace and back down to a motor driven wind up spool where the yarn was rewound after passing through the furnace. The quartz tube on the top char holder was necessary to provide a large smooth turning radius for the yarn, since the yarn could not sustain sharp turns. The motor and spools were contained in a pressurized tank; the test gas passed through the tank and into the furnace. The motor speed was controlled with a Variac.

3.4 PORE SIZE DISTRIBUTION

A 1960 model Aminco-Winslow Porosimeter was used to determine the pore size distribution. This was a 5000 psi hand-operated model which could be used to determine the volume of pores ranging in size from 100 to 0.035 microns. The results were semiquantitative, since the diameter of any pore as determined by the porosimeter was the smallest diameter through which the mercury must pass to enter the pore. This is known as the "bottleneck effect". The data obtained from the mercury porosimeter were the total volume of pores that are filled with mercury at given pressures. From this information one could calculate a capillary pressure curve which in turn could be related to the pore size distribution.

3.5 POROSITY

The porosity was determined by a Boyles' law porosimeter which uses helium gas. In this apparatus a metered amount of helium was brought into the sample chamber. By knowing the total volume of the sample chamber and measuring the pressure before and after the gas was in the apparatus, one could determine the volume of the solids and closed pores, and hence the porosity. The pressure was measured by a fused quartz precision pressure gauge manufactured by the Texas Instrument Company.

3.6 ANALYTICAL BALANCE

All sample weighings were performed on an automatic balance manufactured by Wm. Ainsworth & Sons, Inc. The balance is capable of weighing to 0.001 grams. These weighings, in conjunction with the helium porosimeter results, were used to determine real and apparent densities.

3.7 PRESSURE MEASUREMENT

The pressure drop across the sample was also monitored with the quartz pressure gauge. The gauge output was in digital form; a strip recorder was used to obtain a record of the pressure variation in the course of an experiment.

3.8 FLOW RATES

Rotameters were used for monitoring the flow rates of the gases. These were Brooks rotameters and had maximum flow rates ranging from 51 cc/min. to 24.4 SCFH of air.

3.9 GAS ANALYSIS

The effluent gases from the furnace were analyzed with a gas chromatograph. The analysis did not give the exact composition of the gases leaving the sample since the gases continued to react after that time. This effect was minimized by a side effect of the gas used to keep the sight tube clear. This gas tended to quench the reaction by cooling the effluent gases immediately upon their exit from the sample. A Beckman GC-5 chromatograph equipped with a temperature programmer was used during most of the experimental work.

IV

CHARACTERIZATION OF CHARRED CYLINDERS

4.1 DESCRIPTION OF CYLINDERS AS SUPPLIED

Eight charred cylinders were supplied by Avco/RAD. All cylinders were made from compression molded high purity RAD-6300-HP carbon phenolic material using the dixie cup method with a 30 degree layup angle to the pipe axis. Before charring, the cylinders were twelve inches in length with an outside diameter of 1.25 inches and a wall thickness of 0.25 inches.

Charring was accomplished by passing plasma gases from the Avco/RAD Ten Megawatt Arc Facility through the inside of the cylinders for periods ranging from 14 to 27 seconds. The heat transfer rate to the cylinders was about

$$1100 \frac{\text{Btu}}{\text{ft}^2 \text{ sec.}} .$$

The peak backface temperatures ranged from 1120 to 2000°F. The thickness measured at the center of the cylinders varied from 0.08 to 0.19 inches after charring. The test conditions for the charring are summarized in Table 3.

It should be emphasized that considerable variation of structural properties were evident in the angular direction at any given axial position in the cylinders as supplied. This was apparently due to the non-symmetry of the plasma jet used in the charring process.

4.2 CHARACTERIZATION OF THE CYLINDERS AS SUPPLIED

The cylinders were cut into one inch long segments. The location of these segments from the hot end during the charring process is designated in the sample name. The dimensions of the samples used are listed in Table 4. Also shown are the real and apparent densities, the porosity, the permeability, and the average pore diameters.

Figure 5 is a photomicrograph of an as-received char. Significant deposition may be noted near the inside surface. Almost no deposition is evident near the outside surface.

4.3 COMPARISON WITH COMMERCIAL CARBONS AND GRAPHITES

As-received characterization of commercial carbons and graphites is shown in Table 5 for comparison purposes. The carbons and graphites were obtained from Union Carbide Corporation.

V

CONDITIONING OF THE CHARS

The chars in the as-received condition contained unablated residue. This was eliminated by passing an inert gas through the char at high temperatures in the furnace. The inert gas used was helium. All chars used in deposition runs were conditioned in this manner. The characterization results after conditioning are summarized in Table 6. It can be seen that the real density after conditioning was about 4% higher than before conditioning. The porosity of the samples was typically 28% before conditioning and 32% after conditioning. In general, the after conditioning permeabilities were about one and half times larger than the before conditioning permeabilities. Most of the chars were conditioned at 2600°K for 40 minutes. The time for conditioning at the highest temperature and the highest temperature are both listed in Table 6.

It is of interest to compare the permeabilities of the high purity chars used in the present study with the chars of Reference 1 and also with the commercial carbons and graphites. Figure 6 shows such a comparison. It is immediately obvious that the permeabilities of the present chars are an order of magnitude lower than the previous chars and several orders of magnitude lower than the carbons and graphites. All of the chars shown in Figure 6 were conditioned at about 2600°K for 35 minutes or more.

The pore size distribution of a char before conditioning is compared with a char after conditioning in Figure 7. Conditioning had only a small effect on the pore size.

Three chars were conditioned at high temperature, about 2900°K. All three chars cracked within ten minutes at this temperature. None of these chars was cemented in the sample holders for conditioning. After two chars had cracked at high temperature, great care was taken with the third sample (R6300-HP-DC4-0.6FH-XS) to determine the reasons for cracking. The sample holders were remachined to obtain clean smooth surfaces. The top (spring loaded) support was not used in order to minimize unnecessary mechanical forces on the char. The top holder was needed to prevent radiation losses; it weighed less than 25 grams.

The char was conditioned for ten minutes at 2660°K without difficulty. The temperature was then increased to 2875°K. After less than 4 minutes, the temperature in the char dropped rapidly indicating a crack in the char. When it was removed from the furnace, the crack was confirmed; a picture of the crack is shown in Figure 8. A large pit on the inside surface also developed during conditioning and may be seen in Figure 9. The depth of this pit was about .07". Since there were no mechanical forces on the sample, the crack must be ascribed to thermal stresses.

A photomicrograph of a char after conditioning at 2660°K is shown in Figure 10. Comparing this with a sample as received, the after-conditioning sample is more uniform in the radial direction. Also there are dark deposits visible at the outside surface similar to those at the inside surface. These deposits at the outside surface are a result of the conditioning process. They are deposited carbon, formed during conditioning by the decomposition of the gases coming from the unablated material. The flow direction of the gas was from the inside out, so that the deposition occurred in the outer section of the sample.

VI

CARBON DEPOSITION AND REMOVAL

6.1 EXPERIMENTAL PROCEDURE

To simulate the char densification that occurs in the char, gases typical of the pyrolysis products of phenolic resins (C_2H_2, H_2, CO, H_2O, and CH_4) both singly and in mixtures were passed through char samples while the samples were inductively heated. The effects of these gases on the char were then determined.

For test gases that could be obtained in compressed cylinders (He, CH_4, C_2H_2, H_2, and CO) the general experimental procedure was to heat the sample to the desired temperature using helium only. The test gas was then allowed to flow through the sample. Pressures and flow rates were monitored, and from these permeability as a function of time was calculated.

The procedure for water vapor was the same as that above, except that the water stayed in the liquid form until after it was mixed with the other gases. It was then vaporized and entered the furnace as a gas.

For experiments with yarn, the yarn was first dried in a vacuum oven to remove adsorbed water vapor. It was then placed in the experimental apparatus. The motor pulling the yarn through the furnace was started and the temperature was immediately raised to the test temperature. The weight loss of the yarn was determined by weighing the yarn that had passed through the furnace and also a control piece that was dried but had not passed through the furnace. By measuring the lengths of the two pieces, the weight loss per unit length could be determined, and from this the total weight loss.

6.2 CALCULATION OF PERMEABILITIES FROM THE EXPERIMENTAL DATA

When the experimental data were reduced to obtain permeabilities, the change in gas volume due to reaction was neglected so as to avoid undue complexities in the computations. For the relatively small concentrations of reacting gases used in the experiments this assumption would not cause any appreciable error.

In determining the mobility (the ratio of permeability to initial permeability), the initial value of the permeability used was the value obtained slightly after the test gas was started extrapolated to time zero. Thus errors caused by neglecting the reaction of the test gas cancelled each other in calculating mobility, and any changes in permeability that occurred during startup operations were not erroneously included in the results. The permeabilities after deposition in the chars are summarized in Table 7; the carbon and graphite results are shown in Table 8. A comparison of the

apparent density, permeability, and porosity of the chars in the as-received, after conditioning and after deposition conditions may be found in Table 9. During the experiments the temperature and flow rates varied somewhat. In presenting the results in the tables and figures, average values were used.

6.3 RESULTS USING METHANE

The analysis presented in the previous report for the prediction of the change in permeability as a function of time and position for carbon deposition by the thermal decomposition of methane has been verified.

Complete data and results for deposition in carbon and graphite samples can be found in the dissertation by Schwind (Reference 16).

A comparison of the analysis with the experimental results from two of the runs is shown in Figures 11 and 12. The results are plotted in terms of mobility. It is seen that the analysis provides an accurate means of predicting the effect of carbon deposition from the decomposition of methane in these types of porous media.

Figure 13 shows the effect of methane deposition on the permeability (mobility) of a char sample. Some of the methane decomposed prematurely during this experiment. This can be seen in Figure 14 which is a photomicrograph of the sample after the run. The deposit at the inside surface is the material just slightly different in color from the epoxy resin that was used for impregnating the sample in preparing it for photomicrography. The premature decomposition was due to the low permeability of the char and the resulting low flow rate.

6.4 RESULTS USING ACETYLENE

Acetylene decreases the permeability of the chars by the deposition of carbon. The decrease in permeability is faster than that observed with methane. Some of the experimental results are presented in Figures 15 through 19.

Figures 20 and 21 are photomicrographs of the R6300-HP-DC1-8.2FH-XS sample after carbon deposition using acetylene. Here again, some of the acetylene decomposed prematurely. This can be seen as a deposit at the inside surface with little deposition in the pores of the sample in Figure 21. Figure 20 is a different view of the same sample. In this region of the sample the acetylene did not decompose prematurely and deposit at the inside surface but in the sample, the black spots in Figure 20 being deposited carbon.

6.5 RESULTS USING CARBON MONOXIDE

In Section II it was predicted on the basis of equilibrium data that when carbon monoxide reacts to form carbon, the amount of carbon formed will be

negligible. One sample, R6300-HP-DC1-9.4FH-XS, was tested with carbon monoxide at three temperatures (1620°, 2040°, and 2760°K). At all three temperatures the permeability remained constant; the results agreed with the prediction.

6.6 RESULTS USING HYDROGEN

In Section II it was also predicted that the hydrogen reaction with carbon is equilibrium-limited. Not until temperatures are in excess of 3000°K would it be expected that the effect of hydrogen becomes important in chars. The R6300-HP-DC1-4.2FH-XS sample was used for runs with hydrogen at 1490°, 1995°, 2660°K. The R6300-HP-DC1-5.4FH-XS sample was used for runs with hydrogen at 1585° and 2400°K. Except at the two high temperature values there was no effect on the char permeability.

At the temperatures of 2400° and 2660°K both samples cracked. It is suspected that the cracking occurred because of thermal stresses for the same reason that cracking occurred during conditioning.

For the samples that didn't crack, the experiments agree with what one would predict using equilibrium data. That is, hydrogen has a negligible effect on the permeability for temperatures up to 2000°K and probably for temperatures up to 3000°K.

6.7 RESULTS USING WATER VAPOR

The effect of water on the chars is to increase their permeability. The water reacts with the carbon surfaces in the pores to remove carbon from the char.

Figure 22 shows the effect of water on carbon chars. The permeability increases with time. Figure 23 is a photomicrograph of one of the samples after exposure to water. Comparing this with a sample after conditioning, Figure 10, one can see the dramatic erosion effect of the water. The inside section of the sample has little solid material remaining. This effect of the water can also be seen in the pore size distribution, Figure 24.

6.8 RESULTS USING MIXTURES

Several authors have noted an inhibition of the rate of methane decomposition by hydrogen at relatively low temperatures. Methane-hydrogen mixtures were used in runs with two samples. The results are shown in Figures 25 and 26. To determine the effect of hydrogen, the two experiments were compared with the analysis for methane alone, assuming that the hydrogen was an inert gas. The two experiments using methane are compared with Schwind's experimental data in Figure 27. The data are plotted in terms of the log of the experimental rate constant for methane decomposition versus reciprocal temperature. From this figure it can be seen that for temperatures

greater than 1580°K, hydrogen does not affect the decomposition of methane.

The deviation of Schwind's experimental data from his theoretical line at low temperature was due to the fact that at the low temperatures the carbon deposition was a result of the decomposition of the impurities in his methane gas rather than a result of the decomposition of the methane. For temperatures greater than 2100°K the methane decomposed before actually entering the sample. Since the same purity of methane gas was used for the two methane-hydrogen experiments that Schwind used, the line that best fit his data was used to test the effect of the methane-hydrogen mixture.

Figures 28 and 29 show the results using acetylene and hydrogen. With the char sample the acetylene decomposed prematurely. However, using the results of the acetylene and hydrogen with a carbon sample and comparing them with results with just acetylene, it can be seen that hydrogen does not affect the carbon deposition from acetylene. Figures 30 and 31 show the results for acetylene-methane and acetylene-carbon monoxide mixtures.

Figures 32 through 35 show the effect of carbon deposition and removal occurring simultaneously. By varying the concentrations of the gases, the permeability can be made to increase or decrease. By increasing the concentration of the gases that deposit carbon, CH_4 and C_2H_2, the permeability can be made to decrease more rapidly. By increasing the concentration of the gas which removes carbon from the pores, H_2O, the permeability can be made to increase more rapidly.

6.9 RESULTS USING YARNS IMPREGNATED WITH PHENOLIC

Three experiments were made using yarns impregnated with phenolic so that the effect of actual products of ablation on the permeability of chars could be studied. In all cases the effect of the decomposition products of the yarn was to decrease the permeability of the chars. The yarn used was Union Carbide Co. VYB 70 1/2, impregnated with Monsanto's resin SC 1008. It was prepared by Lockheed Missile and Space Company. The resin content of the yarn was 23.9 weight per cent.

The yarn was quite brittle and required gentle handling. In the design of the experimental apparatus care was taken to insure that the yarn did not have to negotiate any sharp turns. The maximum temperature to which the yarn could be exposed and still be handled satisfactorily was 1500°K.

Before the yarn was used in the furnace it was treated in a vacuum oven to remove adsorbed water vapor. The adsorbed water vapor amounted to more than 10% of the total weight of the yarn.

The R6300-HP-DC8-5.0FH-XS char sample was tested with the yarn in conjunction with a helium flow rate of 0.108 ft^3/min at 1265°K using 56.3 feet of yarn. The mobility decreased from one to 0.642 in 4.3 minutes.

The R6300-HP-DC8-0.6FH-XS sample was tested with the yarn with a helium flow rate of 0.148 ft^3/min at 1265°K using 91.7 feet of yarn. During this

experiment, leaks developed in the cement holding the sample. Even with the leaks the mobility decreased to 0.695 in 6.3 minutes.

The R6300-HP-DC8-3.9FH-XS sample was tested with yarn with a helium flow rate of 0.120 ft^3/min at 1440°K using 97.4 feet of yarn. The mobility decreased to 0.578 in 6.6 minutes.

Exact determination of the resin weight loss of the yarn could not be made. Due to the brittleness of the yarn, the yarn could break at any time during an experiment so that the length of yarn to be used in the furnace was not known beforehand. This meant that average values of the weight per unit length had to be used to determine the weight loss. At the temperatures used the weight loss of the resin was small and of the same order of magnitude as the variation in the weight of the yarn. After the yarn was charred, it was cut into 15 foot lengths, several of which had weights greater than an average value for an uncharred piece.

Another problem in determining the weight loss was the large amount of water that could be adsorbed by the sample. During the time the yarn was exposed to the air after drying (while being transferred from the vacuum oven to the induction furnace and while being transferred from the induction furnace to the gravimetric balance) some water could be adsorbed by the yarn. For all the experiments the resin weight loss was less than 0.005 gm/ft.

Only the final mobility for the yarn experiments is presented rather than a plot of mobility as a function of time. This was done due to the relative values of the volume of the yarn tank as compared to the flow rate of the helium. The actual pressure lagged behind the true pressure due to the time required to change the pressure in the tank using the low flow rate.

VII

CHAR GROWTH SIMULATION

As was described in the Introduction, the ultimate aim of the work which was performed under this and the previous contract was to provide a solid basis for calculations of the change of permeability and pressure drop across a char growing under re-entry conditions. It is believed that this aim has been accomplished, even though the development of the detailed calculational routines was not part of the planned work effort. A simplified model of a growing char was constructed for the case where a methane-inert mixture is the gas flowing through the pores in the char, from the reaction zone to the outside surface. The equations describing carbon deposition for this situation, which had been developed previously (Reference 1), were used for this work. The calculations were intended to demonstrate the feasibility of using the type of data obtained in the course of the project for predicting phenomena more closely associated with actual re-entry situations.

The model employed is a simple model designed to show how char densification affects the permeability of the char. For this reason the rate of char growth and temperature profile were arbitrarily set with the emphasis of the work being on the effect of the carbon formation.

For the present example a linear char growth rate was assumed with the char reaching a thickness of .05 inches in 10 seconds. A linear temperature profile was also used with the temperature at the reaction plane being set at 900°K and the temperature at the outside surface for the maximum char thickness being 2500°K. It was assumed that the phenolic decomposed at a reaction plane rather than throughout a zone of reaction, with the products of the decomposition being methane and argon. The initial char permeability was set at 10^{-11} ft^2, the mass flux of methane at $.469 \times 10^{-2}$ lb_m/ft^2 sec and the mass flux of argon at 7.04×10^{-2} lb_m/ft^2 sec. These conditions were not meant to be necessarily representative of the conditions in an actual re-entry situation. They were used only to illustrate the type of simulation that could be performed if the actual re-entry conditions were used.

Figure 37 presents the effects of carbon deposition occurring in the char pores in a simulated re-entry condition. As in an actual re-entry situation the char thickness increases with time. The gaseous products (in this case methane and argon) coming from the pyrolysis of the resin, flow through the char, decomposing to form carbon in the pores of the char.

It is seen from Figure 37 that the carbon deposition does not have an appreciable effect on the mobility of the outside surface of the char until after six seconds when the surface temperature reaches 1850°K. It is not until this temperature is reached that the rate of decomposition of the methane becomes significant compared to the residence time of the methane

in the char. The mobility versus time curve becomes constant because all the methane has decomposed by the time it has reached the outside surface for times greater than 9 seconds. The pressure drop from the reaction plane to any point in the char, the outside surface temperature, and char thickness are also plotted for the assumed conditions.

The program for this solution is in the Appendix.

The general outline for this program could be utilized in developing a more realistic model, including the actual gas mixtures involved, variations in the temperature gradient through the char with time, etc. This should permit prediction of the properties of the char (permeability, porosity, and density) and the composition, pressure, and flow rate of the gaseous ablation products as a function of position in the char and of time. This information, coupled with structural analyses of the char, would make it possible for the designer to determine what combination of conditions might lead to mechanical failure of the char. He would then be able to specify variation of such properties as weave of the reinforcing cloth, polymer composition, and shield thickness in order to alter the performance of the char, if desired.

It should be noted, however, that, for the reasons already discussed, experimental data on chars alone, as obtained in the present work, are not sufficiently accurate to serve as a reliable base for this type of model. It is believed that a combination of information from more uniform (and more permeable) porous carbonaceous materials and from the chars is required for the analysis. To be more specific, results for the deposition kinetics of gases and gas mixtures obtained on the more uniform (and reproducible) materials could be combined with data on the pore size distribution and internal surface area of heat shield materials in various stages of charring to yield fairly accurate results. The term "fairly accurate" must be inserted here because of the inherent inhomogeneities and nonuniformities of all practical ablative composites, as well as the difficulty in predicting external effects.

A necessary input for the exact char growth analysis would be the heat flux at the surface as a function of time, the composition of the original gaseous ablation products, the rate of decomposition of the polymer as a function of temperature, the thermal conductivity and density of the char, and the permeability of the initial char material formed. With this information the rate of char growth, the char thickness, the temperature profile, the gas flow rate, the porosity, the density, the pressure and the permeability of the char could be calculated as a function of time and position. Also the assumption used in the simplified char growth simulation program (with methane), of the polymer decomposing at a plane rather than throughout a zone, could be eliminated.

VIII

CONCLUSIONS AND RECOMMENDATIONS

The effect of carbon deposition and removal in ablative chars was studied, using gases typical of the ablation products of phenolic decomposition both singly and in mixtures. It was found that, by themselves, carbon monoxide and hydrogen had a negligible effect on the permeability of chars. Methane and acetylene decreased the permeability, the effect of acetylene being more rapid than methane. Hydrogen did not affect the rate of carbon formation from either methane or acetylene, it acted only as a diluent. Water increased the permeability of chars. The composition of mixtures of C_2H_2, CH_4, H_2, CO, and H_2O could be adjusted to make the permeability increase or decrease. Actual phenolic ablation products, obtained from impregnated yarns, were used with the char samples. Their effect was to decrease the permeability of the samples. It was also found that the chars would crack from thermal stresses when they were exposed to high temperatures (above 2800°K) for more than five minutes.

The analysis presented in the previous report for the prediction of the change in permeability by carbon deposition from methane has been verified. (Reference 16). Two figures are shown comparing this analysis with experiment. This analysis was also extended to demonstrate how it could be used to predict the permeability in the char layer during re-entry.

It has been found that the experiments with the ablative char samples alone were not a sufficient basis on which to base a precise analytical model of carbon deposition and removal in ablative chars. The primary difficulty was the low permeability of the chars. The low permeability required the use of small gas flow rates which in turn limited the experimental temperatures to prevent premature reaction of the test gas. Even using low temperatures, premature reaction of the test gas was frequently observed with the char samples. Using uniform more permeable porous carbon or graphite samples, the functional kinetic relationships among the various gases interacting with the chars can be determined. Some results have already been obtained doing this and are included in this report.

It is recommended that the analytical work which has been initiated be extended to include increasingly complex ablation models, so that maximum use can be made of the results obtained during the present project. In conjunction with this, further experimental data should be obtained on the kinetics of the reactions undergone by gas mixtures typical of the decomposition products of ablative materials. Also there is need for more detailed information on the internal structure of heat shield materials at various stages of decomposition.

IX

REFERENCES

1. Weger, E., Brew, J., and Schwind, R. A., "An Investigation of Carbon Deposition in Chars", BSD TR 66-385, Final Report USAF Contract AF 05 (694)-695, Washington University, November 1966.

2. Darcy, H., "Les Fontaines Publiques de Ville de Dijon", Dalmont, Paris, 1856.

3. Scheidegger, A. E., "The Physics of Flow through Porous Media", The MacMillan Company, New York, 1960.

4. Kozeny, J., Akademie der Wissenschaften, Vienna Almanach, Mathematisch-naturwissenschaftliche Klosse-Anzeiger-Sitzungsberichte, Vol. IIa, No. 136, (271 - 282), 1927.

5. Palmer, H. B., and Cullis, C. F., "The Formation of Carbon from Gases", Chemistry and Physics of Carbon, edited by P. L. Walker, Marcel Dekker, New York, No. 1, Chapter 5, 1965.

6. Kevorkian, V., Heath, C. E., and Boudart, M., "The Decomposition of Methane in Shock Waves", The Journal of Physical Chemistry, Vol. 64, (964 - 968), August 1960.

7. Skinner, G. B., and Ruehrwein, R. A., "Shock Tube Studies on the Pyrolysis and Oxidation of Methane", Journal of Physical Chemistry, Vol. 63, (1736 - 1742), 1959.

8. Porter, G., "Carbon Formation in the Combustion Wave", Fourth Symposium on Combustion, (Massachusetts Institute of Technology), (228 - 232), 1952.

9. Kozlov, G. I., and Knorre, V. G., "Single-pulse Shock Tube Studies on the Kinetics of the Thermal Decomposition of Methane", Combustion and Flame, Vol. 6, (253 - 263), 1962.

10. Silcocks, C. G., "The Kinetics of the Thermal Polymerization of Acetylene", Proceedings of the Royal Society of London, Series A, Vol. 242, (411 - 429), 1957.

11. Kassel, L. S., "Thermodynamic Functions of Nitrous Oxide and Carbon Dioxide", Journal of American Chemical Society, Vol. 56, (1838 - 1842), 1934.

12. Gaydon, A. G., and Wolfhard, H. G., "Flames", Chapman and Hall, London, Chapter VIII, 1953.

13. Sanders, W. A., "Rates of Hydrogen-Graphite Reaction Between 1550 and 2260°C", National Aeronautics and Space Administration NASA TN D-2738.

14. Ergun, S., and Mentser, M., "Reactions of Carbon with CO_2 and Steam", Chemistry and Physics of Carbon, edited by P. L. Walker, Marcel Dekker, New York, Vol. 1, Chapter 4, 1965.

15. Brown, A. R. G., and Watt, W., "The Preparation and Properties of High-Temperature Pyrolytic Carbon", Industrial Carbon and Graphite, Papers Conference, London (86 - 100), 1957.

16. Schwind, R. A., "Carbon Deposition in Porous Media by the Thermal Decomposition of Methane", Doctor of Science Dissertation, Sever Institute of Washington University, January 1968.

TABLE 1

Equilibrium Constant for Boudouard Reaction

T, (°K)	K_{eg}
300	1.63×10^{-21}
400	5.40×10^{-14}
500	1.82×10^{-9}
600	1.90×10^{-6}
700	2.71×10^{-4}
800	1.11×10^{-2}
900	0.195
1000	1.91
1100	1.23×10
1200	5.73×10
1250	1.12×10^{2}
1300	2.09×10^{2}
1400	6.28×10^{2}
1500	1.63×10^{3}
1750	1.06×10^{4}
2000	4.21×10^{4}
2500	2.72×10^{5}
3000	8.80×10^{5}

Boudouard Reaction: $CO_2 + C \rightleftharpoons 2CO$

Equilibrium Constant: $K_{eq} = \dfrac{P^2_{CO}}{P_{CO_2}}$

TABLE 2

Equilibrium Constants for the Dehydrogenation Reaction of Some Hydrocarbons

Hydrocarbon	Temperature	
	1527° C (1800° K)	2327° C (2600° K)
	Equilibrium constant, K	Equilibrium constant, K
Methane (CH_4)	$7.54X10^{-4}$	$1.19X10^{-4}$
Acetylene (C_2H_2)	$1.98X10^{-4}$	$1.81X10^{-2}$
Ethylene (C_2H_4)	$4.78X10^{-6}$	$9.91X10^{-6}$
Methyl radical (CH_3)	$9.47X10^{-6}$	$1.30X10^{-4}$
Methylene radical (CH_2)	$3.50X10^{-7}$	$1.06X10^{-4}$
Methenyl radical (CH)	$3.67X10^{-12}$	$7.08X10^{-7}$

TABLE 3

Data on AVCO/RAD Charred Cylinders

Material Code	PRE-TEST Wgt. (gms)	Length (in)	O.D. (in)	I.D.[a] (in)	Wall Thick. (in)	POST-TEST Test Time (sec)	Wgt. (gms)	I.D.[a] (in)	Char Thick (in)	Peak Backface (°F)
R6300 HP-DC1[b]	227.3	12	1.25	0.734	0.25	14.36	63.8	1.004	0.123	1500
R6300 HP-DC2[c]	225.7	12	1.25	0.734	0.25	24.9	68.8	1.037	0.1065	1500
R6300 HP-DC3[d]	223.0	12	1.25	0.726	0.25	26.01	115.7	0.868	0.191	1580
R6300 HP-DC4[e]	225.0	12	1.25	0.732	0.25	27.00	118.0	0.876	0.187	1200
R6300 HP-DC5[f]	225.0	12	1.25	0.749	0.25	14.49	66.9	1.034	0.108	1900
R6300 HP-DC6[g]	223.0	12	1.25	0.747	0.25	17.77	50.0	1.094	0.078	1820+[g]
R6300 HP-DC7[h]	226.9	12	1.25	0.753	0.25	22.55	62.5	1.059	0.0955	1600[i]
R6300 HP-DC8[h]	225.3	12	1.25	0.752	0.25	18.00	59.5	1.070	0.090	1410

a - measured at center of cylinder

b - supplied 5 April 1967; two consecutive tests were performed on this cylinder, first test was 7.94 sec. with a post-test weight of 127.7 gms, and second test was 6.42 sec. with a post-test weight of 63.8 gms.

c - supplied 12 April 1967; two consecutive tests were performed on this cylinder, first test was 10.17 sec. with post-test weight of 122.0 gms and second test was 14.73 sec. with a post-test weight of 68.8 gms.

d - supplied 5 May 1967; two consecutive runs were performed, first test was 5.41 sec. with a post-test weight of 181.5 gms, and second test was 20.60 sec. with a post-test weight of 115.7 gms.

e - supplied 5 May 1967

f - supplied 29 May 1967

g - thermocouple burn-out at approximately 15 seconds, it is estimated that a peak backface temperature of approximately 2000°F was reached.

h - supplied 5 July 1967 (DC8 was an extra charred cylinder)

i - approximation based upon the downstream thermocouple reading for DC7, as well as, the peak backface temperature for DC8 since DC7 and DC8 were run at same test conditions.

TABLE 4

AS RECEIVED CHARACTERIZATION (CHARS)

Sample	Thickness (in)	O.D. (in)	Real Density (gm/cm^3)	Apparent Density (gm/cm^3)	Porosity (%)	Permeability ($\times 10^{13}$ ft^2)	Average Pore Diameter (Microns)	Conditioned	Deposition
R6300-HP-DC1-0.9FH-XS	0.049	1.241	1.4124	1.079	23.6	5.9	--	X	X
R6300-HP-DC1 2.6FH-0 $\frac{1}{2}$	0.038	1.224	1.4329	0.935	33.4	---	--	--	-
R6300-HP-DC1-3.2FH-H $\frac{1}{3}$	0 036	1.208	1.3505	0.957	29.2	---	8.4	--	--
R6300-HP-DC1-4.2FH -XS	0.080	1.249	1.3508	1.095	18.9	5 1	---	X	X
R6300-HP-DC1-5.4FH-XS	0 092	1.246	1.3378	0.986	26.7	5.7	---	X	X
R6300-HP-DC1-6.1FH-I $\frac{1}{2}$	0.070	1.157	1.2192	0.783	35.8	---	---	---	-
R6300-HP-DC1-6.5FH-0 $\frac{1}{2}$	0 046	1.239	1.4957	1.047	30.0	---	---	---	-
R6300-HP DC1-7.3FH-H $\frac{1}{3}$	0.039	1.165	1.3084	0.957	26 9	---	7.4	--	---
RS300-HP-DC1-8.2FH-XS	0.111	1.244	1.3369	0.994	25.7	4.2	--	-	-
R6300 HP-DC1-8.2FH-XS (Machined)	0.049	1.25	---	---	28 0	6.6	--	X	X
R6300 HP-DC1-9 4FH-XS	0.115	1 244	1.3275	0.911	31.4	4.9	---	X	X
R6300-HP-DC1-10.0FH-1 $\frac{1}{2}$	0.073	1.143	1.2088	0.906	25.1	---	-		
R6300-HP-DC1-10 6FH-0 $\frac{1}{2}$	0.067	1 244	1 4033	1.027	26.8	---	8.1	---	---
R6300-HP-DC1-11 2FH-XS	0.122	1.246	1.3183	0.920	30.2	2.1	---	X	---
R6300-HP-DC2-3.15FH-XS	0.076	1.254	1.4018	0.983	30.4	8.0	---	X	X
R6300-HP-DC3-1.75FH-XS	0.153	1 251	1.4621	1.043	28.7	6.5	---	X	X
R6300-HP-DC4-0.6FH-XS	0.123	1.254	1.4453	0.942	34.8	7.0	---	X	---
R6300 HP-DC5-0 7FH-XS	0.041	1.246	1.2769	0.996	22.0	4.2	---	X	X
R6300-HP-DC5-2.55FH-XS	0.085	1.248	1.3359	0.976	26.9	6.2	---	X	X
R6300-HP-DC5-4.6FH-XS	0 098	1.246	1.3565	0.958	29.4	4.9	---	X	---
R6300-HP-DC5-5.5FH-I $\frac{1}{2}$	0.066	1.171	1.3075	0.948	27.5	3.6	4.1	---	---

TABLE 4 (CONT.)

Sample	Thickness (in)	O.D. (in)	Real Density (gm/cm^3)	Apparent Density (gm/cm^3)	Porosity (%)	Permeability ($\times 10^{13}$ Ft^2)	Average Pore Diameter (Microns)	Conditioned	Deposition
R6300-HP DCS 6 0FH O $\frac{1}{2}$	0.055	1.253	1.4671	1.008	31.3	6.4	5.7	--	
R6300 HP DCS-6 55FH-K $\frac{1}{3}$	0.039	1.181	1.4218	0.969	31.8	4.0	6.1		
R5300-HP DCS 7 3FH XS	0.116	1.247	1.3788	0.977	29.2	6.3		X	
R6300 HP DCS 8 4FH-XS	0.123	1.247	1.3826	0.967	30.1	7		X	X
R6300 HP DCS 9 5FH XS	0.127	1.248	1.3892	0.966	30.6	7.8		X	
R6300 HP DCS-10 5FH XS	0.132	1.250	1.3921	0.961	30.9	8.8		X	X
R6300 HP DCS 11 5FH XS		-					6.1*		
R6300 HP DC6 2 2FH XS	0.032	1.262	1.2856	0.954	25.8	4.4		X	
R6300 HP DC7 1 35FH XS	0 31	1.259	1.4134	1.052	25.6	8.1		X	X
R6300 HP DC8 0 6FH XS	0.045	1.250	1.3664	1.023	25.1	4.5		X	X
R6300 HP DC8 1 7FH XS	51	1.253	1.3720	0.973	29.4	4.9		X	X
R6300 HP-DC8 2 8FH XS	3.067	1.254	1.3833	0.966	31.6	5.7		X	X
R6300 HP DC8 3 3FH XS	0.078	1.257	1.3889	0.961	30.8	5.5		X	X
R6300 HP DC8 5 3FH XS	0.087	1.253	1.3762	0.957	30.5	5.7		X	X
R6300 HP DC8 5 85FH L $\frac{1}{4}$	0.043	1.151	1.3376	0.926	30.5	4.9	5.2	-	
R6300 HP XC8 6 45FH O $\frac{1}{2}$	[illegible]	[illegible]	1.4663	0.997	31.0	7.5	6.3		
R6300 HP XC8 6 95FH M $\frac{1}{3}$	[illegible]	1.168	1.3769	0.965	29.9	4.3	9.4	-	
R6300 HP XC8 7 3FH XS	0.134	1.253	1.3837	0.981	29.1	6.1		X	X
R6300 HP XC8 8 8FH XS	0.139	1.252	1.3821	0.967	30.0	6.3	-	X	X
R6300 HP DC8 9 3FH XS	0.101	1.256	1.3775	1.000	27.4	5.4	-	X	X
R6300 HP DC8 11 0FH XS	0.135	1.252	1.3691	1.006	26.5	3.3	-	X	--

* Surface Area = 8.3 m^2/gm

TABLE 5
As Received Characterization (Carbons and Graphites)

Sample	Thickness (in)	O.D. (in)	Real Density (gm/cm^3)	Apparent Density (gm/cm^3)	Porosity (%)	Permeability ($\times 10^{13}$ Ft^2)
PC-45G-1	0.151	1.254	2.0058	1.064	47.0	1700.
PC-45G-2	0.104	1.254	2.0314	1.058	47.9	1700.
PC-45G-3	0.261	1.251	2.0203	1.062	47.5	1400.
PG-45D-2	0.218	1.232	2.085	1.082	48.1	3200.
PG-45F-2	0.217	1.250	2.1010	1.101	47.6	2300.
PG-45F-3	0.217	1.250	2.0991	1.095	47.8	2400.
*PG-25D-3	0.232	1.250	2.055	0.98	52.2	13000.
*PC-60A-1	0.202	1.248	1.995	1.11	44.6	800.

* Data from Ref. 16

TABLE 6
AFTER CONDITIONING CHARACTERIZATION

Sample	Thickness (in)	O.D (in)	Real Density (gm/cm^3)	Apparent Density (gm/cm^3)	Porosity (%)	Permeability ($\times 10^{13}$ Ft^2)	Temperature (°K)	Time (Min)	Remarks
R6333 HP XC1-0 9FH-XS	-	- -	--	- -	---	26.	2410	35	-
R6333 HP XC1-4 2FH XS	0.090	1.235	1.3856	0.971	23.9	5.1	2693	55.	-
R6333 HP XC1-5 4FH-XS	-	---	-	-	---	9.2	1856	28	-
R6333 HP XC1-8 2FH XS (Machined)	0.045	1.253	1.551	1.058	31.8	16	2665.	45	-
[illegible] HP XC1-9 4FH XS	0.117	1.236	1.3739	0.910	33.7	4.6	2693	45	
R633[illegible] HP XC1-11 2FH XS		--	---	- -	---		2810	10	Sample Cracked
R633[illegible] HP XC1-13 15FH XS	0.07	1.263	1.4330	0.970	35.1	13	2660	43.	-
R63[illegible] HP XC1-13 15FH XS	0.154	1.241	1.5173	0.984	34.7	14	2663	45	-
R633 HP XC1-14 4FH XS			- -	-	- -		2875	4	Sample Cracked
R633[illegible] XC1-15FH XS	0.118	1.247	1.3145	1.337	22.7	4.5	2477	50	
R633[illegible] XC1-15FH XS	0.184	1.235	1.3863	0.947	31.8	7.6	2670	45	
R633 HP XC1-16 4FH XS	0.146	1.235		--	32.1	7.3	2693	40	-
R633[illegible] XC1-17FH XS				-			2450	10	Sample Cracked
R633[illegible] XC1-18FH XS	118	1.237	1.4035	0.964	33.2	14	2633	47	-
R633[illegible] XC1-19FH XS			—				2660	35	Sample Cracked, Water Leak Inside Furnace Caused Sample Frosion
R6[illegible] XC1-20FH XS	124	1.233	1.4283	0.951	33.4	14	2596	45	-
R633[illegible] XC1-21FH XS	0.1[illegible]	1.[illegible]	1.3[illegible]	1.[illegible]	25.4	5.3	2663	45	Not Used for Deposition
R633[illegible] XC1-22FH XS	0.[illegible]	1.[illegible]	1.4[illegible]	0.974	32.8	15	2660	45	

TABLE 6 (CONT.)

Sample	Thickness (in)	O.D (in)	Real Density (gm/cm^3)	Apparent Density (gm/cm^3)	Porosity (%)	Permeability ($\times 10^{13}$ Ft^2)	Temperature (°K)	Time (Min)	Remarks
R6300-HP-DC8-0.6FH-XS	0.042	1.241	1.4024	1.06	24.4	5.4	2660.	20.	- -
R6300 HP DC8-1.7FH-XS	---	---	- -	---	---	7.9	2660.	30.	- -
R6300-HP-DC8-2.8FH-XS	0.066	1.242	1.4784	0.938	36.6	6.9	2667.	45.	- -
R6300-HP-DC8-3.9FH-XS	0.078	1.238	1.4746	0.929	37.0	8.2	2660.	43.	---
R6300-HP-DC8-5.0FH-XS	0.085	1.237	1.4365	0.951	33.8	10.	2660.	40.	---
R6300-HP-DC8-7.7FH-XS	0 103	1.242	1.4578	0.957	34.4	8.0	2660.	46.	-
R6300-HP-DC8-8.8FH-XS	0.103	1.241	1.4486	0.978	32.5	9.1	2660.	40.	---
R6300-HP-DC8-9.9FH-XS	0.103	1.243	1.4527	0.957	34.2	8.5	2660.	45.	---
R6300-HP-DC8-11.0FH-XS	0.104	1.236	1.4255	0.990	30.5	4.9*	2660.	45.	---

* Average Diameter - 5.4 Microns

TABLE 7
AFTER DEPOSITION CHARACTERIZATION (CHARS)

Sample	Thickness (in)	O.D. (in)	Real Density (gm/cm³)	Apparent Density (gm/cm³)	Porosity (%)	Permeability (x 10^{13} ft²)	Average Diameter (Microns)	Gases							Average Temperature (°K)	Remarks
								N_2	CH_4	C_2H_2	H_2	CO	H_2O	Vacuum		
[illegible]	--	---	---	--	---	No Effect	-	X	X	--	-	-	- -	---	2380	--
[illegible]	-		- -	---	---	No Effect	--	X	-	--	X	--			1690, 1995 2665,	Sample Cracked at High Temperature
[illegible]		--	- -	--	---	No Effect	5.2	X	-	- -	X	-	-	--	1585 2455	Sample Cracked at High Temperature
[illegible] (Machined)	0.149	1.251	1.5299	1.020	33.3	6.7	7.6	X	-	X	--			-	1574	Premature Decomposition
[illegible]	0.111	1.235	1.3729	0.916	33.4	No Effect	6.1	X				X	-		1670 2760 2765	
[illegible]	0.175	1.245	1.4231	3.689	17.6	22		X	-			-	X	-	1368	
[illegible]	1.167	1.243	1.7176	0.560	68.6	38	9.3	X					X		1671	
[illegible]	1.161	1.329	1.3337	3.373	27.0	1.1	6.9	X	X		-				1655	Premature Decomposition
[illegible]	1.183	1.232	1.3791	3.378	29.4	4.0			X		X		-		1585,	
[illegible]	1.95	1.235	1.3667	3.930	28.5	3.7	6.2			X	X				1607	Premature Decomposition
[illegible]	1	1.731	1.6673	1.946	33.4	6.4	-			X		X			1566	
[illegible]		.91	1.6733	1.318	31.2	9.2		X	X				X		1550	Probable Leak in Cement
[illegible]	1.14	1.261	1.6191	1.327	27.6	3.8		X						X	1760	Leak in Cement
[illegible]	.4	1.734	1.6769	0.961	35.4	3.6		X	X	X					1534	
[illegible]	1.184	1.1			-	9.2		X		X			X		1584	
[illegible]	1.4	1.8	1.673	1.374	34.1	4.7		X						X	1669,	
[illegible]	.94	1.4	1.6658	1.063	36.7	6.6		X						X	1784,	Leak in Graphite Tube
[illegible]	1.4	1.33	1.3823	1.111	75.9	1			X	X	X	X	X		1653	
		1.34	1.5144	3.677	58.6	23		X			X		X		1592	
[illegible]	1	1	1.1658	3.8[illegible]	61.7	7.1			X	X	X	X	X	-	1691	

TABLE 8
AFTER DEPOSITION CHARACTERIZATION (CARBONS AND GRAPHITES)

Sample	Thickness (in)	O.D. (in)	Real Density (gm/cm^3)	Apparent Density (gm/cm^3)	Porosity (%)	Permeability ($\times 10^{13}$ ft^2)	Average Pore Diameter (Microns)	Gases				Average Temperature (°K)	Remarks
								H_e	CH_4	C_4H_2	H_2		
PC-45G-1	0.152	1.264	1.9347	1.238	36.0	250.	---	X	X	---	X	1992.	
PC-45G-2	0.106	1.254	1.9956	1.347	32.5	430.	---	X	---	X	--	1445.	
PC-45G-3	0.202	1.255	1.9542	1.188	39.2	670.	36.	X	---	X	X	1890.	
PG-45D-2	0.221	1.253	2.0148	1.175	41.7	1800.	---	X	---	X	--	1767.	No Radiation Shield
PG-45F-2	0.221	1.253	2.0417	1.242	39.2	1060.	---	X	---	X	--	1923.	
PG-45[illegible]-3	0.221	1.252	2.0529	1.230	40.1	690.	---	X	--	X	--	1914.	
*PG-25D-3	0.233	1.247	1.782	1.410	20.9	1430.	---	X	X	---	-	1730.	
*PC-60A-1	0.200	1.245	1.923	1.342	30.3	350.	---	X	X	---	--	1763.	

* Data Taken From Ref. 14

TABLE 9
SUMMARIZED COMPARISON OF CHARS

Sample	Apparent Density (gm/cm³)			Porosity (%)			Permeability (x 10^{13} ft^2)			Gases
	As Received	After Conditioning	After Deposition	As Received	After Conditioning	After Deposition	As Received	After Conditioning	After Deposition	
R6300-HP-DC1-0.9FH XS	1.079	----	----	23.6	----	----	5.9	26.	No Effect	CH_4
R6300 HP-DC1-9.4FH-XS	0.911	0.910	0.914	31.4	33.7	33.4	4.9	4.6	No Effect	CO
R6300-HP-DC2-3.15FH-XS	0.983	0.970	0.688	30.4	35.0	57.6	8.0	13.	22.	H_2O
R6300-HP-DC3-1.75FH-XS	1.043	0.984	0.540	28.7	34.7	68.6	6.5	14.	38.	H_2O
R6300-HP-DC5-3.55FH-XS	0.976	0.947	0.978	26.9	31.8	28.6	6.2	7.6	4.0	CH_4, H_2
R6300-HP-DC5-8.4FH-XS	0.967	0.964	0.964	30.1	33.2	33.4	7.7	14.	6.4	C_2H_2, CO
R6300-HP-DC8-1.7FH-XS	0.973	---	0.961	29.4	----	34.8	4.9	7.9	3.4	CH_4, C_2H_2
R6300-HP-DC8-2.8FH-XS	0.946	0.938	----	31.6	36.6	----	5.7	6.9	9.1	C_2H_2, H_2O
R6300-HP-DC8-3.9FH XS	0.961	0.929	0.974	30.8	37.0	34.1	5.5	8.2	4.7	Yarn
R6300 HP-DC8-7.7FH-XS	0.981	0.957	1.011	29.1	34.4	25.9	6.1	8.0	10.	CH_4,C_2H_2,H_2,CO, H_2O
R6300-HP-DC8-8.6FH-XS	0.967	0.978	0.677	30.0	32.5	58.6	6.3	9.1	23.	H_2, H_2O
R6300-HP-DC8-9.9FH-XS	1.000	0.957	0.902	27.4	34.2	41.7	5.4	8.5	7.3	CH_4,C_2H_2,H_2,CO,H_2O

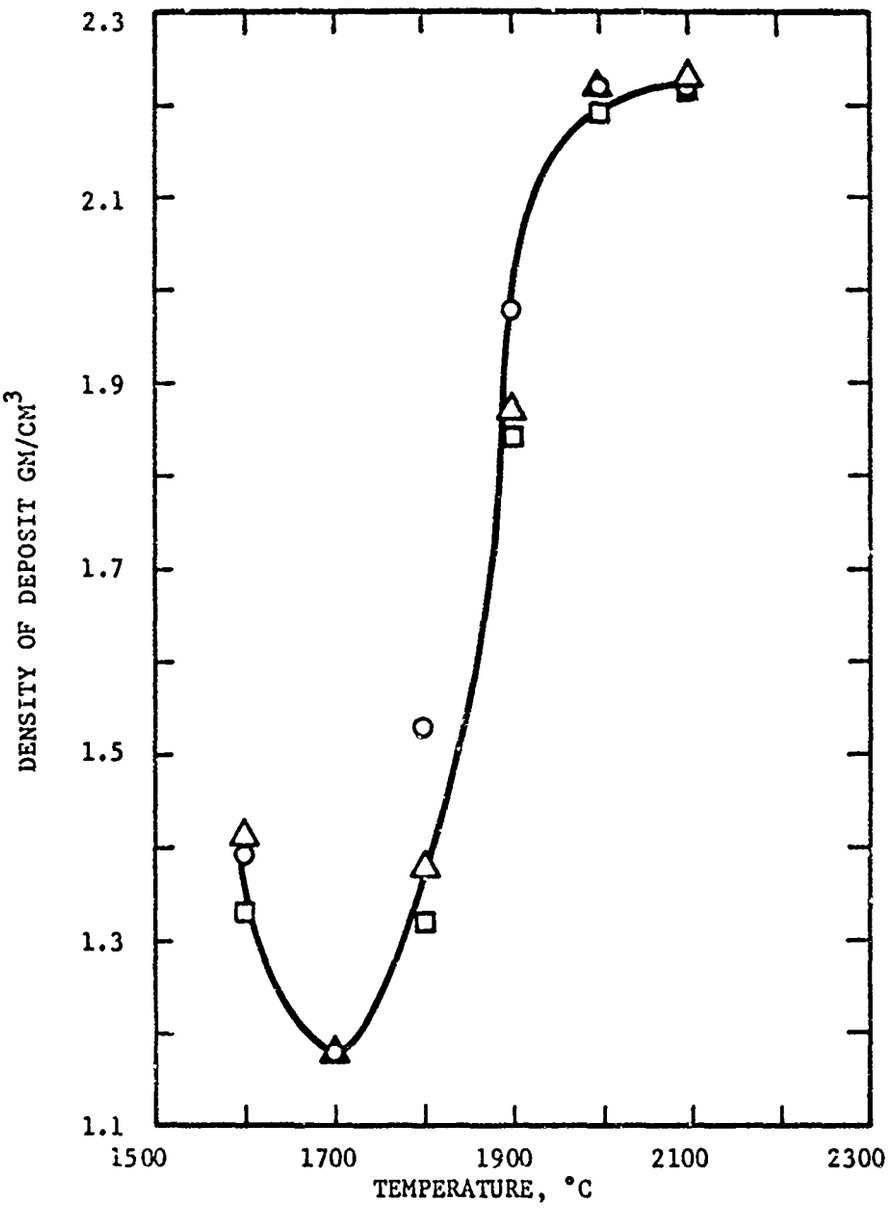

FIGURE 1: VARIATION OF DENSITY OF CARBONACEOUS DEPOSIT WITH TEMPERATURE

- ○ DEPOSITED FROM METHANE AT 15 CM Hg PARTIAL PRESSURE
- □ DEPOSITED FROM BENZENE AT 2.5 CM Hg PARTIAL PRESSURE
- △ DEPOSITED FROM PROPANE AT 15 CM Hg PARTIAL PRESSURE

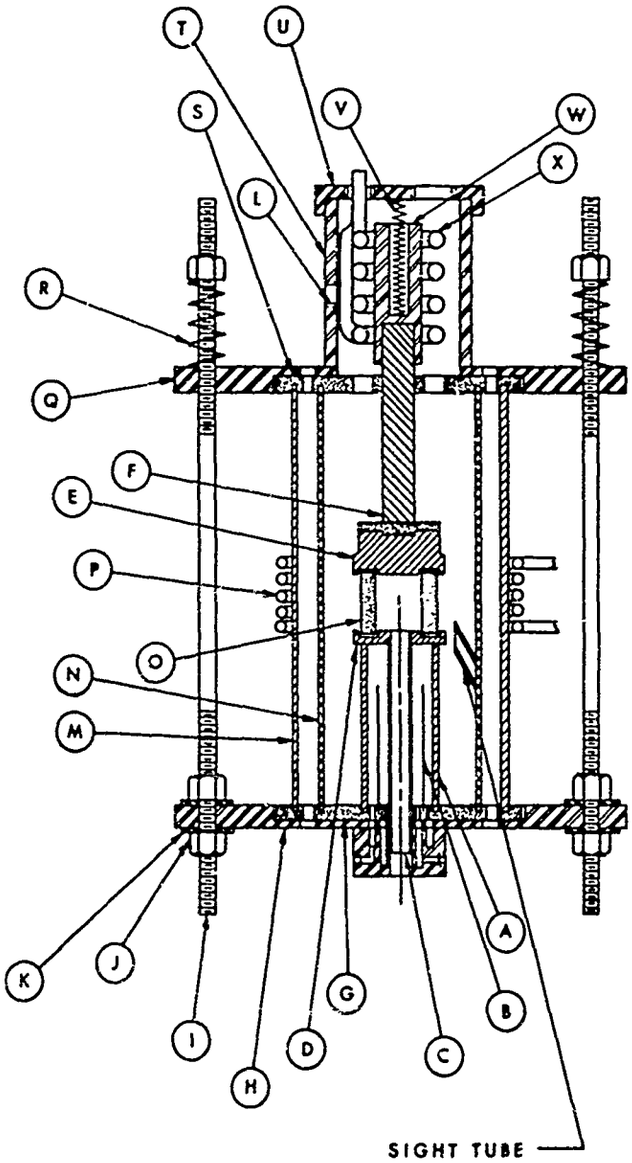

NO	PART	MATL.
A	LOWER SUPPORT	PYRO. G
B	BAFFLE	STAINLESS STEEL
C	GAS TUBE	PYRO. G
D	BOTTOM HOLDER	BORON NITRIDE
E	TOP HOLDER	BORON NITRIDE
F	TOP SUPPORT	PYRO G.
G	BOTTOM SHIELD	PYRO G.
H	BOTTOM PLATE	STAINLESS STEEL
I	THREADED ROD	INCONEL
J	NUT	STAINLESS STEEL
X	WASHER	STAINLESS STEEL
L	MANOMETER LEAD	
M	INNER PYREX TUBE	PYREX
N	QUARTZ TUBE	QUARTZ
O	SAMPLE	
P	INDUCTION COILS	COPPER
Q	TOP PLATE	STAINLESS STEEL
R	ROD SPRING	STEEL
S	TOP SHIELD	PYRO G.
T	COOLING CYLINDER	STAINLESS STEEL
U	CYLINDER CAP	STAINLESS STEEL
V	H. T. SPRING	INCONEL X
W	SPRING GUIDE	STAINLESS STEEL
X	COOLING COIL	STAINLESS STEEL

FIGURE 2: INDUCTION FURNACE

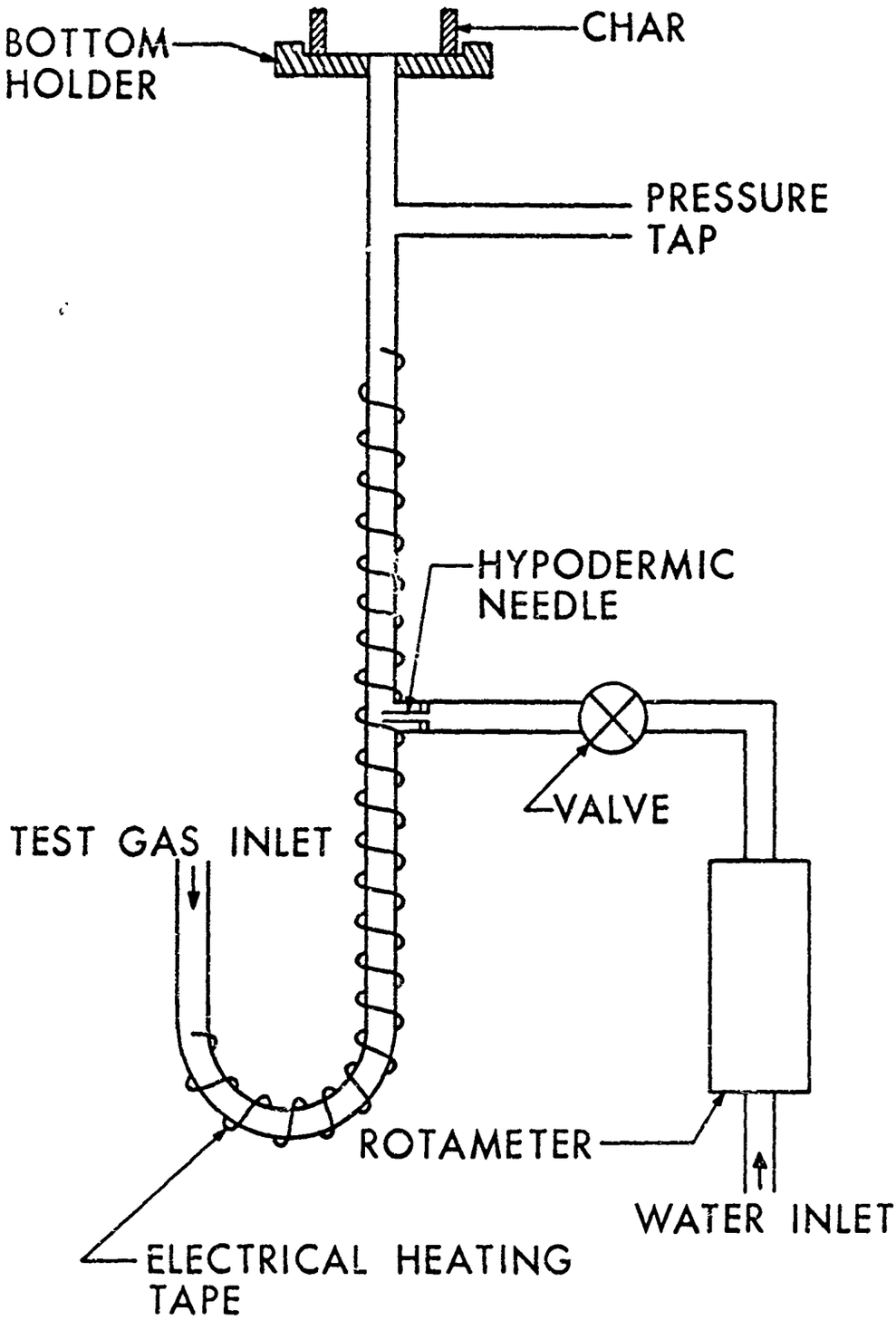

FIGURE 3: WATER INJECTION SYSTEM

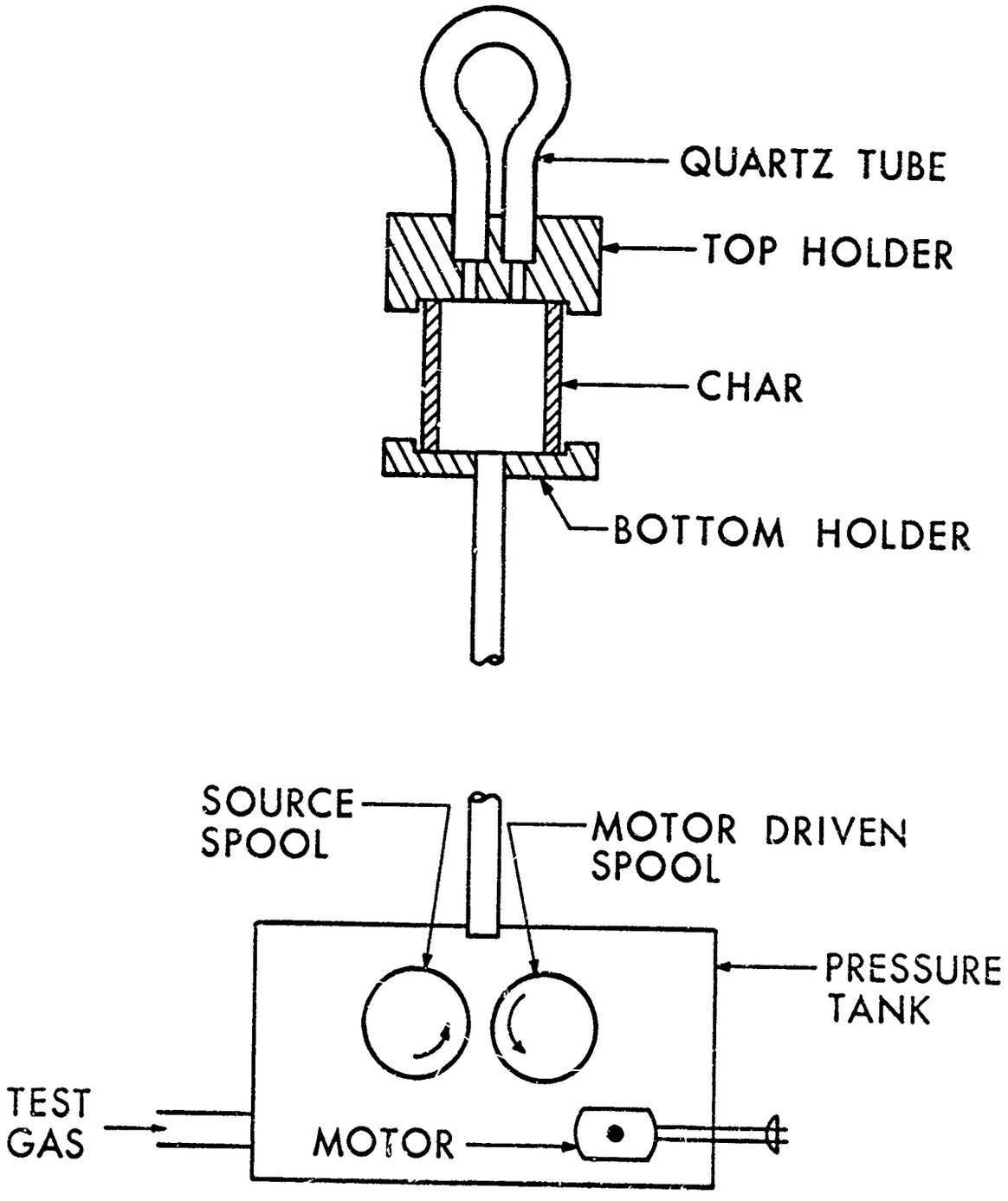

FIGURE 4: YARN APPARATUS

FIGURE 5: PHOTOMICROGRAPH OF R6300-HP-DC5-11.0FH-XS
AS RECEIVED

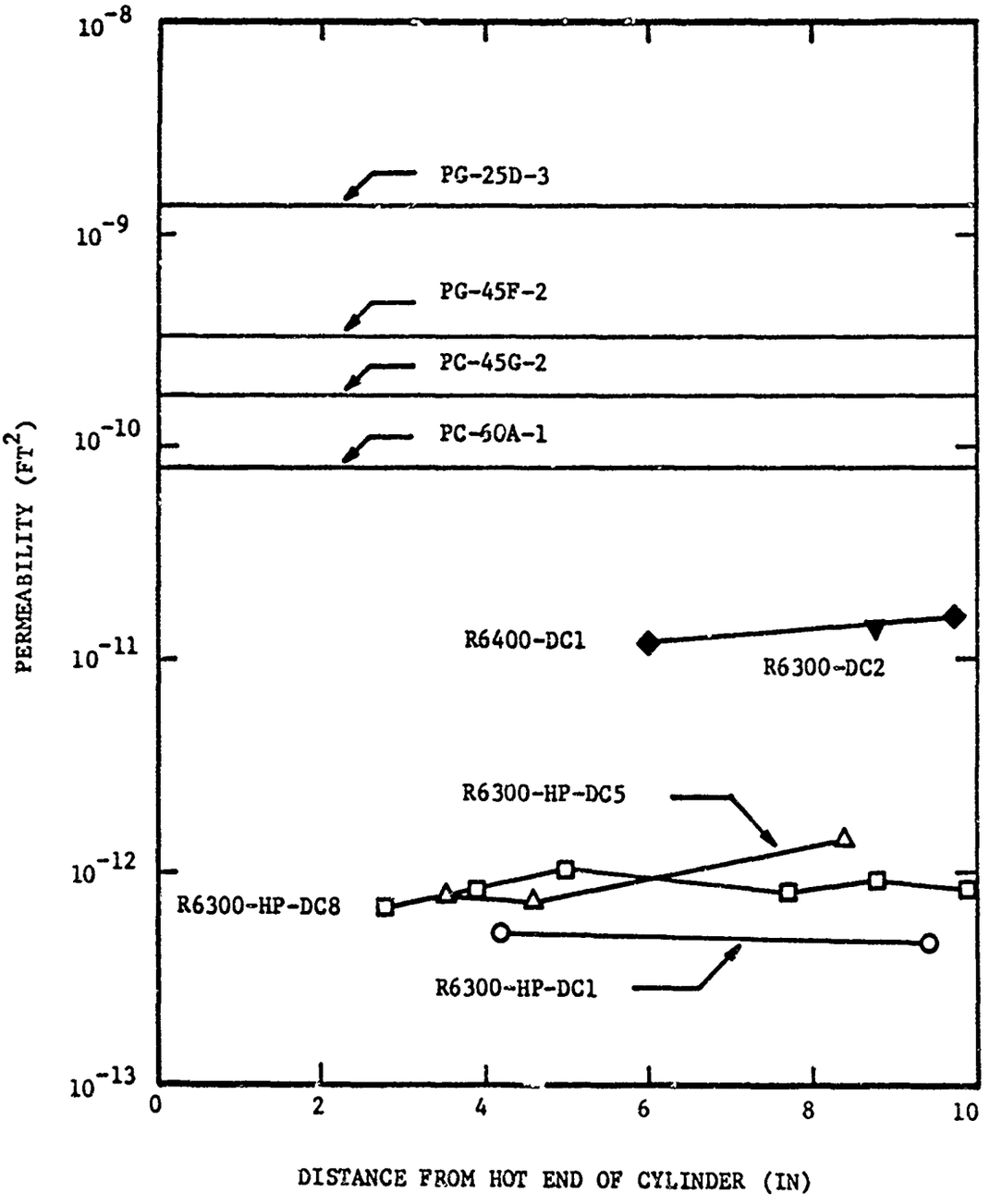

FIGURE 6: COMPARISON OF AFTER CONDITIONING PERMEABILITIES

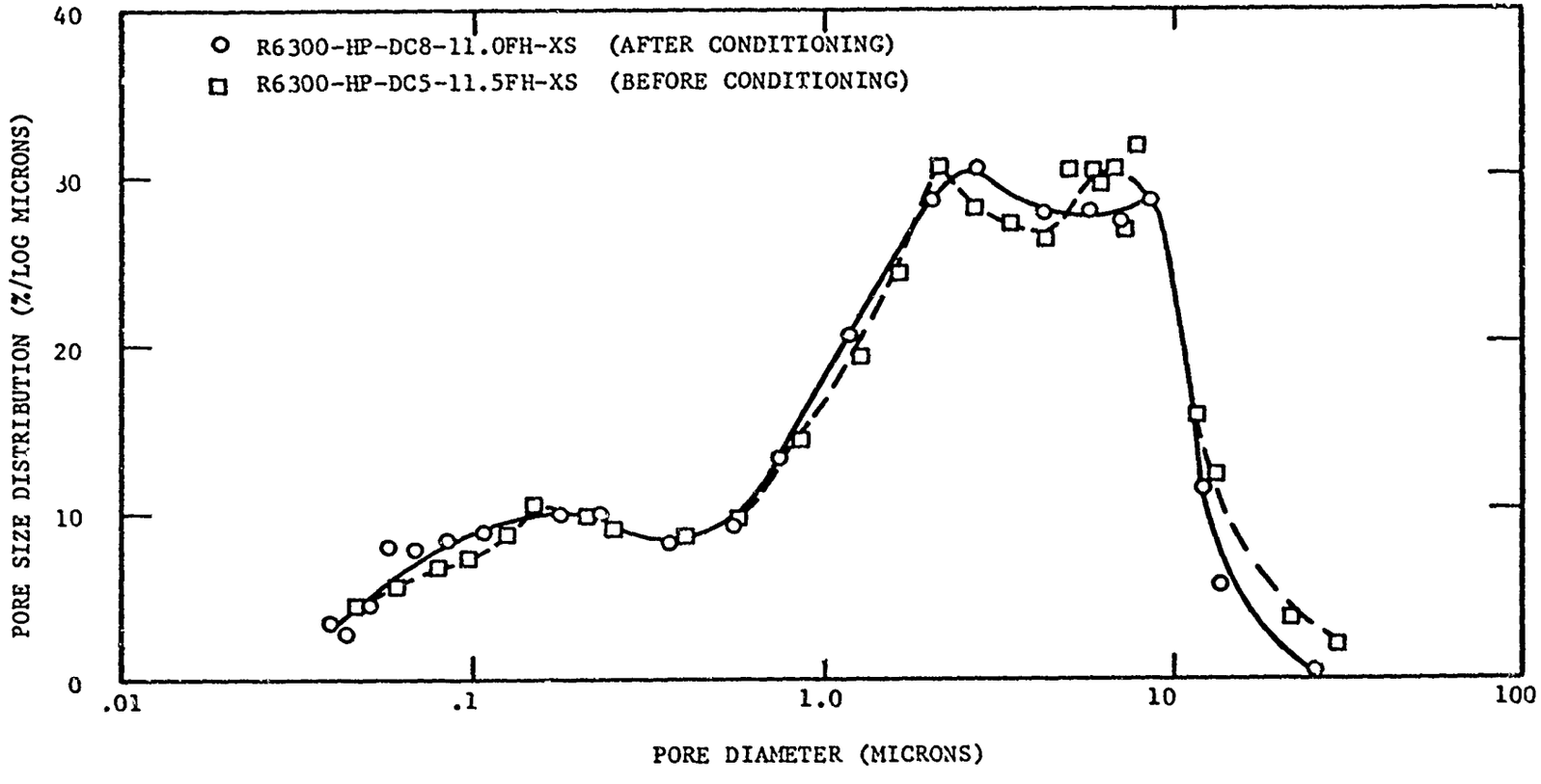

FIGURE 7: PORE SIZE DISTRIBUTION BEFORE AND AFTER CONDITIONING

FIGURE 8: R6300-HP-DC4-0.6FH-XS
AFTER CONDITIONING AT 2875°K
EXTERIOR VIEW

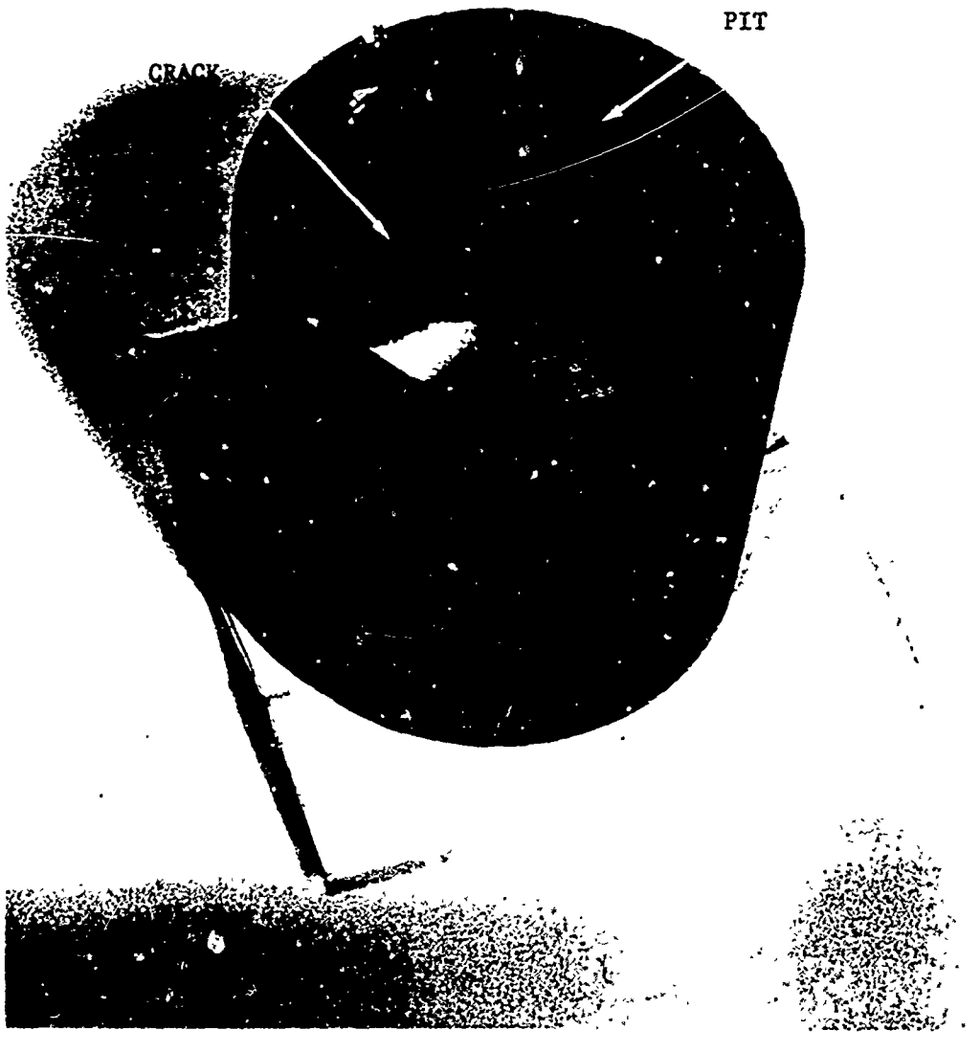

FIGURE 9: R6300-HP-DC4-0.6FH-XS
AFTER CONDITIONING AT 2875°K
INTERIOR VIEW

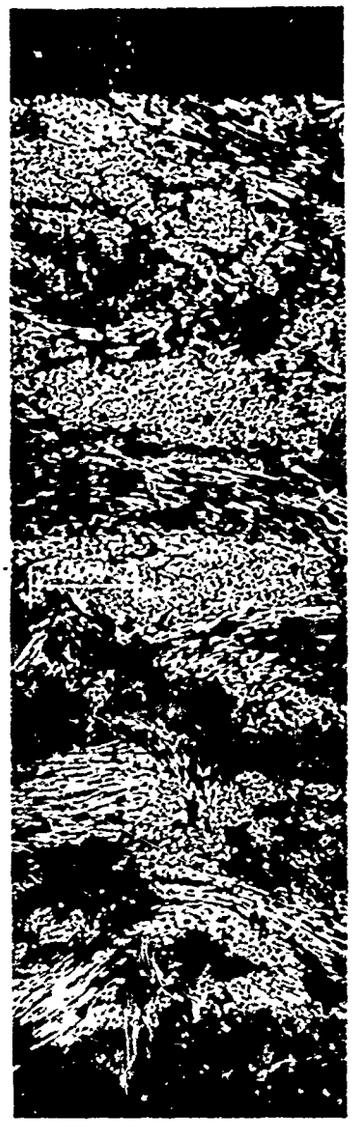

FIGURE 10: PHOTOMICROGRAPH OF R6300-HP-DC8-11.0FH-XS
AFTER CONDITIONING

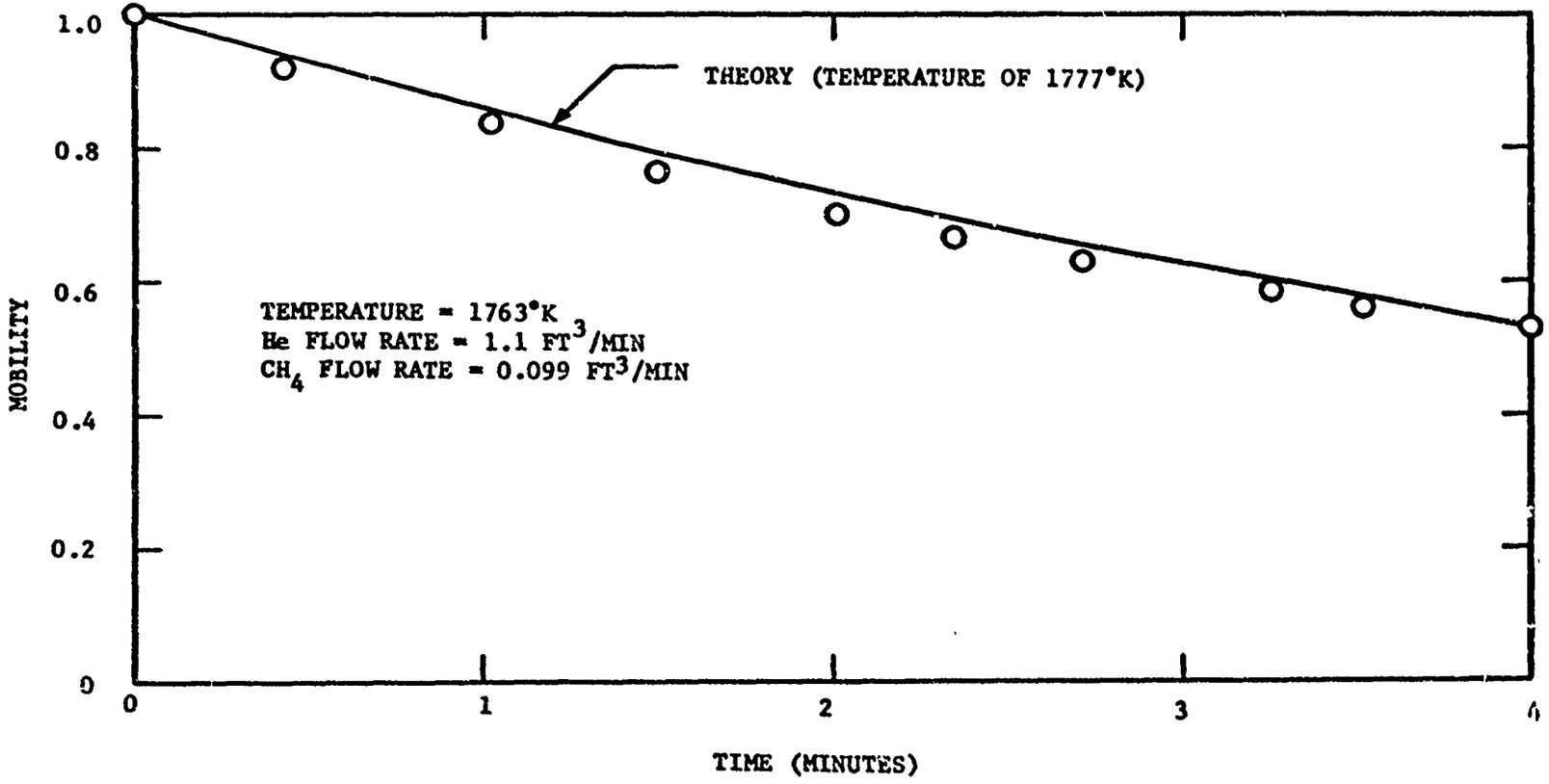

FIGURE 11: COMPARISON OF EXPERIMENTAL AND THEORETICAL MOBILITIES IN PC-60A-1 SAMPLE FOR CARBON DEPOSITION FROM METHANE

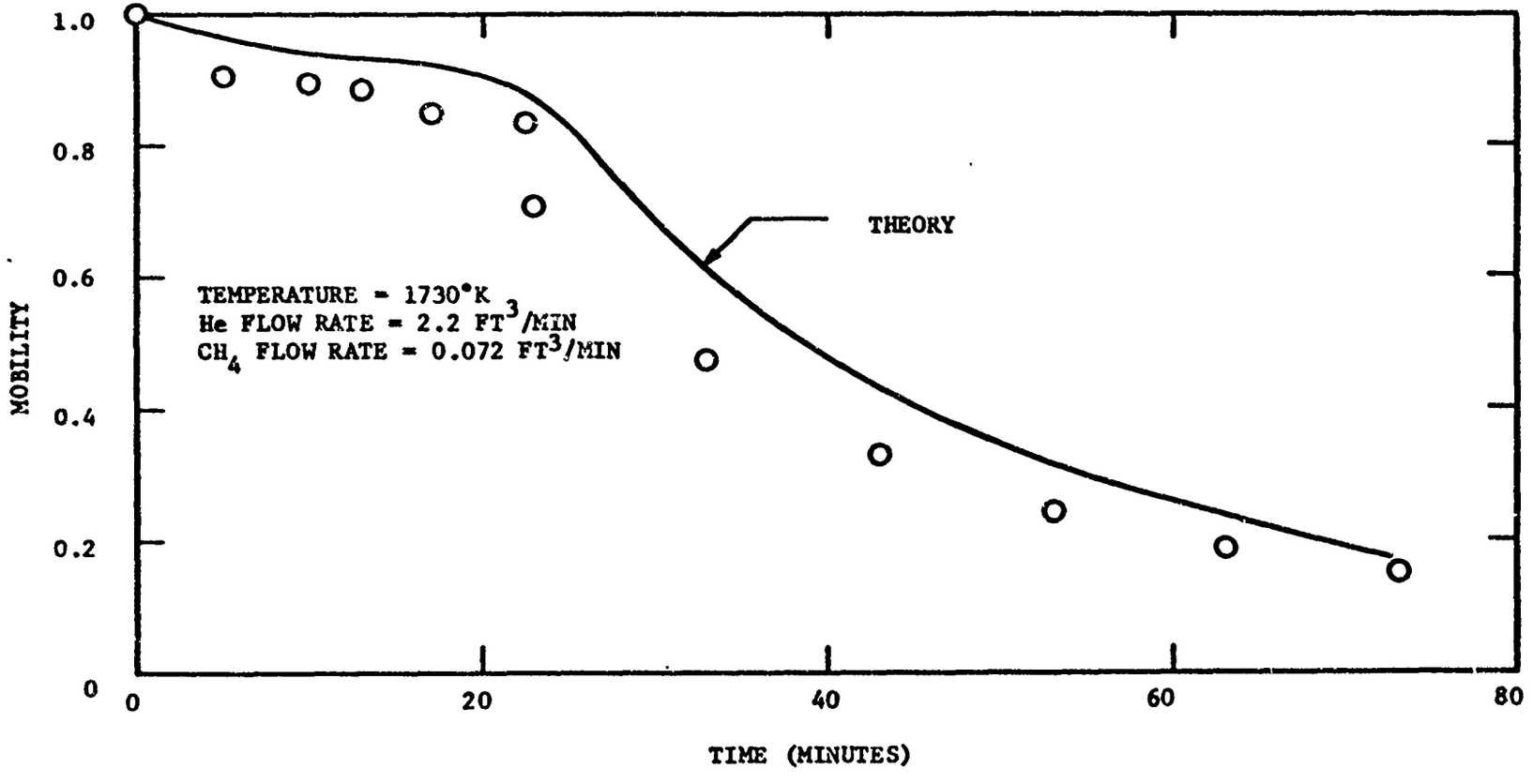

FIGURE 12: COMPARISON OF EXPERIMENTAL AND THEORETICAL MOBILITIES IN PG-25D-3 SAMPLE FOR CARBON DEPOSITION FROM METHANE

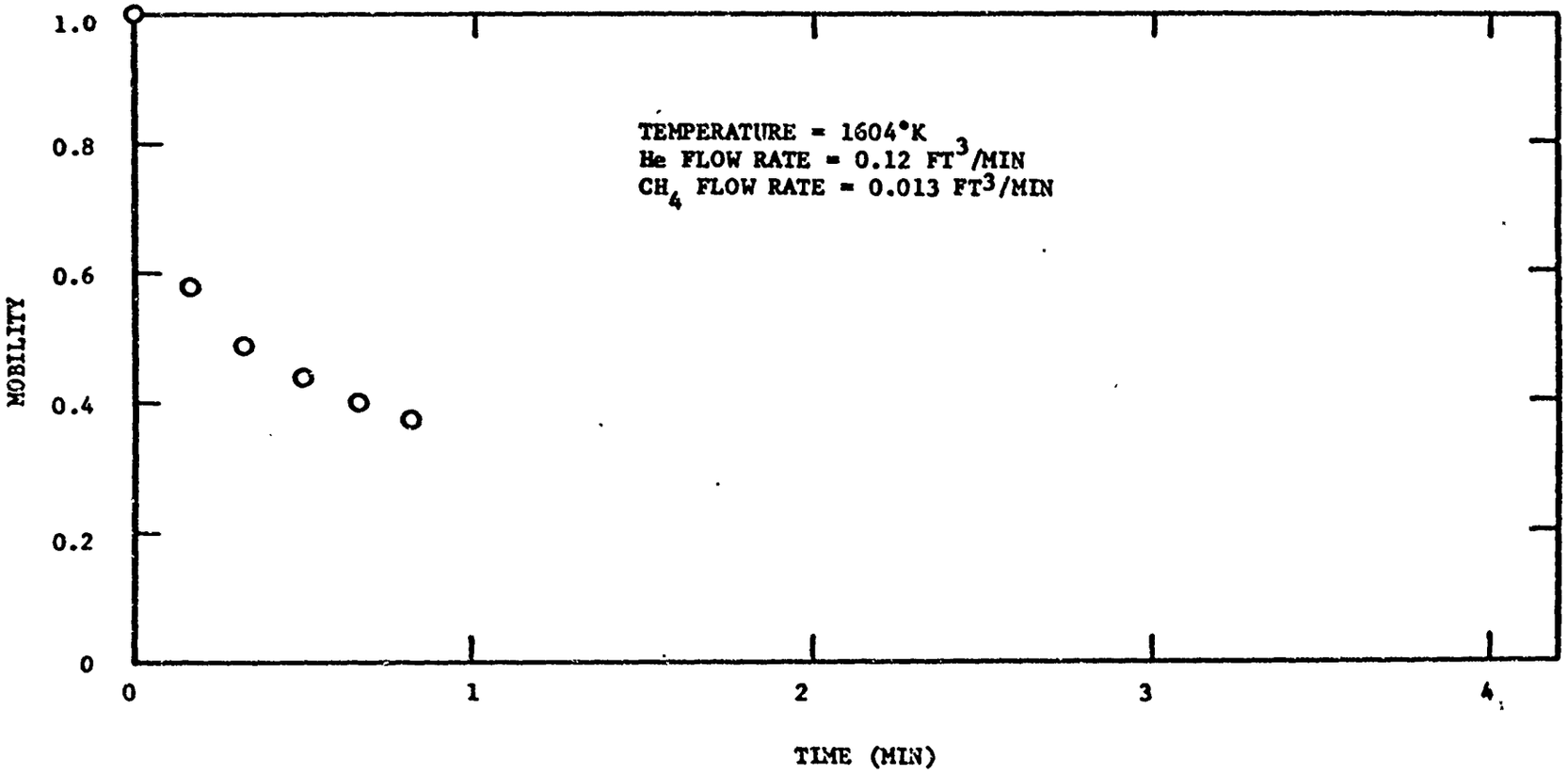

FIGURE 13: EFFECT OF METHANE ON R6300-HP-DC5-0.7FH-XS

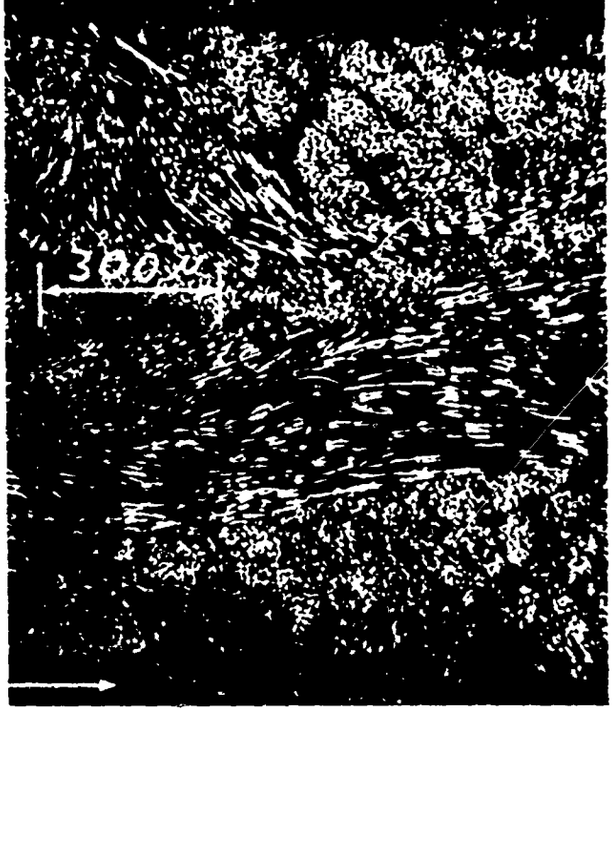

FIGURE 14: PHOTOMICROGRAPH OF R6300-HP-DC5-0.7FH-XS AFTER EXPOSURE TO METHANE

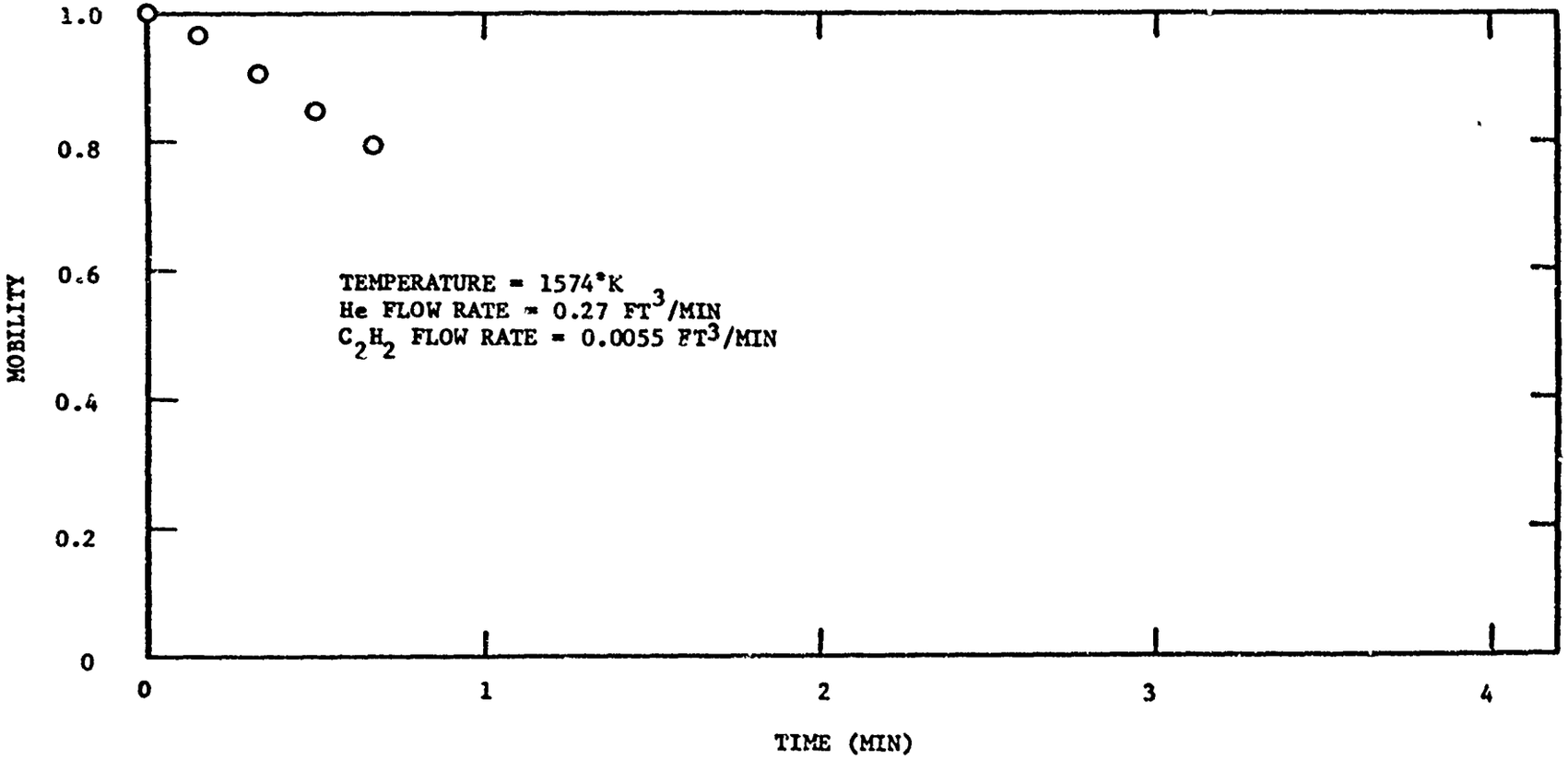

FIGURE 15: EFFECT OF ACETYLENE ON R6300-HP-DC1-8.2FH-XS (MACHINED)

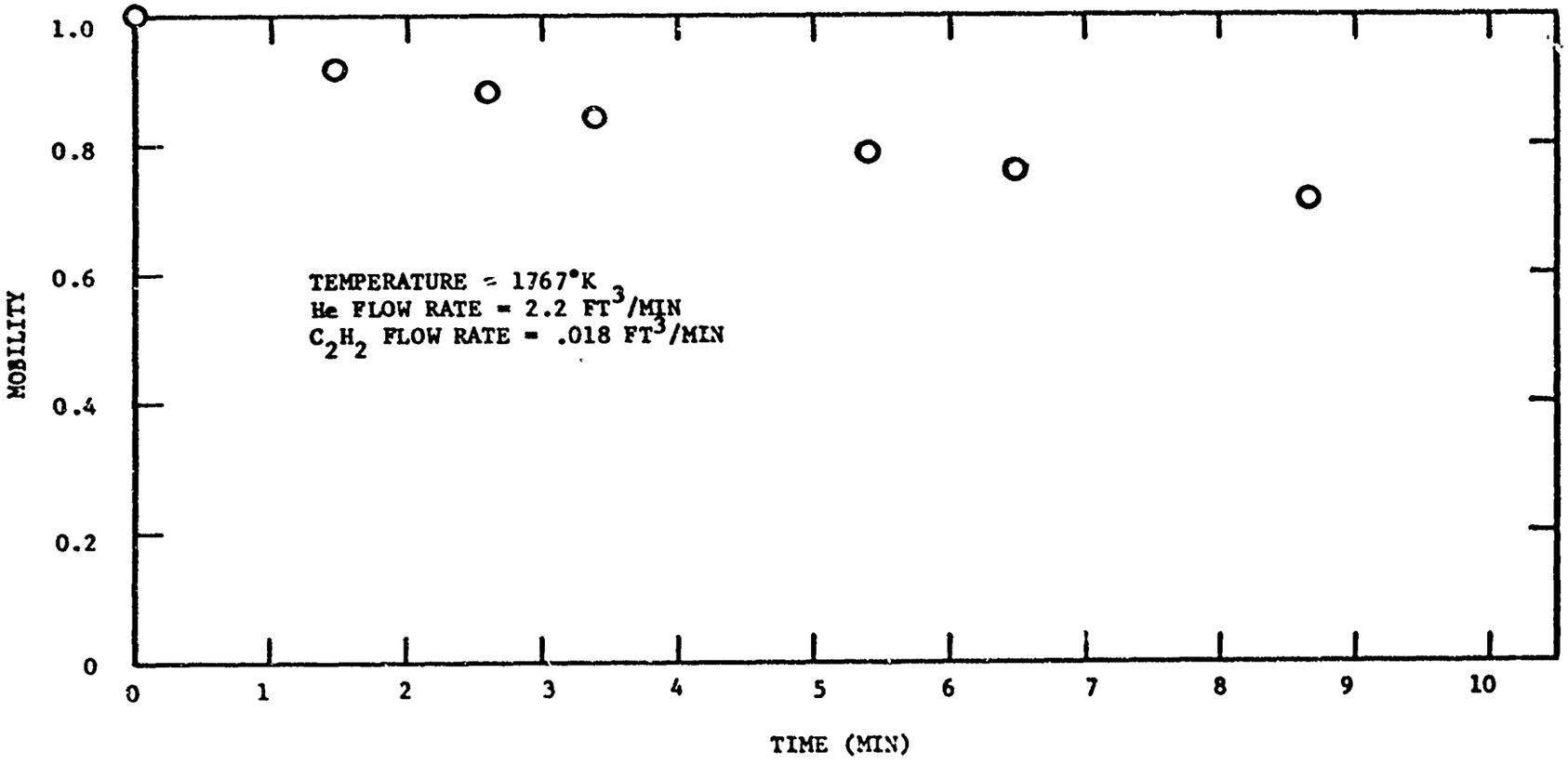

FIGURE 16: EFFECT OF ACETYLENE ON PG-45D-2

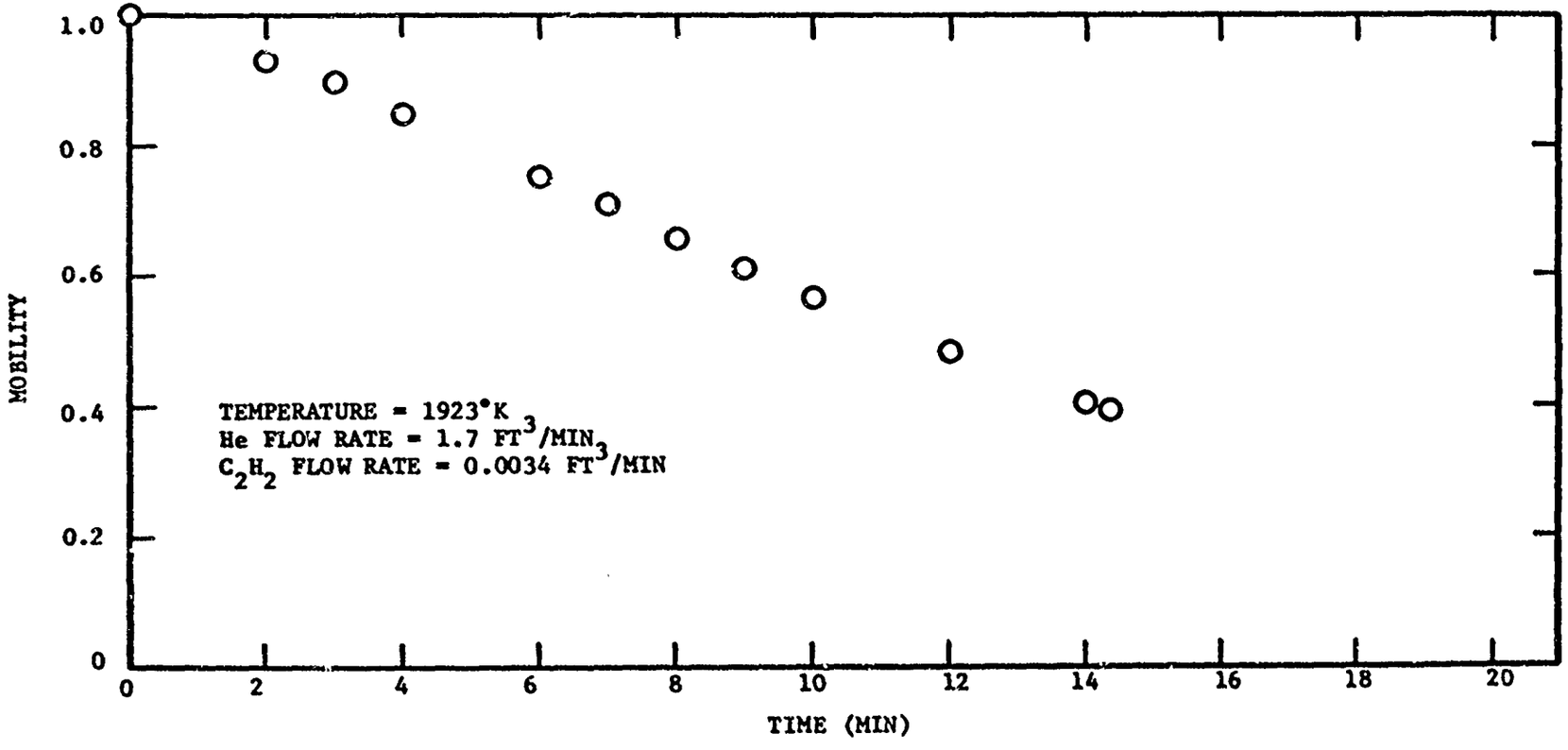

FIGURE 17: EFFECT OF ACETYLENE ON PG-45F-2

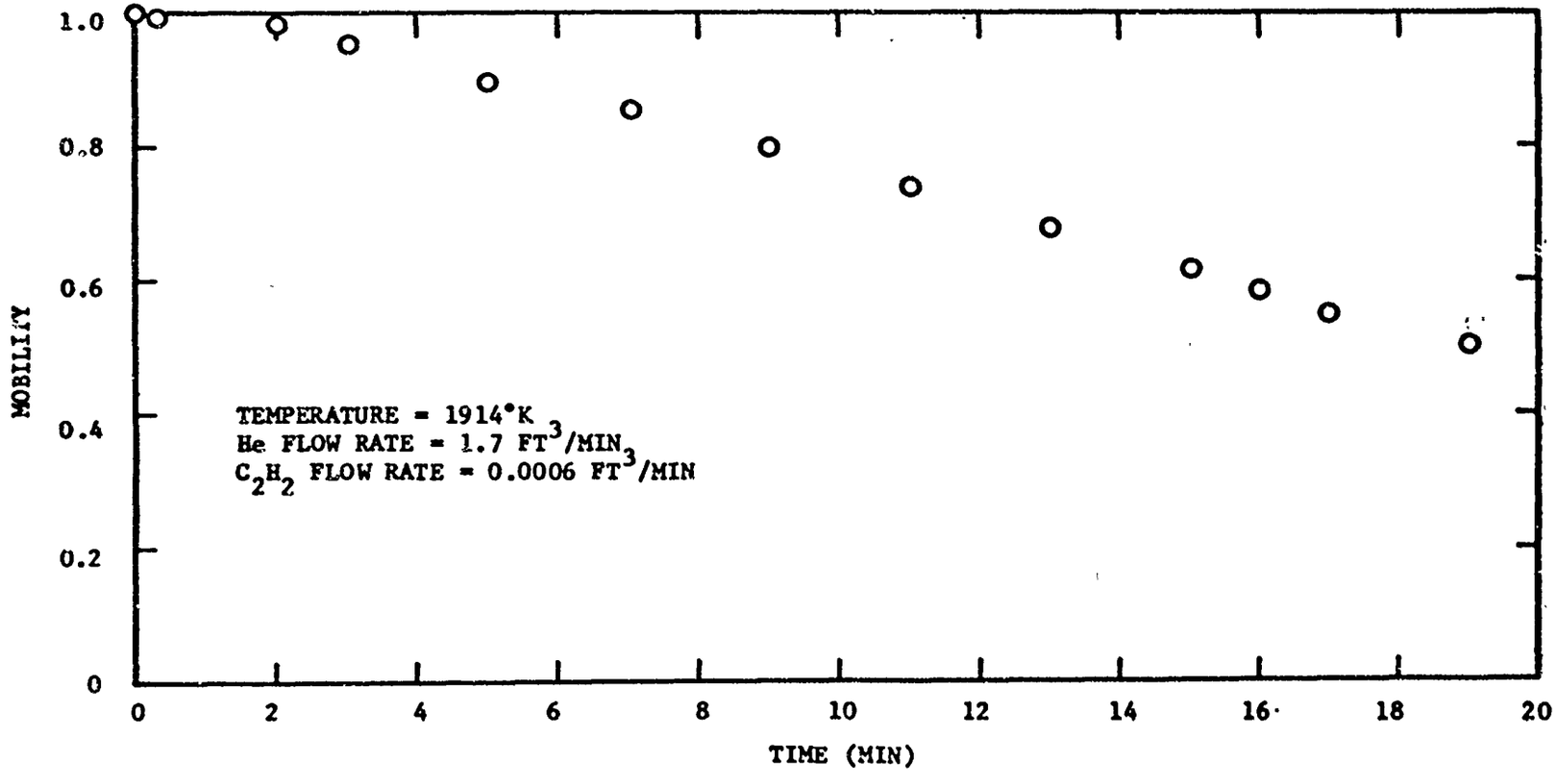

FIGURE 18: EFFECT OF ACETYLENE ON PG-45F-3

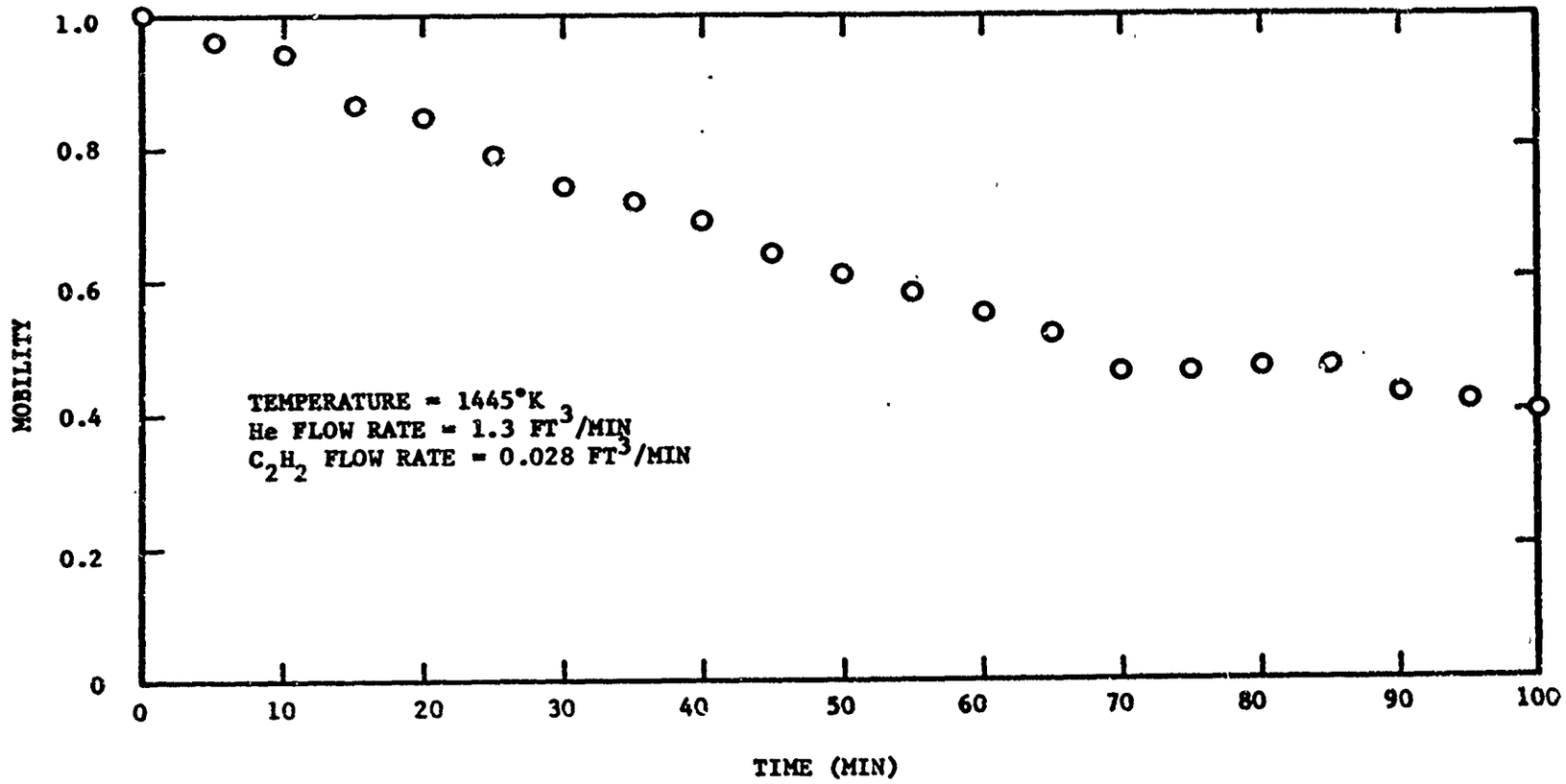

FIGURE 19: EFFECT OF ACETYLENE ON PC-45C-2

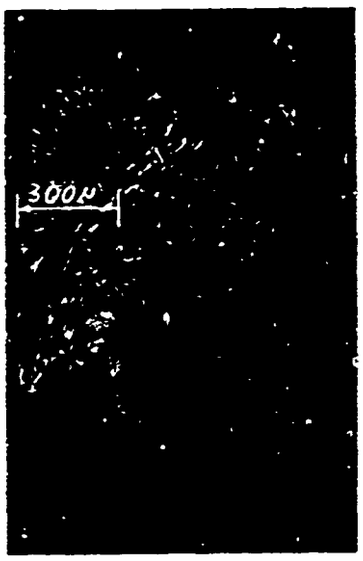

FIGURE 20: PHOTOMICROGRAPH OF R6300-HP-DC1-8.2FH-XS
(MACHINED)
AFTER EXPOSURE TO ACETYLENE

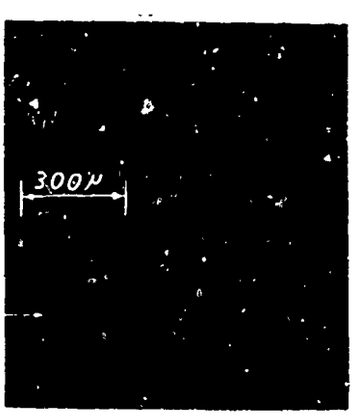

FIGURE 21: PHOTOMICROGRAPH OF R6300-HP-DC1-8.2FH-XS
(MACHINED)
AFTER EXPOSURE TO ACETYLENE

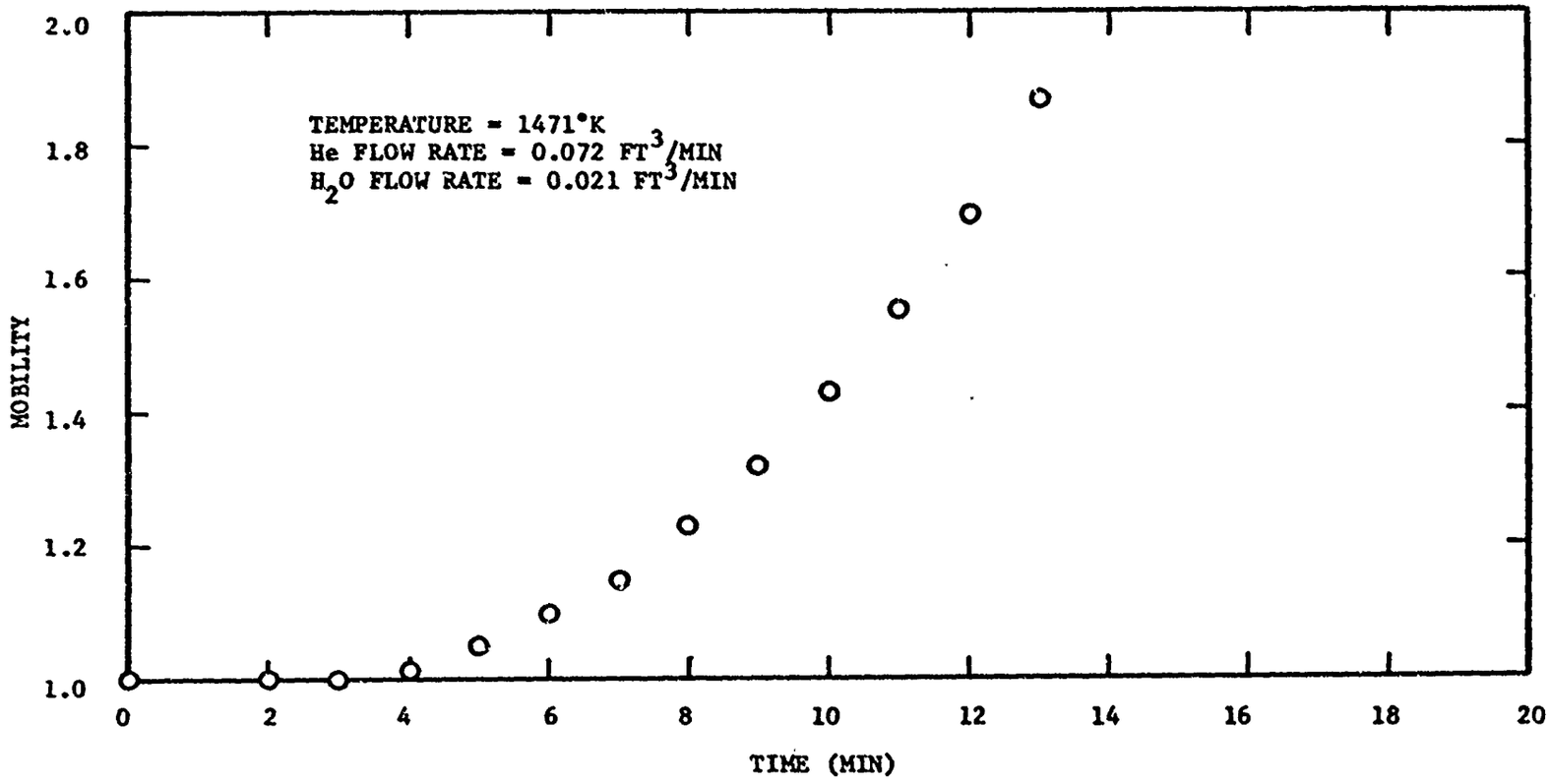

FIGURE 22: EFFECT OF WATER ON R6300-HP-DC3-1.75FH-XS

FIGURE 23: PHOTOMICROGRAPH OF R6300-HP-DC3-1.75FH-XS
AFTER EXPOSURE TO WATER

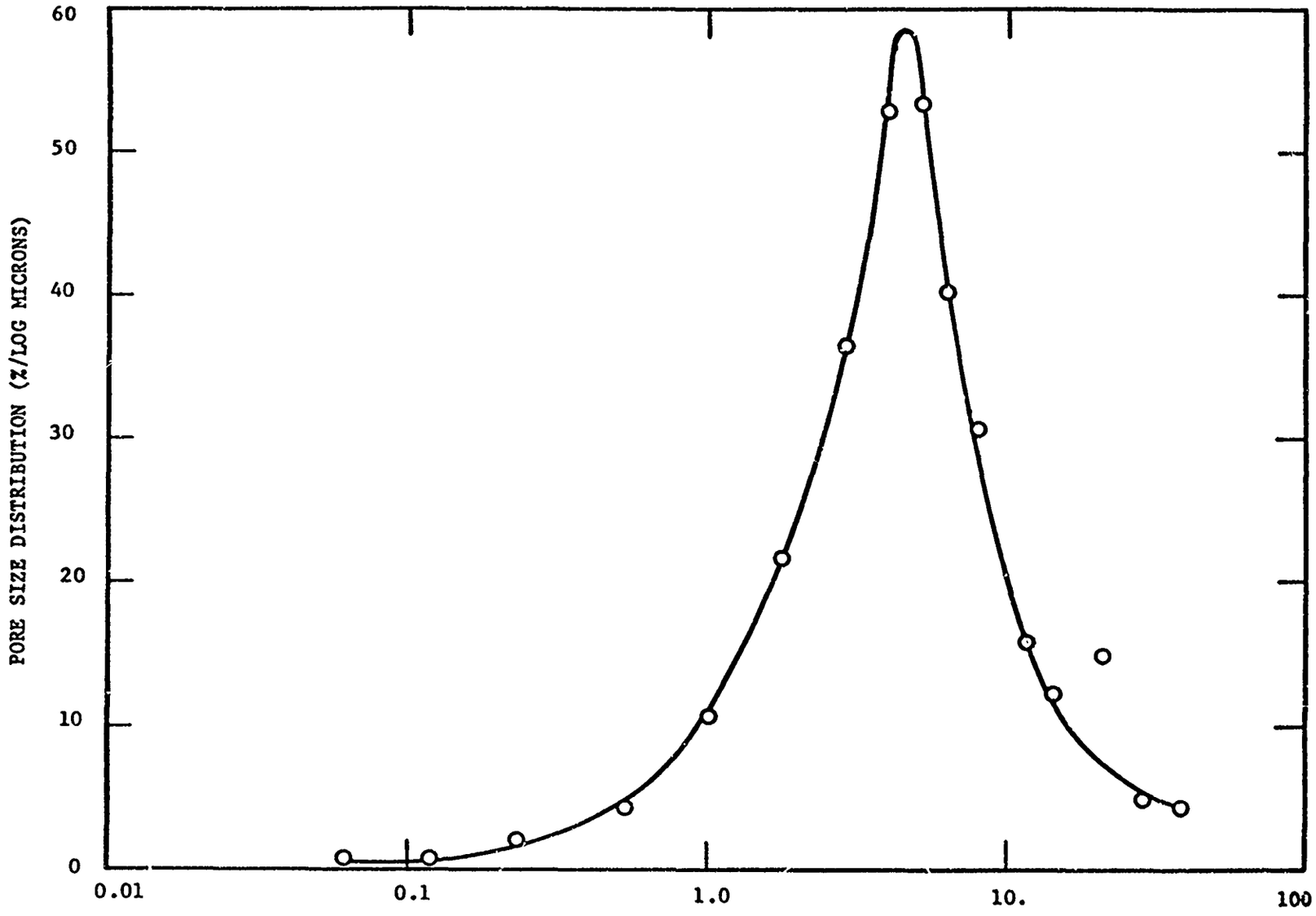

FIGURE 24: PORE SIZE DISTRIBUTION OF R6300-HP-DC3-1.75FH-XS AFTER EXPOSURE TO WATER

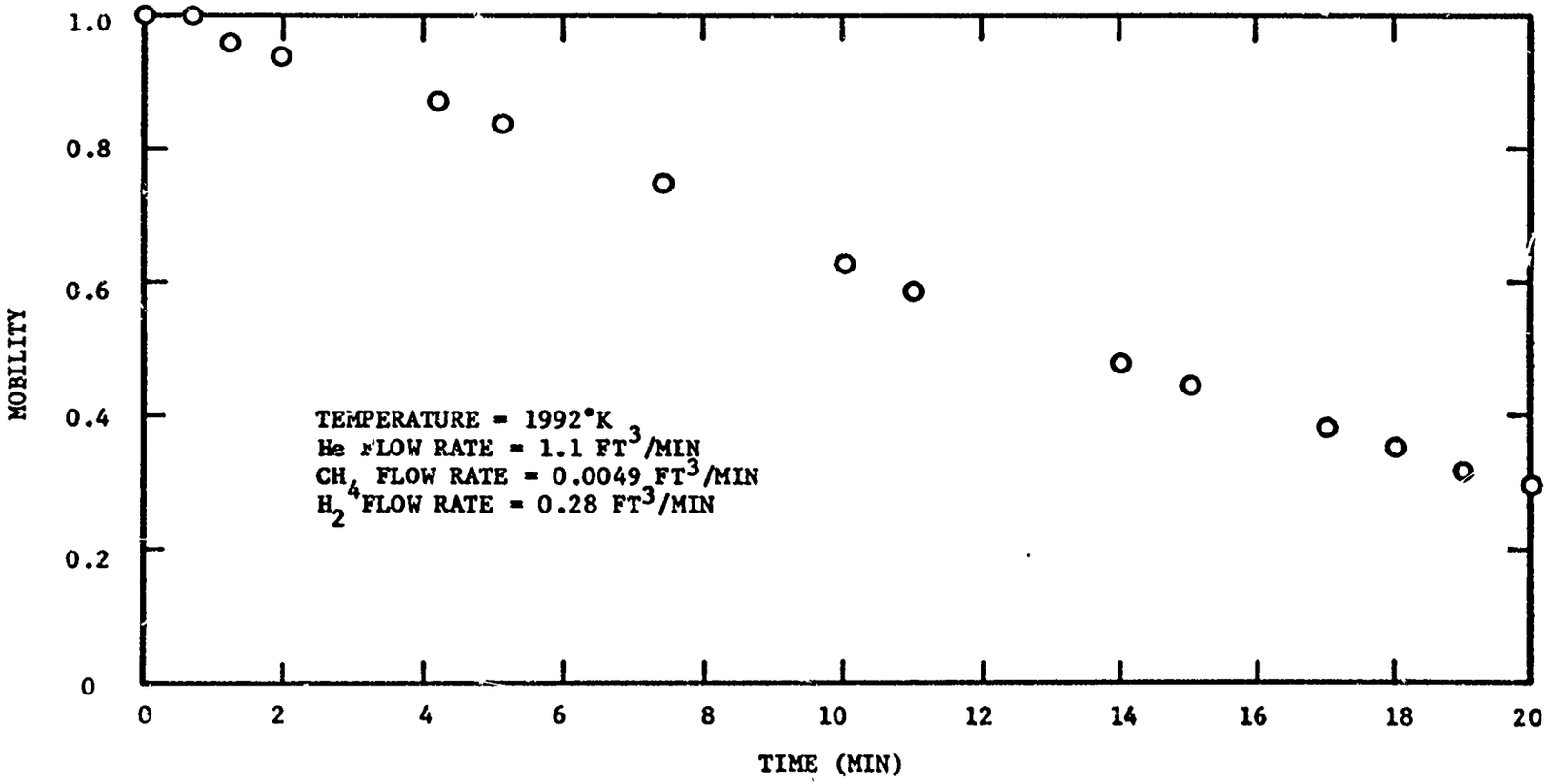

FIGURE 25: EFFECT OF METHANE AND HYDROGEN ON PG-45G-1

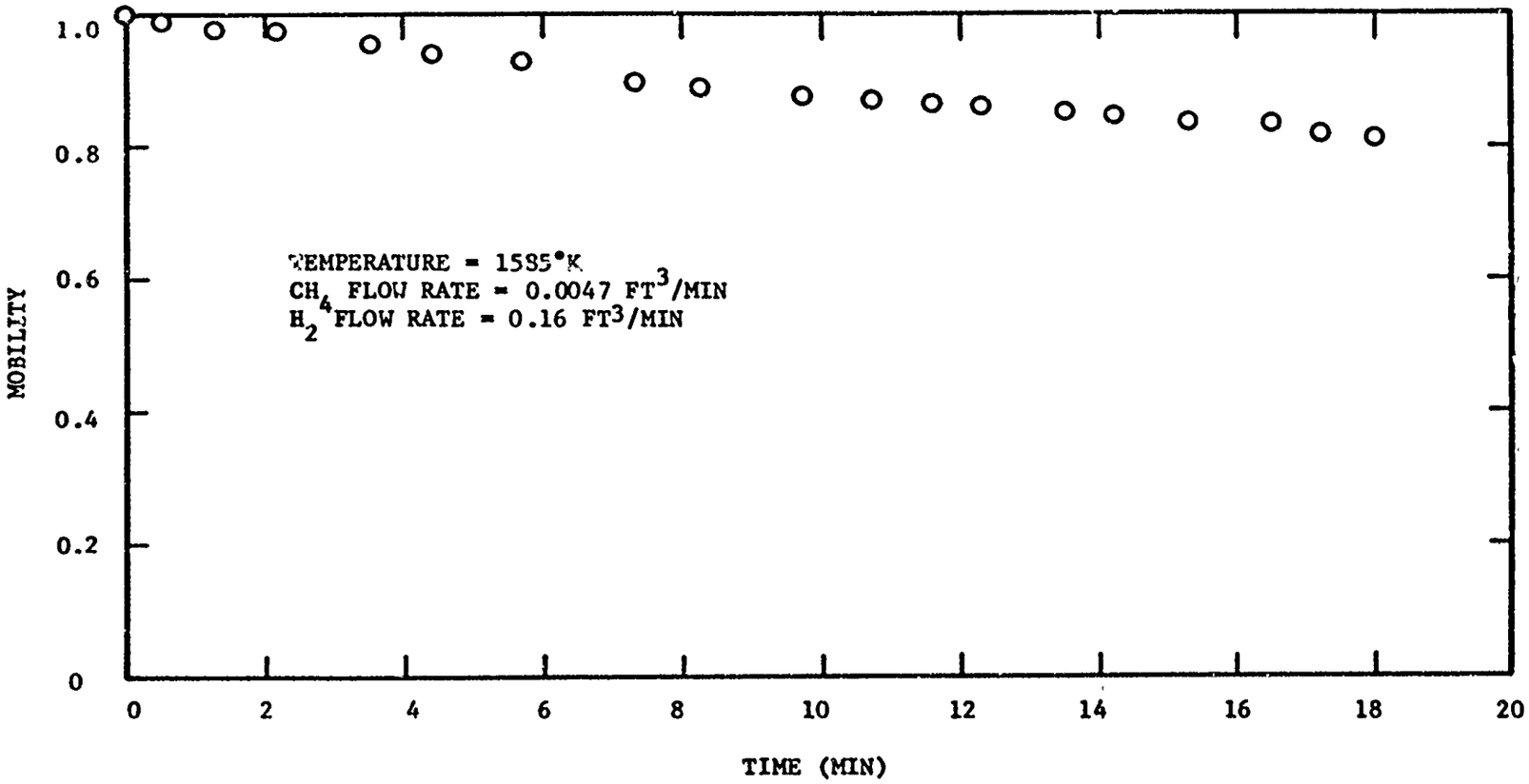

FIGURE 26: EFFECT OF METHANE AND HYDROGEN ON R6300-HP-DC5-3.55-FH-XS

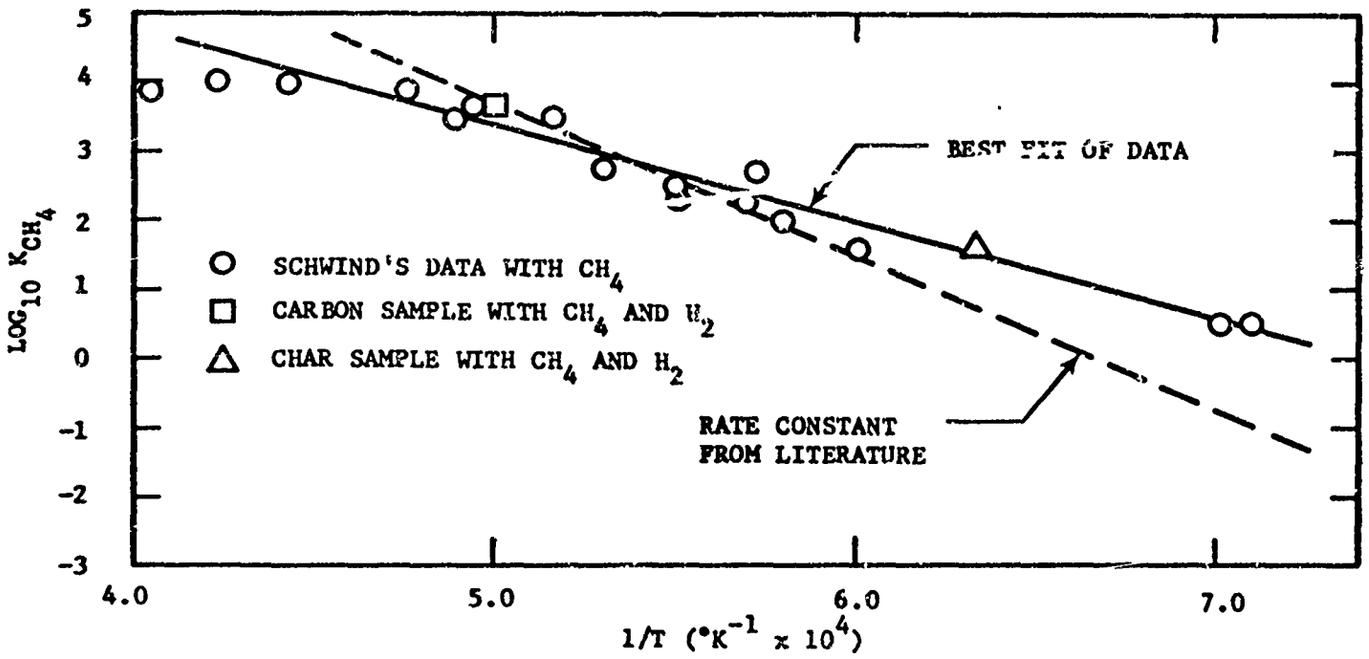

FIGURE 27: ARRHENIUS RATE CONSTANT NEEDED TO FIT SCHWIND'S EXPERIMENTAL METHANE DATA

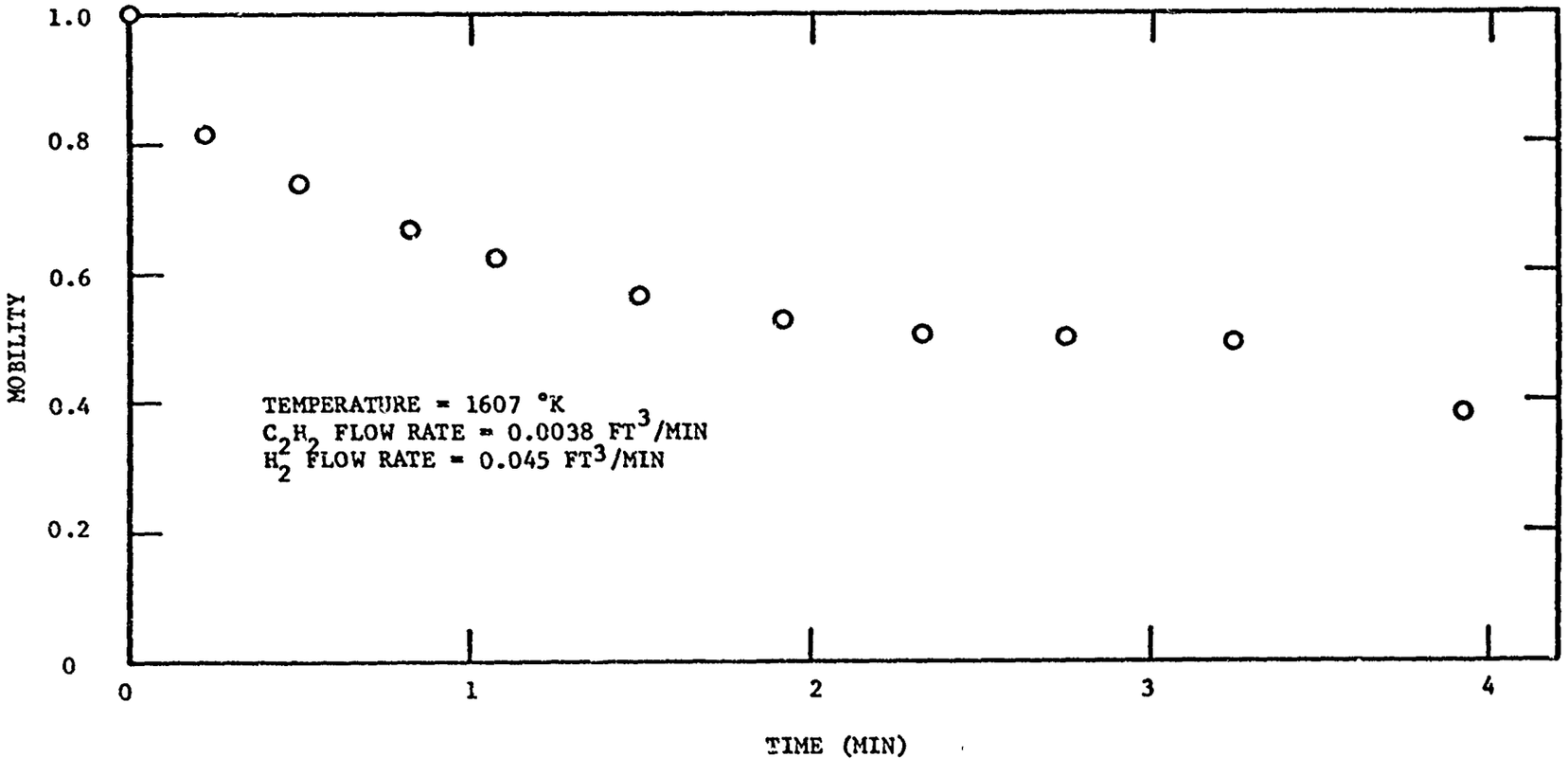

FIGURE 28: EFFECT OF ACETYLENE AND HYDROGEN ON R6300-HP-DC5-4.6FH-XS

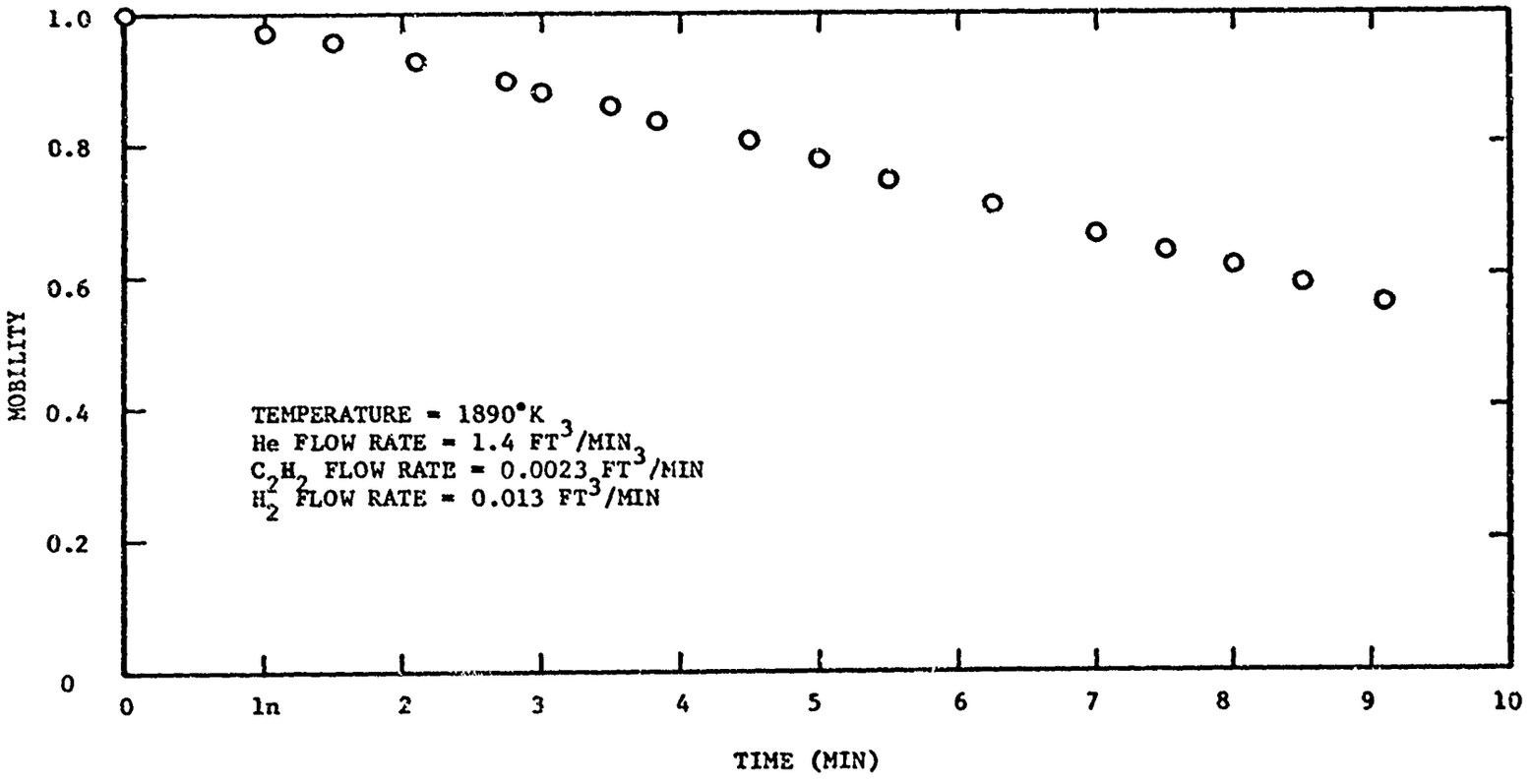

FIGURE 29: EFFECT OF ACETYLENE AND HYDROGEN ON PC-45-G

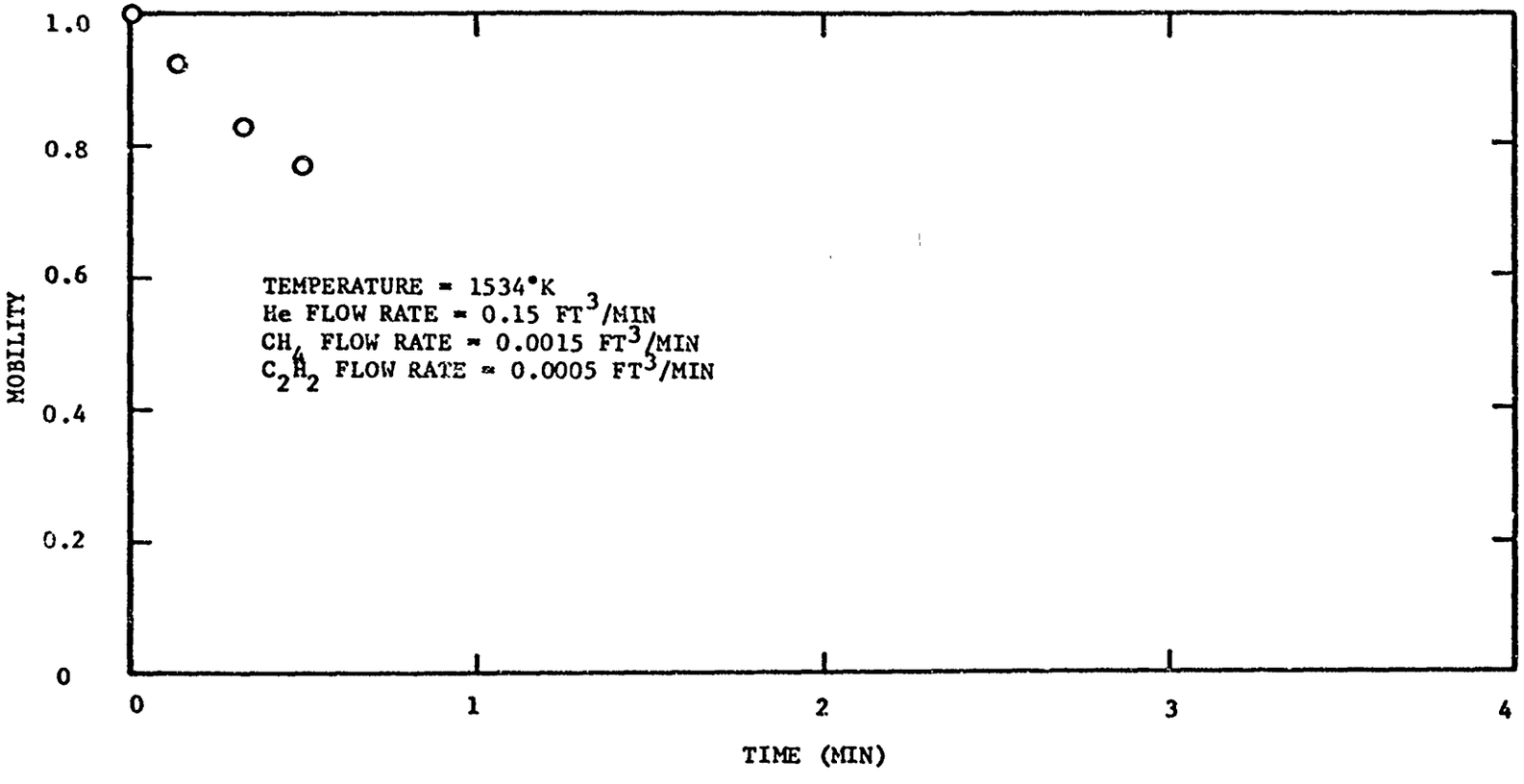

FIGURE 30: EFFECT OF METHANE AND ACETYLENE ON R6300-HP-DC8-1.7FH-XS

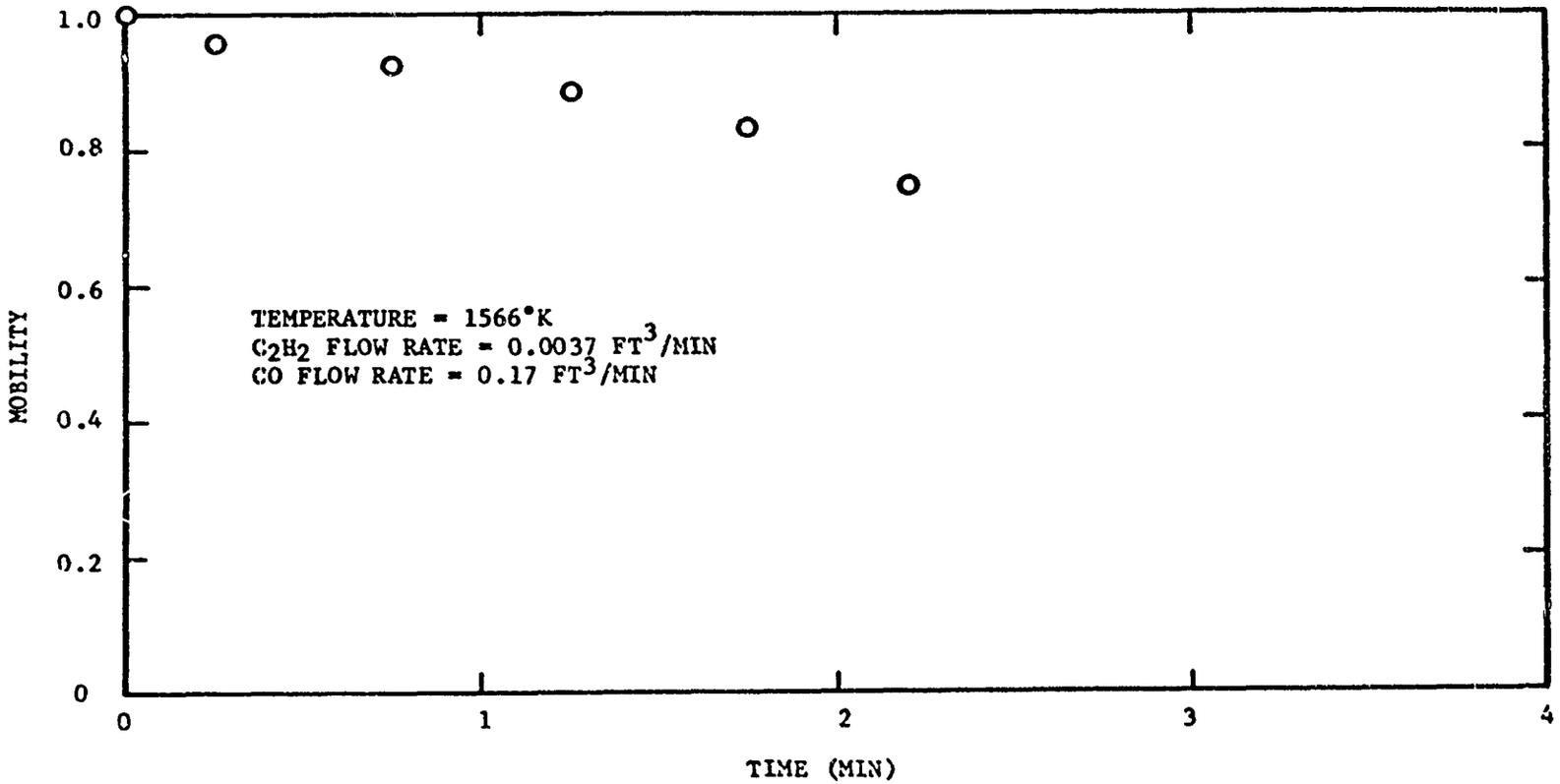

FIGURE 31: EFFECT OF ACETYLENE AND CARBON MONOXIDE ON R6300-HP-DC5-8.4FH-XS

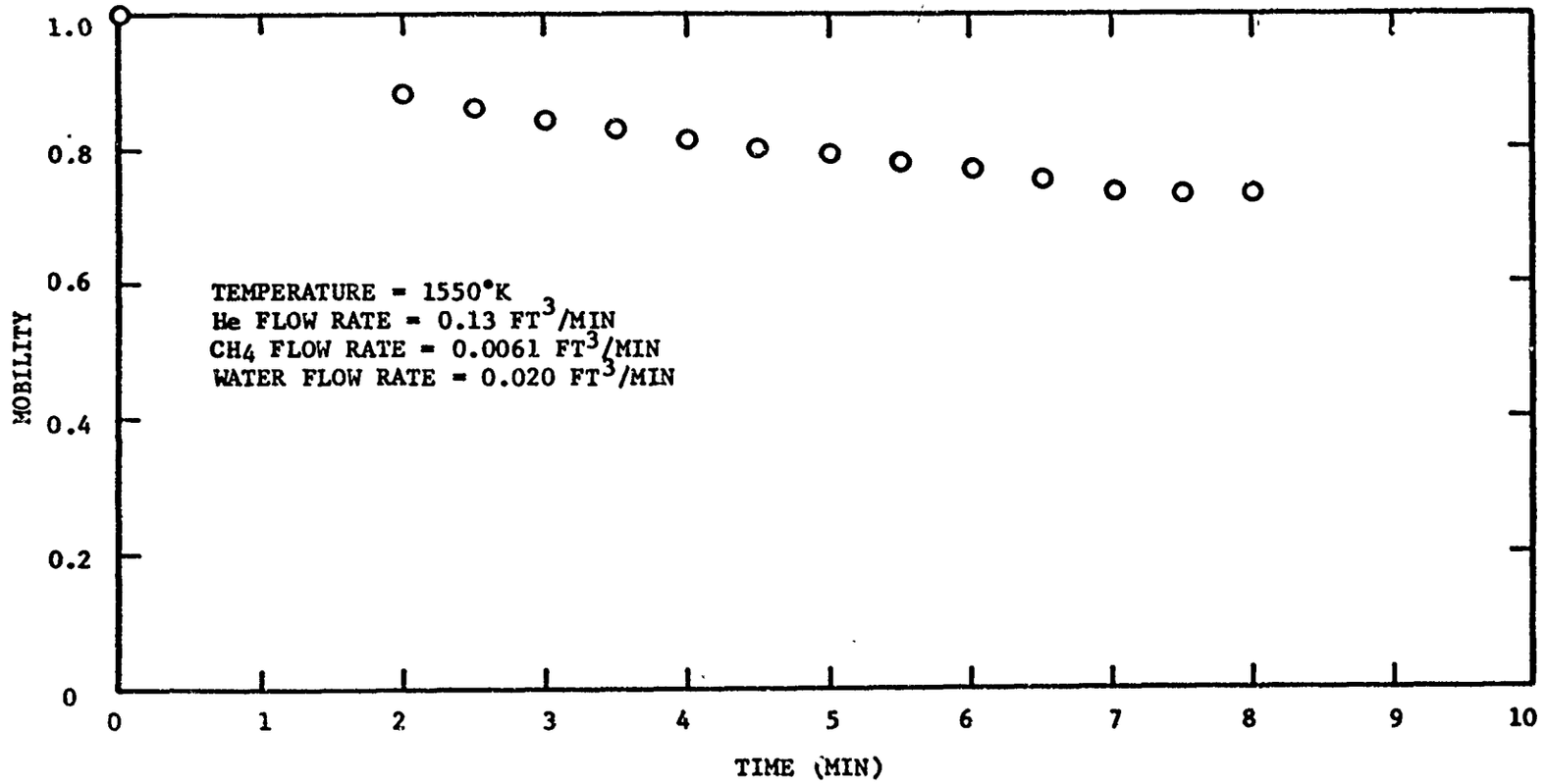

FIGURE 32: EFFECT OF METHANE AND WATER ON R6300-HP-DC7-1.35FH-XS

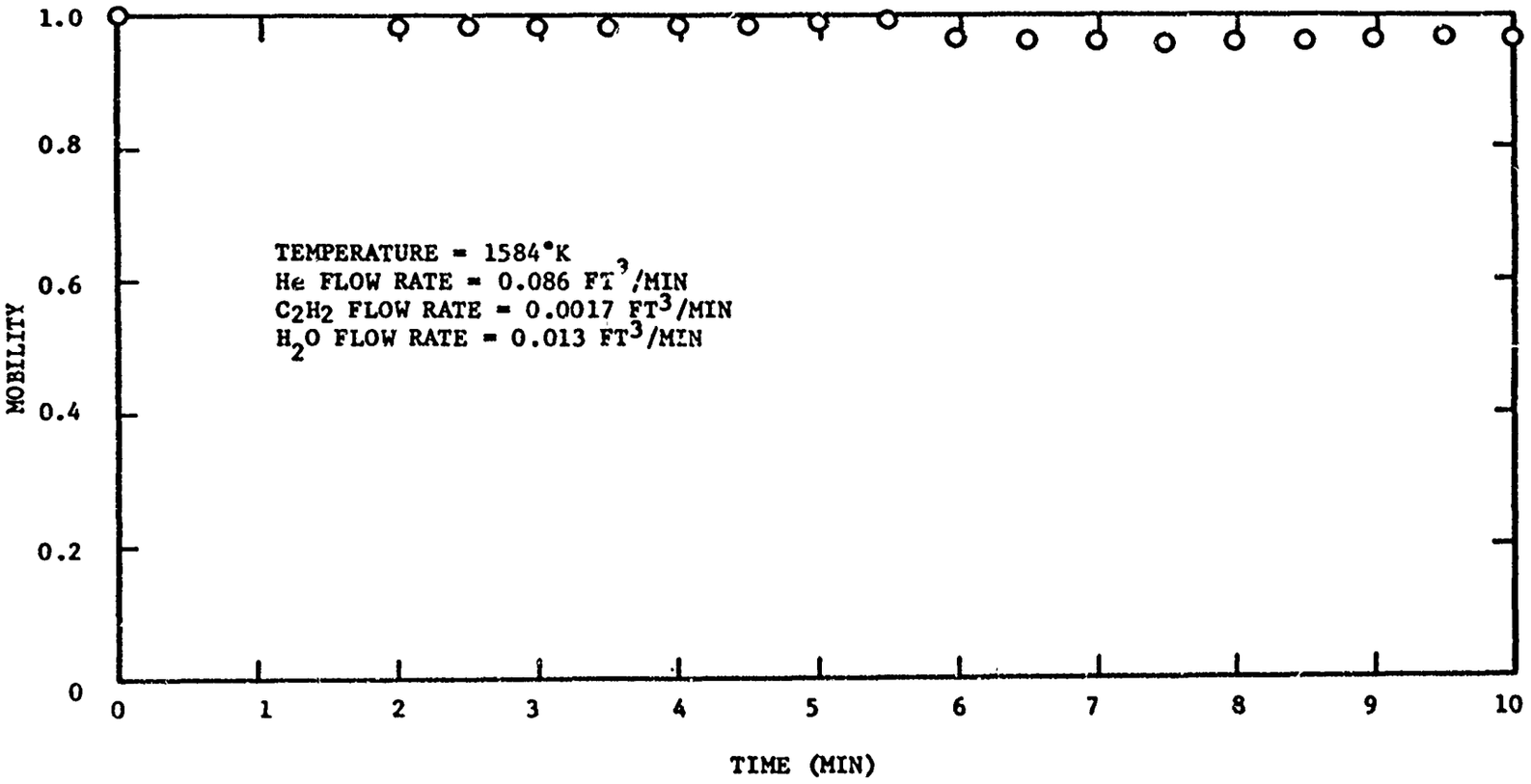

FIGURE 33: EFFECT OF ACETYLENE AND WATER ON R6300-HP-DC8-2.8FH-XS

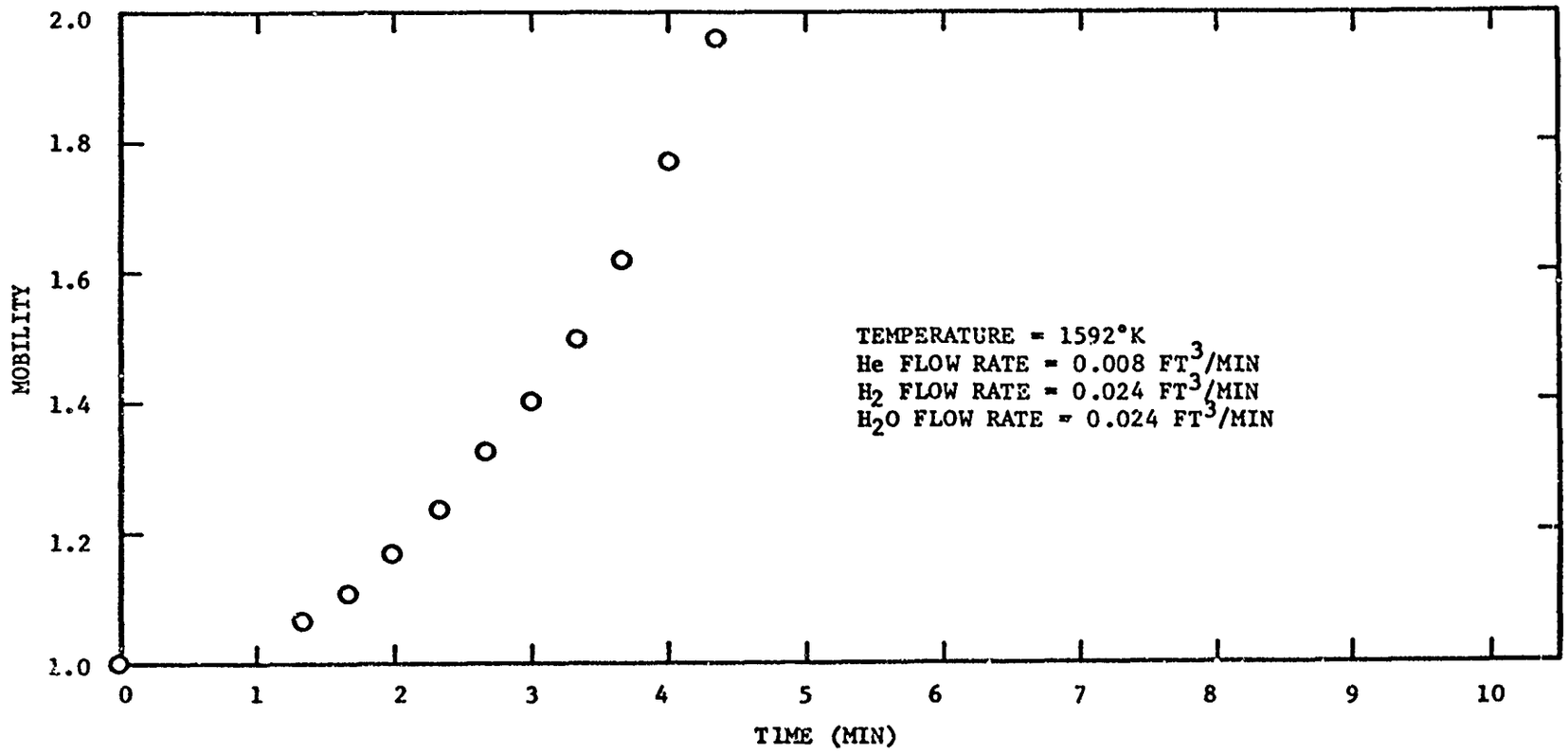

FIGURE 34: EFFECT OF HYDROGEN AND WATER ON R6300-HP-DC8-8.8FH-XS

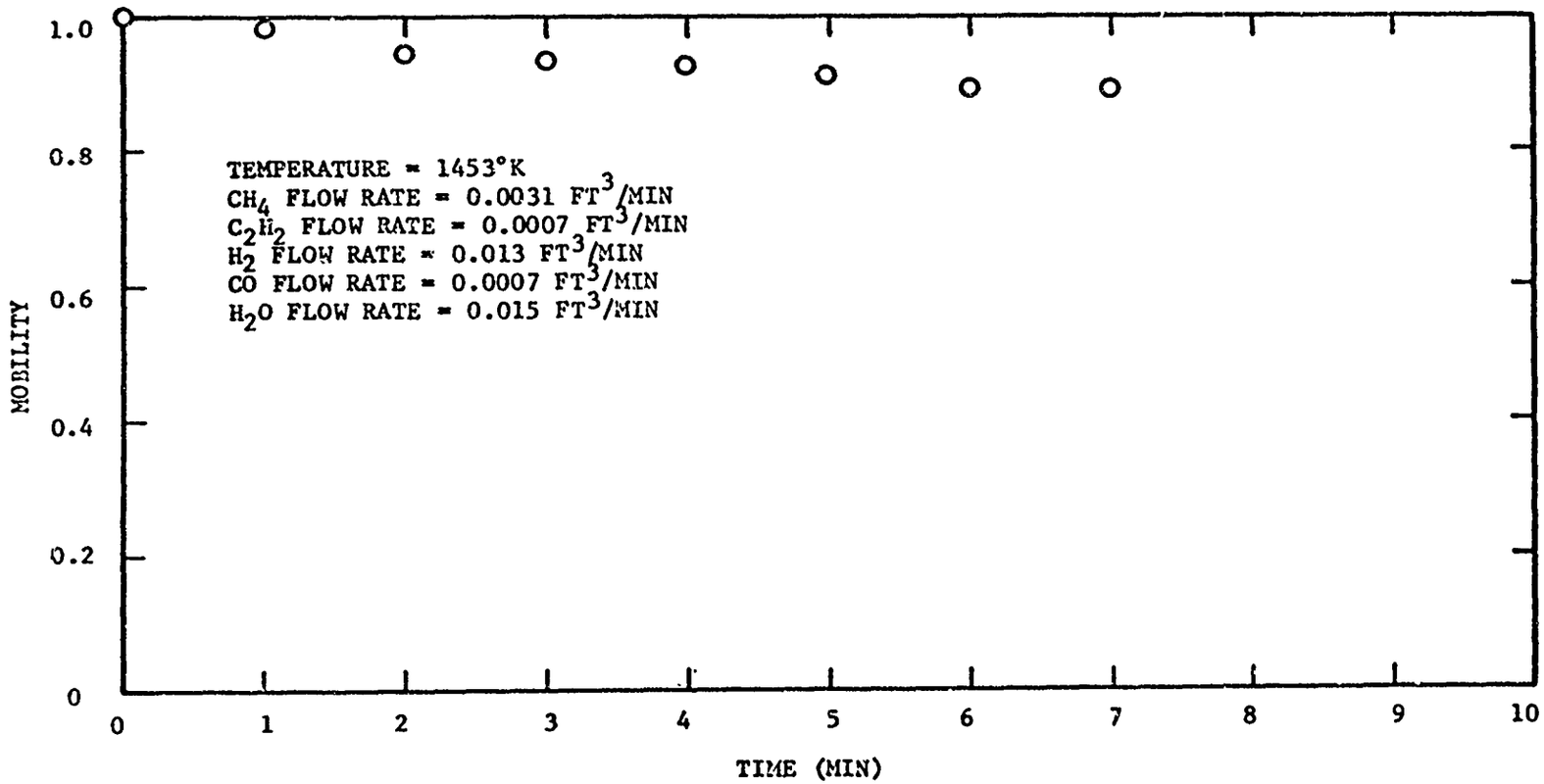

FIGURE 35: EFFECT OF METHANE, ACETYLENE, HYDROGEN, CARBON MONOXIDE, AND WATER ON R6300-HP-DC8-7.7FH-XS

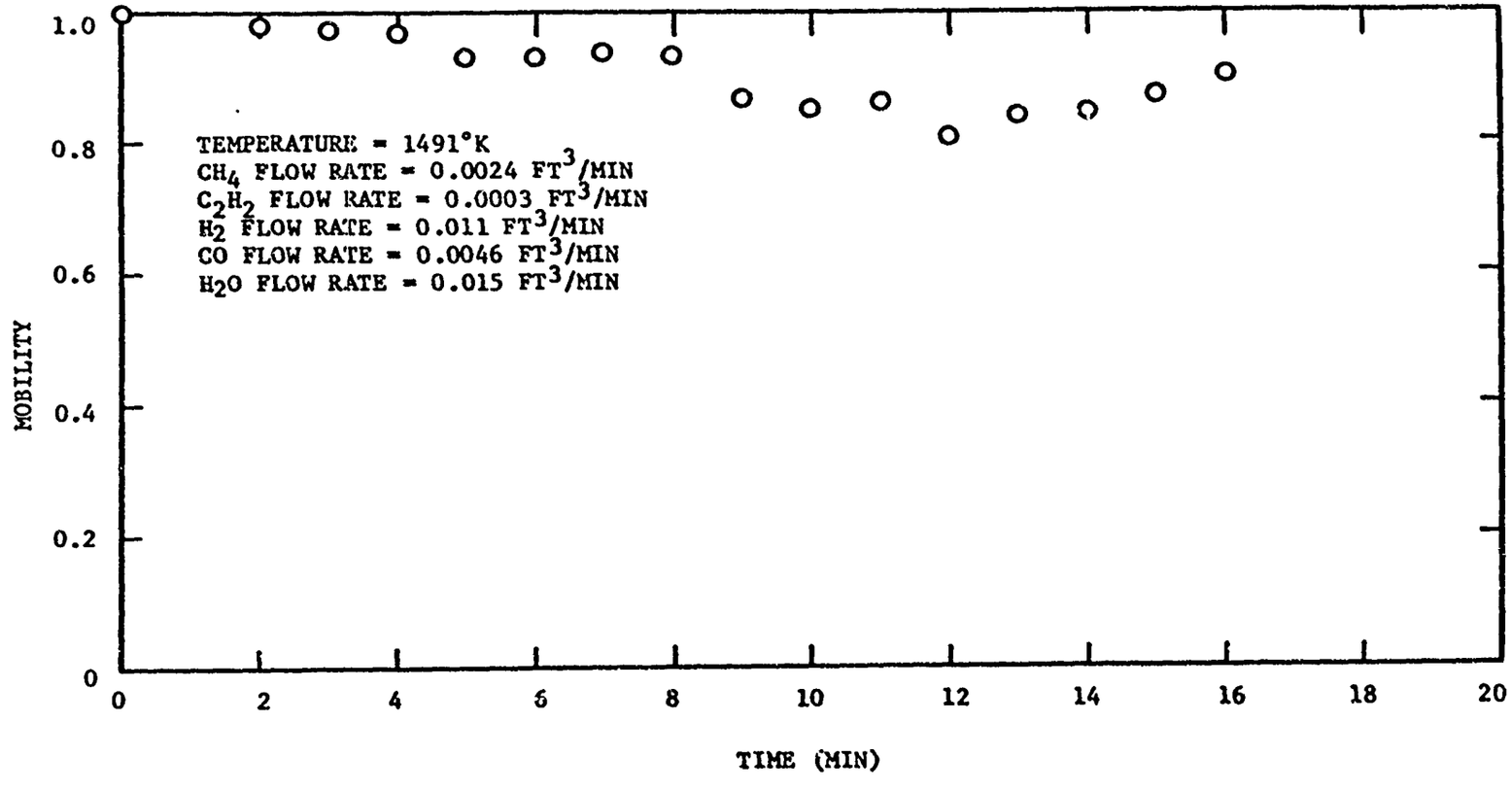

FIGURE 36: EFFECT OF METHANE, ACETYLENE, HYDROGEN, CARBON MONOXIDE, AND WATER ON R6300-HP-DC8-9.9FH-XS

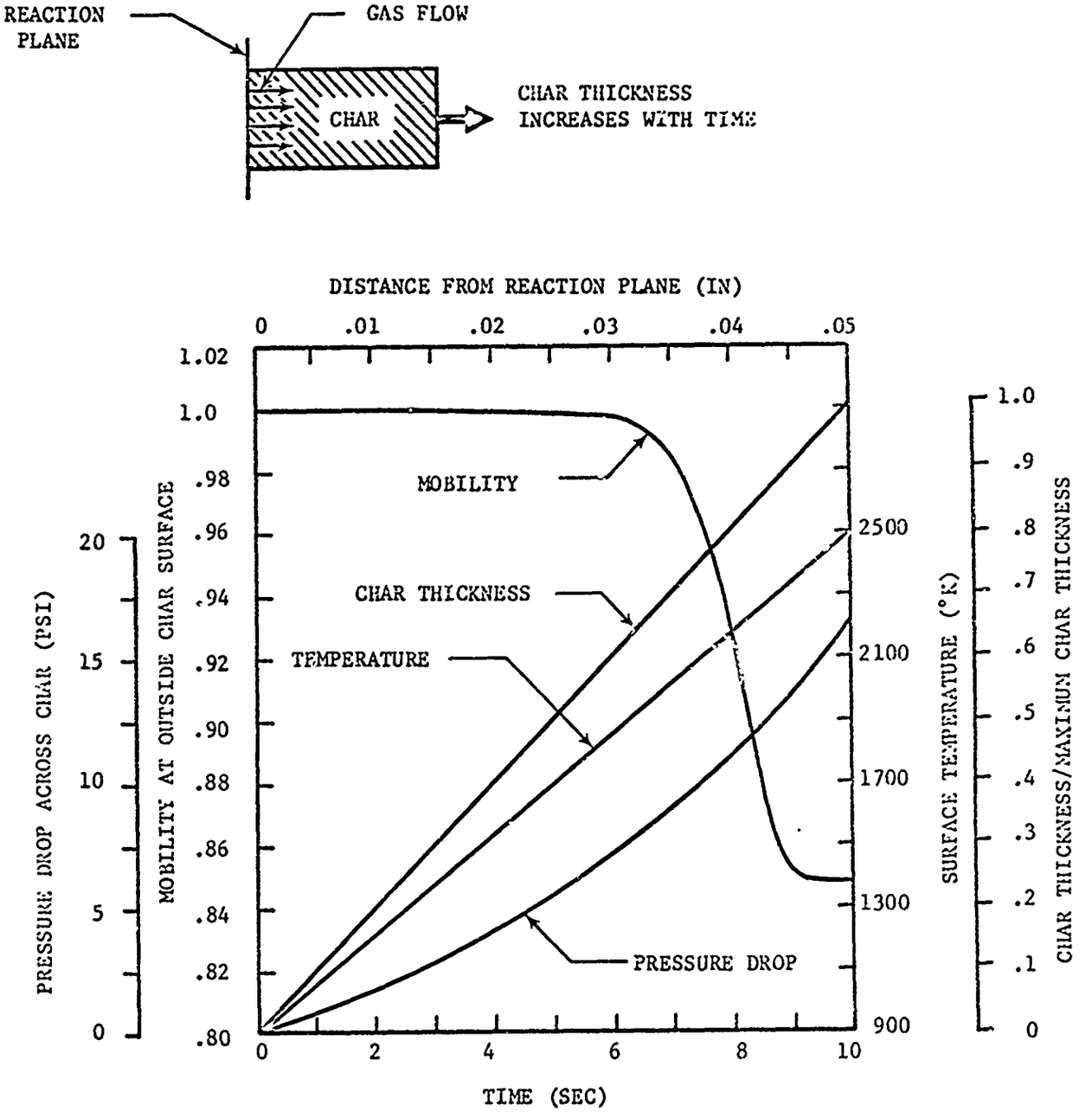

FIGURE 37: CHAR GROWTH SIMULATION

X

APPENDIX: CHAR GROWTH SIMULATION PROGRAM

10.1 CARBON DEPOSITION EQUATIONS

The char simulation program is based on the solution of the equations predicting the change in permeability due to carbon deposition from methane. These equations are listed below and were derived in the previous report (BSD TR 66-385).

$$\frac{\partial M}{\partial t_y} = \frac{C_2 \frac{P}{P_1} \exp\left[C_4 \int_o^Y \frac{M^{1/2}(r_1+y)}{Q}\, dy\right]}{1 + f_1\left[1-\exp\left(C_4 \int_o^Y \frac{M^{1/2}(r_1+y)}{Q}\, dy\right)\right]} \tag{10.1}$$

$$Q = \frac{RT}{p}\left[n_{T_1} + n_{(CH_4)_1} - n_{(CH_4)}\right] \tag{10.2}$$

$$P = \left(P_2^2 - \frac{RT}{\pi L K_o} \int_{Y_2}^{Y} \frac{\mu\left[n_{T_1} + n_{(CH_4)_1} - n_{(CH_4)}\right]}{(r_1 + y)\, M}\, dy\right)^{1/2} \tag{10.3}$$

$$n_{(CH_4)} = n_{(CH_4)_1} \exp\left[C_4 \int_o^Y \frac{M^{1/2}(r_1 + y)}{Q}\, dy\right] \tag{10.4}$$

where

$$C_2 = -\frac{2k_{(CH_4)}\,(M.W.)_c\, f_1 P_1}{RT\rho_d} \tag{10.5}$$

$$C_4 = -2k_{(CH_4)}\,\pi L\varepsilon_o \qquad (10.6)$$

The program solves these equations for a linear char growth rate, a linear temperature profile, and a constant methane and inert gas flow rate at a plane where the gas enters the char for a cylindrical char. A simplified flow chart showing the calculation procedure is found on page 82. The input variables are listed on page 83. The program was written in Fortran IV for use on an IBM 360 computer operating with a RACS system.

10.2 COMPUTER PROGRAM NOMENCLATURE

The following subroutines and function programs were used in the char simulation program.

Function SUMN(I, IM)--calculates the sum of the squares of the difference between the last two iterations on the number of moles of methane at a given time, I. The summation is over each radial position existing at that time.

Function SUMM(I,IM)--calculates the sum of the squares of the difference between the last two iterations in the value of the mobility at a given time, I. The summation is over each radial position existing at that time.

Function FF(I,J)--calculates the right hand side of equation 10.1 for time, I and position J.

Subroutine TEMP--calculates the values of the temperature dependent variables for each radial position existing at time I.

Subroutine PC2--performs a second order predictor-corrector solution of equation 10.1. Also includes Euler's method followed by second order corrector.

Subroutine PC4--performs a Hamming's fourth order predictor-corrector solution of equation 10.1.

Subroutine RFND--calculates the root of equation 10.4 for given values of mobility and pressure. The secant method is used to find the root.

Subroutine INTEG--performs integration in equation 10.4 by trapezoidal rule.

Subroutine PRES--solves equation 10.3 for given values of the moles of methane and the mobility for each radial position at time I. Again the trapezoidal rule was used.

10.3 NONSUBSCRIPTED VARIABLES

ANAR	molar flow rate of inert gas
ANCH4	molar flow rate of methane gas
AVM	average mobility at any time
CCI	convergence criterion
CC2	square of convergence criterion
CSTEP	determines whether step size is to be changed
C2	constant defined by equation 10.5
C4	constant defined by equation 10.6
DELT	time step size
DELY	step size in y direction
DTDTH	constant temperature gradient across the char
DTMX	final step size, maximum step size
HEAD	sample designation
HT	height of the sample
I	index to keep track of times stored in the computer
IM	index to keep track of actual time that the times stored in the computer represent
JS	counter to keep track of the value of the index corresponding to the inside surface of the char
MPOUT	determines whether intermediate pressure and number of moles of CH_4 output is printed out
MSEP	determines if mobilities and pressures at each y should be printed out at selected increments in time
MOUT	allows mobilities at each y for all times to be printed out

NR	input tape number
NS	indicates new sample follows
NTH	indicates the number of increments in y which are used
NW	output tape number
N2	indicates type of inert gas used
ODIA	outside diameter of the sample
PERO	initial permeability of the sample
PORO	initial porosity of the sample
P2B	atmospheric pressure
RADIF	inside radius of the sample in feet
RK	rate constant for the decomposition of methane
ROAR	inert gas flow rate
ROCH4	methane gas flow rate
T	temperature of the sample during the carbon deposition
TH	thickness of the sample
THEND	maximum thickness of the char
TIME	total time
TMAX	maximum time of the deposition experiment
TMPO	time increment for normal output
TREF	temperature of outside surface of the char
TREFI	temperature of inside surface of the char
VISAR	viscosity of the inert gas
VISCH4	viscosity of the methane
VISMX	viscosity of the inert gas-methane mixture

10.4 SUBSCRIPTED VARIABLES

BM(I, J)	mobility at time I and position J
BNCH4(I, J)	number of moles of methane at time I and position J
FNCH4(J)	number of moles of methane at position J
P(I, J)	pressure at time I and position J
RK(I, K)	rate constant for decomposition of CH_4 at time I and position K
SINT(I, J)	value of integral in equation 10.4 for time I and position J
SPINT(K)	integral of equation 10.3
T(I, K)	temperature of char at time I and position K
VISMX(I, K)	viscosity of the methane-inert gas mixture at time I and position K

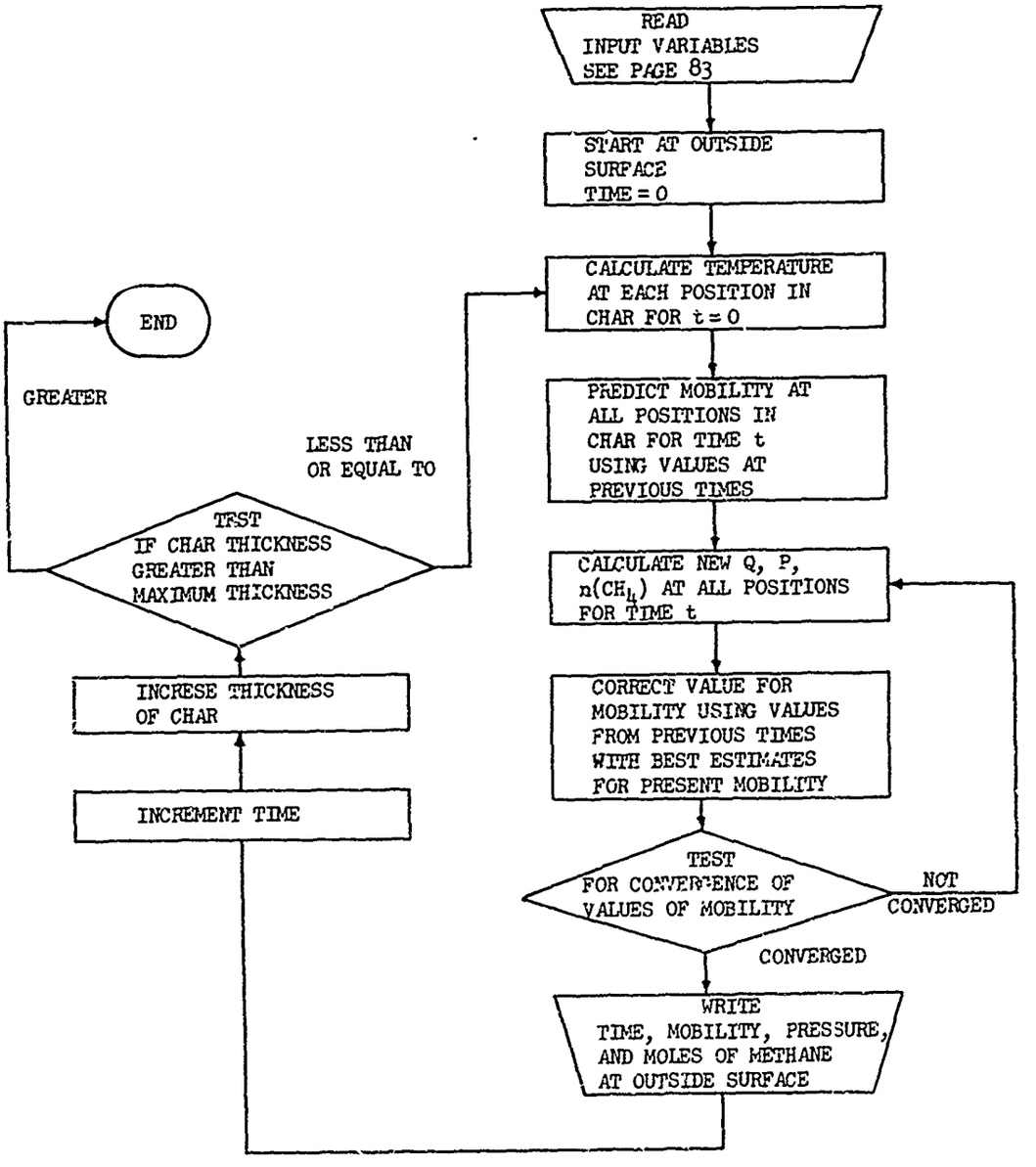

FIGURE A-1: SIMPLIFIED FLOW CHART FOR CHAR SIMULATION PROGRAM

TABLE A-1

INPUT FOR CHAR SIMULATION COMPUTER PROGRAM

Card Number	Columns	Type of Field	Variable	Description	Units
1	1-60	A	HEAD	Heading describing test	----
2	1-2	I	N2	Inert gas used (0 for Argon, 1 for H_e, 2 for N_2)	----
3	1-10	D	ROCH4	Methane flow rate (1 atm., 25°C)	ft^3/min
	11-20	D	ROAR	Inert gas flow rate (1 atm., 25°C)	ft^3/min
	21-30	D	ODIA	Outside diameter of sample	in.
	31-40	D	HT	Height of sample	in.
	41-50	D	THEND	Maximum thickness of char	in.
4	1-10	D	TMAX	Time for char to reach maximum thickness	sec.
5	1-10	D	TREF	Maximum temperature of outside surface of char	°K
	11-20	D	TREFI	Temperature of inside surface of char (usually taken as phenolic decompesition temperature)	°K
	21-30	D	PERO	Permeability of initially formed char	ft^2
	31-40	D	PORO	Porosity of initially formed char	----
	41-42	I	NTH	Number of increments used to reach maximum char thickness (must be an even number)	----

COMPUTER LISTING OF CHAR SIMULATION PROGRAM

```
C     CHAR SIMULATION PROGRAM
C     EXACT THEORY          T = T(TIME,Y)   THICKNESS VARIES
C     THIS PROGRAM SOLVES FOR  THE MOBILITY, PRESSURE,AND
C     THE MOLES OF CH4 IN THE CHAR OF A REENTERING ABLATOR
C     WHERE THE CHAR THICKNESS IS ALLOWED TO VARY FROM 0 TO TH.
C     INPUT IS READ INTO THE COMPUTER AS FOLLOWS
C     CARD 1.  COL. 1-60 HEADING, A FIELD
C     CARD 2.  COL. 1-2 INERT GAS USED (0 FOR ARGON, 1 FOR HE,
C     2 FOR N2
C     CARD 3.  COL. 1-10 CH4 FLOW RATE, COL. 11-20 INERT GAS
C     FLOW RATE, COL. 21-30 OUTSIDE DIAMETER, COL. 31-40
C     HEIGHT, COL. 41-50 FINAL THICKNESS OF THE CHAR,
C     FORMAT(5D10.4)
C     CARD 4.  COL. 1-10 LENGTH OF TIME FOR THE THICKNESS
C     TO REACH A STEADY STATE VALUE
C     CARD 5.  COL. 1-10 MAXIMUM TEMPERATURE THAT THE
C     OUTSIDE SURFACE OF THE CHAR WILL REACH, COL. 11-20
C     TEMPERATURE OF INSIDE SURFACE OF THE CHAR (USUALLY
C     TAKEN AS THE DECOMPOSITION TEMPERATURE OF PHENOLIC RESIN),
C     COL. 21-30 PERMEABILITY OF CHAR WHICH IS ORIGINALLY
C     FORMED, COL. 31-40 ORIGIANL POROSITY OF THE CHAR,
C     COL. 41-42 NUMBER OF STEPS USED ACROSS CHAR
      DOUBLE PRECISION P(5,21),BNCH4(5,21),BM(5,21),AFT(21),
     1SINT(5,21),T(5,21),RK(5,21),VISMX(5,21),FNCH4(21),
     2GM(21),ROCH4,
     3ODIA,HT,THEND,DELT,XCH4,RAD1,RAD1F,VCH4M,ANCH4,VN2M,
     4ANAR,VARM,
     5VHEM,ANTOT,ANTCH,PERO,PORO,TREF,DTDTH,DELY,TMAX,ANTH,
     6C5,C6,ROAR
     7,XAR,TIME,PRED,TREFI
      DIMENSION HEAD(15)
      COMMON P,BNCH4,BM,AFT,SINT,T,RK,VISMX,FNCH4,GM,C6,C5,
     1XCH4,NTH
      NR=1
      NW=2
  500 READ(NR,5) HEAD
    5 FORMAT(15A4)
C     N2=0 FOR ARGON  =1 FOR HE.    =2 FOR N2
      READ (NR,105) N2
  105 FORMAT(I2)
      N2=N2+1
      WRITE (NW,40)  HEAD
   40 FORMAT(1H1,15A4,///)
C     SAMPLE DIMENSIONS ARE IN INCHES
C     FLOW RATES ARE FT3/MIN
      READ (1,10) ROCH4,ROAR,ODIA,HT,THEND
   10 FORMAT(5D10.4)
C     TMAX=10 ,20, 30 SEC.
```

```
C      TMAX = LENGTH OF TIME FOR THICKNESS TO REACH STEADY
      1STATE VALUE
       READ (1,16) TMAX
   16  FORMAT(D10.4)
       RAD1=.5D0*GDIA-THEND
       RAD1F=RAD1/12.
       VCH4M = ROCH4
       ANCH4 = VCH4M * .0025620000/60.
       GO TO (8,12,9),N2
    9  VH2M = ROAR
       ANAR = VH2M * (7.2035D-2)/(28.*60.)
       GO TO 11
    8  VARM = ROAR
       ANAR = VARM * (2.554D-3)/60.
       GO TO 11
   12  VHEM = ROAR
       ANAR=VHEM*(2.55D-3)/60.
   11  ANTOT=ANCH4+ANAR
       WRITE (NW,45) ANCH4,ANAR
   45  FORMAT(8HONCH4 = ,D14.6,8HPER SEC.,4X,6HNAR = ,D14.6,
      18HPER SEC.,/)
       ANTCH=ANTOT+ANCH4
C      NTH= NUMBER OF INTERVALS IN Y-DIRECTION  MUST BE EVEN
      1NO.
C      TREF IS TEMPERATURE OF OUTSIDE SURFACE
C      TREFI IS TEMPERATURE OF PHENOLIC DECOMPOSITION
    1  READ (NR,15) TREF,TREFI,PERO,PORO,NTH
   15  FORMAT(4D10.4,I2)
       XCH4=ANCH4/ANTOT
       XAR=ANAR/ANTOT
       ANTH=DFLOAT(NTH)
       DTDTH=(TREF-TREFI)/THEND*12.
       DELT=TMAX/ANTH
       DELY=THEND/(12.*ANTH)
       WRITE (NW,30) TREF,THEND,TMAX
   30  FORMAT(9H-TEMP. = ,D10.4,5X,7H TH. = ,D10.4,8H TMAX =
      1,D10.4,//)
       C5=-24.*2000./140.*XCH4/39.35D0
       C6=-6.283185307*HT*PORO/12.
       NTH=NTH+1
       IM=1
       I=1
       BM(1,NTH)=1.
       BNCH4(1,NTH)=ANCH4
       SINT(1,NTH)=0.
       FNCH4(NTH)=ANCH4
       J=NTH
       TIME=0.
       CALL TEMP(I,IM,TIME,DELY,DTDTH,ANCH4,ANTOT,ANAR,XAR,
      1HT,N2)
       CALL PRES(DELY,ANTCH,RAD1F,I,IM,HT,PERO)
```

```
      WRITE (NW,68) TIME,BM(IM,NTH),P(IM,NTH),BNCH4(IM,NTH)
   68 FORMAT(8H TIME = ,D10.4/(3D20.8))
      IM=2
      I=2
      RAD1F=RAD1F-DELY
      JS=NTH-IM+1
      BM(I,JS)=1.
      BNCH4(I,JS)=ANCH4
      FNCH4(JS)=ANCH4
      TIME=TIME+DELT/60.
      CALL TEMP(I,IM,TIME,DELY,DTDTH,ANCH4,ANTOT,ANAR,XAR,
     1HT,N2)
      J=NTH
      PRED=1.
      CALL PC2(I,IM,J,PRED,ANTOT,ANCH4,RAD1F,DELY,ANTCH,HT,
     1PERO,DELT)
      GO TO 151
  111 IF (SUMM(I,IM)-(1.0D-26)) 151,151,152
  151 JS=NTH-IM+1
      WRITE (NW,68) TIME,(BM(I,JJ),P(I,JJ),BNCH4(I,JJ),
     1JJ=JS,NTH)
      I=I+1
      IM=IM+1
      RAD1F=RAD1F-DELY
      IF (I-6) 108,109,109
  108 JS=NTH-IM+1
      BM(I,JS)=1.
      GM(JS)=1.
      BNCH4(I,JS)=ANCH4
      FNCH4(JS)=ANCH4
      KK=JS+1
      DO 201 K=KK,NTH
      BM(I,K)=BM(I-1,K)
  201 BNCH4(I,K)=BNCH4(I-1,K)
      IF (IM-NTH) 116,116,112
  116 TIME=TIME+DELT/60.
      CALL TEMP(I,IM,TIME,DELY,DTDTH,ANCH4,ANTOT,ANAR,XAR,
     1HT,N2)
  152 JS=NTH-IM+2
      DO 211 K=JS,NTH
  211 GM(K)=BM(I,K)
      J=JS
      PRED=1.
      CALL PC2(I,IM,J,PRED,ANTOT,ANCH4,RAD1F,DELY,ANTCH,HT,
     1PERO,DELT)
      J=J+1
  106 PRED=2.
      CALL PC2(I,IM,J,PRED,ANTOT,ANCH4,RAD1F,DELY,ANTCH,HT,
     1PERO,DELT)
      IF (J-NTH) 101,111,111
  101 J=J+1
```

```
      IF (J-(NTH-IM+4)) 106,106,107
  107 CALL PC4(I,IM,J,PRED,ANTOT,ANCH4,RADIF,DELY,ANTCH,HT,
     1PERO,DELT)
      IF (J-NTH) 101,111,111
  109 I=0
      JS=NTH-IM+6
      DO 200 K=2,5
      I=I+1
      JS=JS-1
      DO 200 J=JS,NTH
      BM(I,J)=BM(K,J)
      P(I,J)=P(K,J)
      SINT(I,J)=SINT(K,J)
      T(I,J)=T(K,J)
      RK(I,J)=RK(K,J)
      VISMX(I,J)=VISMX(K,J)
  200 BNCH4(I,J)=BNCH4(K,J)
      I=5
      GO TO 108
  112 GO TO 500
  600 END
/FTC
      DOUBLE PRECISION FUNCTION SUMN(I,IM)
      DOUBLE PRECISION P(5,21),BNCH4(5,21),BM(5,21),AFT(21),
     1SINT(5,21),T(5,21),RK(5,21),VISMX(5,21),FNCH4(21),
     2GM(21)
     3,C6,C5,XCH4,X,Q
      COMMON P,BNCH4,BM,AFT,SINT,T,RK,VISMX,FNCH4,GM,C6,C5,
     1XCH4,NTH
      X=0.
      JSS=NTH-IM+2
      DO 61 K=JSS,NTH
      IF (BNCH4(I,K)) 63,63,62
   63 Q=0.
      GO TO 61
   62 Q=(FNCH4(K)-BNCH4(I,K))/BNCH4(I,K)
   61 X=X+Q*Q
      SUMN=X
      RETURN
      END
/FTC
      DOUBLE PRECISION FUNCTION SUMM(I,IM)
      DOUBLE PRECISION P(5,21),BNCH4(5,21),BM(5,21),AFT(21),
     1SINT(5,21),T(5,21),RK(5,21),VISMX(5,21),FNCH4(21),
     2GM(21),
     3C6,C5,XCH4,R,Y
      COMMON P,BNCH4,BM,AFT,SINT,T,RK,VISMX,FNCH4,GM,C6,C5,
     1XCH4,NTH
      Y=0.
      JSS=NTH-IM+2
      DO 81 K=JSS,NTH
```

```
      R=(GM(K)-BM(I,K))/BM(I,K)
   81 Y=Y+R*R
      SUMM=Y
      RETURN
      END
/FTC     REF
      DOUBLE PRECISION FUNCTION FF(I,J)
      DOUBLE PRECISION P(5,21),BNCH4(5,21),BM(5,21),AFT(21),
     1SINT(5,21),T(5,21),RK(5,21),VISMX(5,21),FNCH4(21),
     2GM(21)
     3,C6,C5,XCH4,Z
      COMMON P,BNCH4,BM,AFT,SINT,T,RK,VISMX,FNCH4,GM,C6,C5,
     1XCH4,NTH
      Z=DEXP(C6*SINT(I,J))
      FF=C5*BM(I,J)*P(I,J)*RK(I,J)*Z/(T(I,J)*T(I,J)*
     1(1.+XCH4*(1.-Z)))
      RETURN
      END
/FTC
      SUBROUTINE TEMP(I,IM,TIME,DELY,DTDTH,ANCH4,ANTOT,ANAR,
     1XAR,HT,N2)
      DOUBLE PRECISION P(5,21),BNCH4(5,21),BM(5,21),AFT(21),
     1SINT(5,21),T(5,21),RK(5,21),VISMX(5,21),FNCH4(21),
     2GM(21),C6,C5,
     3DTDTH,ANCH4,ANTOT,ANAR,HT,Y,VISCH4,VISAR,XAR,PH12,
     4PH21,XCH4,TIME
     5,DELY
      COMMON P,BNCH4,BM,AFT,SINT,T,RK,VISMX,FNCH4,GM,C6,C5,
     1XCH4,NTH
      K=NTH
      IY=IM-1
   12 Y=DELY*DFLOAT(IY)
      T(I,K)=DTDTH*Y+2.D3
      VISCH4=(2.93D-2)*(6.7197D-4)
C     THIS IS VISCOSITY OF CH4 AT 1000 K (PERRYS)     LBM/
     1FT-SEC
      GO TO (212,216,213),N2
  213 VISAR=(6.7197D-8)*174.*397.*((T(I,K)/293.)**1.5)/(T(I,
     1K)+104.)
      GO TO 214
  212 VISAR=(6.717D-8)*222.*435.*((T(I,K)/293.)**1.5)/(T(I,
     1K)+142.)
      GO TO 214
  216 VISAR=(6.7197D-8)*194.*363.*((T(I,K)/293.)**1.5)/(T(I,
     1K)+70.)
C     1=CH4  AND  2= N2  OR AR
  214 PH11=1.
      PH12=.35355DC/(1.401800**.5)*(1.+(2.48900**.25)*
     1((VISCH4/VISAR)
     2**.5))**2.
```

```
      PH21=.3535500/(3.48900**.5)*(1.+(.40180**.25)*
     1((VISAR/VISCH4)
     2**.5))**2.
      PH22=1.
      VISMX(I,K)=XCH4*VISCH4/(XCH4*PH11+XAR*PH12)+XAR*VISAR/
     1(XCH4*PH21
     2+XAR*PH22)
      RK(I,K)=10.**(15.1600-2.2804/T(I,K))
      K=K-1
      IY=IY-1
      IF (IY) 11,12,12
   11 RETURN
      END
/FTC     REF
      SUBROUTINE PC2(I,IM,J,PRED,ANTOT,ANCH4,RAD1F,DELY,
     1ANTCH,HT,PERO,
     2DELT)
      DOUBLE PRECISION P(5,21),BNCH4(5,21),BM(5,21),AFT(21),
     1SINT(5,21),T(5,21),RK(5,21),VISMX(5,21),FNCH4(21),
     2GM(21),C6,C5,
     3PN1,PRED,ANTOT,ANCH4,RAD1F,DELY,ANTCH,HT,PERO,XCH4,
     4DELT,FM
      COMMON P,BNCH4,BM,AFT,SINT,T,RK,VISMX,FNCH4,GM,C6,C5,
     1XCH4,NTH
      IF (PRED-1.1) 51,51,61
C     FOLLOWING USES EULERS METHOD TO APPROX. M AT T=T+DELT
   51 BNCH4(I,J)=BNCH4(I-1,J)
      TRUN=0.
   69 BM(I,J)=BM(I-1,J)+DELT*FF(I-1,J)
      GO TO 71
C      NOW USE 2 ND. ORDER PRED.
   61 BNCH4(I,J)=BNCH4(I-1,J)
      TRUN=1.
      BM(I,J)=BM(I-2,J)+2.*DELT*FF(I-1,J)
      PN1=BM(I,J)
   71 CALL PRES(DELY,ANTCH,RAD1F,I,IM,HT,PERO)
      CALL RFND(DELY,I,IM,ANTOT,ANCH4,RAD1F)
      IF (SUMN(I,IM)-(1.0D-26)) 74,71,71
C    NOW USE 2 ND ORDER CORRECTOR
   74 FM=BM(I-1,J)+DELT/2.*(FF(I-1,J)+FF(I,J))
      IF (DABS(FM-BM(I,J))-(1.0D-13)) 80,73,73
   73 BM(I,J)=FM
      GO TO 74
   80 BM(I,J)=FM
   85 IF (TRUN) 681,685,681
  681 BM(I,J)=BM(I,J)+1./5.*(PN1-BM(I,J))
  685 CALL PRES(DELY,ANTCH,RAD1F,I,IM,HT,PERO)
      CALL RFND(DELY,I,IM,ANTOT,ANCH4,RAD1F)
      IF(SUMN(I,IM)-(1.0D-26)) 87,685,685
   87 RETURN
      END
```

```
FTC     REF
      SUBROUTINE PC4(I,IM,J,PRED,ANTOT,ANCH4,RAD1F,DELY,
     1ANTCH,HT,PERO,
     2DELT)
      DOUBLE PRECISION P(5,21),BNCH4(5,21),BM(5,21),AFT(21),
     1RK(5,21),
     2SINT(5,21),T(5,21),VISMX(5,21),FNCH4(21),GM(21),X,C6,
     3C5,XCH4
     4,ANTCT,ANCH4,RAD1F,DELY,ANTCH,HT,PERO,PN1,C,PRED,DELT
      COMMON P,BNCH4,BM,AFT,SINT,T,RK,VISMX,FNCH4,GM,C6,C5,
     1XCH4,NTH
      MOD4=0
      BNCH4(I,J)=BNCH4(I-1,J)
      BM(I,J)=BM(I-4,J)+4.*DELT/3.*(2.*FF(I-1,J)-FF(I-2,
     1J)+2.*FF(I-3,J))
      PN1=BM(I,J)
      IF (MOD4) 92,392,92
  392 X=0.
   92 BM(I,J)=PN1-112./121.*X
   51 CALL PRES(DELY,ANTCH,RAD1F,I,IM,HT,PERO)
      CALL RFND(DELY,I,IM,ANTOT,ANCH4,RAD1F)
      IF (SUMN(I,IM)-(1.0D-26)) 78,51,51
   78 C4TM=0.
  178 C=1./8.*(9.*BM(I-1,J)-BM(I-3,J)+3.*DELT*(FF(I,J)+2.*
     1FF(I-1,J)
     2-FF(I-2,J)))
      IF(DABS(C-BM(I,J))-(1.0D-13)) 170,76,76
   76 BM(I,J)=C
      C4TM=C4TM+1.
      IF (C4TM-10) 178,178,602
  602 WRITE (NW,610) C,GM(J)
  610 FORMAT(47H 4 TH. ORDER CORR. DOESNT CONVERGE IN 10
     1CYCLES,2D15.8)
  170 BM(I,J)=C
   82 CALL PRES(DELY,ANTCH,RAD1F,I,IM,HT,PERO)
      CALL RFND(DELY,I,IM,ANTOT,ANCH4,RAD1F)
      IF (SUMN(I,IM)-(1.0D-26)) 77,82,82
   77 X=PN1-C
      BM(I,J)=C+9./121.*X
   81 CALL PRES(DELY,ANTCH,RAD1F,I,IM,HT,PERO)
      CALL RFND(DELY,I,IM,ANTOT,ANCH4,RAD1F)
      IF (SUMN(I,IM)-(1.0D-26)) 195,81,81
  195 RETURN
      END
/FTC
      SUBROUTINE RFND(DELY,I,IM,ANTOT,ANCH4,RAD1F)
      DOUBLE PRECISION P(5,21),BNCH4(5,21),BM(5,21),AFT(21),
     1SINT(5,21),T(5,21),RK(5,21),VISMX(5,21),FNCH4(21),
     2GM(21),FNC(2),
     3ANTCH,DELY,ANTOT,ANCH4,RAD1F,Y,CNCH4,DNCH4,C6,C5,XCH4
```

```
      COMMON P,BNCH4,BM,AFT,SINT,T,RK,VISMX,FNCH4,GM,C6,C5,
     1XCH4,NTH
      ANTCH=ANTOT+ANCH4
      CONV=0.
      NCON=0
      JSR=NTH-IM+1
      Y=0.
      AFT(JSR)=39.350C*T(I,JSR)/P(I,JSR)*ANTOT
      SINT(I,JSR)=0.
      IF (I-1) 201,201,211
  211 JSR=JSR+1
      DO 200 L=JSR,NTH
      IRT=0
      Y=Y+DELY
      CNCH4=BNCH4(I,L)
  203 IRT=IRT+1
      GO TO (205,204),IRT
  205 AFT(L)=39.3500*T(I,L)/P(I,L)*(ANTCH-CNCH4)
      CALL INTEG(I,L,DELY,Y,RAD1F)
      GO TO (208,204),IRT
  208 CNCH4=ANCH4*DEXP(C6*SINT(I,L))
      FNC(1)=BNCH4(I,L)-CNCH4
      GO TO 203
  204 FNC(2)=CNCH4-ANCH4*DEXP(C6*SINT(I,L))
      IF (FNC(2)-FNC(1)) 212,213,212
  212 DNCH4=CNCH4-(CNCH4-BNCH4(I,L))/(FNC(2)-FNC(1))*FNC(2)
      CONV=CONV+1.
      IF (CNCH4) 305,207,305
  305 IF(DABS((CNCH4-DNCH4)/CNCH4)-(1.0D-13)) 207,206,206
  206 FNC(1)=FNC(2)
      BNCH4(I,L)=CNCH4
      CNCH4=DNCH4
      IF(CONV-30.) 205,205,209
  209 NCON=NCON+1
      WRITE (NW,210) CNCH4,BNCH4(I,L)
  210 FORMAT(20H ROOT NOT CONVERGING,2D15.8)
      IF(NCON-4) 207,207,200
  213 DNCH4=CNCH4
  207 CONV=0.
      BNCH4(I,L)=DNCH4
  200 CONTINUE
  201 RETURN
      END
/FTC
      SUBROUTINE INTEG(I,L,DELY,Y,RAD1F)
      DOUBLE PRECISION P(5,21),BNCH4(5,21),BM(5,21),AFT(21),
     1SINT(5,21),T(5,21),RK(5,21),DELY,Y,RAD1F,XRAD,DINT,A,B
      COMMON P,BNCH4,BM,AFT,SINT,T,RK
      XRAD=RAD1F+Y
      A=DSQRT(BM(I,L-1))*(XRAD-DELY)/AFT(L-1)*RK(I,L-1)
      B=DSQRT(BM(I,L))*XRAD/AFT(L)*RK(I,L)
```

```
      DINT=DELY/2.*(A+B)
      SINT(I,L)=SINT(I,L-1)+DINT
      RETURN
      END
/FTC
      SUBROUTINE PRES(DELY,ANTCH,RAD1F,I,IM,HT,PERO)
      DOUBLE PRECISION P(5,21),BNCH4(5,21),BM(5,21),AFT(21),
     1SINT(5,21),T(5,21),RK(5,21),VISMX(5,21),GM(21),C6,C5,
     2XCH4,FNCH4(21),SPINT(21),DELY,ANTCH,RAD1F,HT,PERO,
     3XRAD,A,B,DPINT,
     4ANTH,Y
      COMMON P,BNCH4,BM,AFT,SINT,T,RK,VISMX,FNCH4,GM,C6,C5,
     1XCH4,NTH
      FNCH4(NTH)=BNCH4(I,NTH)
      ANTH=DFLOAT(NTH)
      Y=DELY*ANTH
      P(I,NTH)=29.921D0
      IF (I-1) 410,410,405
  405 SPINT(NTH)=0.
      K=NTH-1
  400 Y=Y-DELY
      XRAD=RAD1F+Y
      A=(ANTCH-BNCH4(I,K+1))/(XRAD*BM(I,K+1))*VISMX(I,K+1)*
     1T(I,K+1)
      B=(ANTCH-BNCH4(I,K))/((XRAD-DELY)*BM(I,K))*VISMX(I,K)*
     1T(I,K)
      DPINT=DELY/2.*(A+B)
      SPINT(K)=SPINT(K+1)+DPINT
      P(I,K)=DSQRT(895.266D0+(6.6018D-2)/(HT*PERO)*
     1SPINT(K))
      FNCH4(K)=BNCH4(I,K)
      IF (K-(NTH-IM+1)) 410,410,420
  420 K=K-1
      GO TO 400
  410 RETURN
      END
```

UNCLASSIFIED

Security Classification

DOCUMENT CONTROL DATA - R&D

(Security classification of title, body of abstract and indexing annotation must be entered when the overall report is classified)

1. ORIGINATING ACTIVITY (Corporate author)	2a. REPORT SECURITY CLASSIFICATION
Washington University St. Louis, Missouri 63130	Unclassified
	2b. GROUP

3. REPORT TITLE

An Investigation of Carbon Deposition in Chars. II

4. DESCRIPTIVE NOTES (Type of report and inclusive dates)

Final Report

5. AUTHOR(S) (Last name, first name, initial)

Weger, Eric
Brew, Jere R.
Servais, Ronald A.

6. REPORT DATE	7a. TOTAL NO. OF PAGES	7b. NO. OF REFS
January 1968	96	16

8a. CONTRACT OR GRANT NO.	9a. ORIGINATOR'S REPORT NUMBER(S)
F04694-67-C-0013 new b. PROJECT NO.	
c.	9b. OTHER REPORT NO(S) (Any other numbers that may be assigned this report)
d.	SAMSO TR 68-123

10. AVAILABILITY/LIMITATION NOTICES This document is subject to special export controls and each transmittal to foreign governments or foreign nationals may be made only with prior approval of Space and Missile Systems Organization (SMSD) Los Angeles AFS, California 92409.

11. SUPPLEMENTARY NOTES	12. SPONSORING MILITARY ACTIVITY
	Space and Missile Systems Organization Air Force Systems Command United States Air Force

13. ABSTRACT

The techniques for the investigation of char densification phenomena which had been developed under a previous contract (see BSD TR-66-385) were extended to include transpiration experiments with gases and gas mixtures typical of the decomposition products of phenolic resins. As before, the chars used in the experiments were produced by charring high performance carbon cloth phenolic composites in a plasma jet. Data on the structural characteristics and permeabilities of the chars, and the change occurring during transpiration, are presented. Comparisons of the experimental data with kinetic rate data from the literature are made. A simplified program for calculating the change in permeability of and pressure drop across a growing char is presented. The effort required to extend this program to more complex situations is discussed.

DD FORM 1 JAN 64 1473

UNCLASSIFIED

Security Classification

UNCLASSIFIED

Security Classification

14. KEY WORDS	LINK A		LINK B		LINK C	
	ROLE	WT	ROLE	WT	ROLE	WT
Ablation Carbon Deposition and Removal Char Densification Permeability Phenolic Porous Media Thermal Stresses High Temperature Reactions						

INSTRUCTIONS

1. ORIGINATING ACTIVITY: Enter the name and address of the contractor, subcontractor, grantee, Department of Defense activity or other organization *(corporate author)* issuing the report.

2*a*. REPORT SECURITY CLASSIFICATION: Enter the overall security classification of the report. Indicate whether "Restricted Data" is included. Marking is to be in accordance with appropriate security regulations.

2*b*. GROUP: Automatic downgrading is specified in DoD Directive 5200.10 and Armed Forces Industrial Manual. Enter the group number. Also, when applicable, show that optional markings have been used for Group 3 and Group 4 as authorized.

3. REPORT TITLE: Enter the complete report title in all capital letters. Titles in all cases should be unclassified. If a meaningful title cannot be selected without classification, show title classification in all capitals in parenthesis immediately following the title.

4. DESCRIPTIVE NOTES: If appropriate, enter the type of report, e.g., interim, progress, summary, annual, or final. Give the inclusive dates when a specific reporting period is covered.

5. AUTHOR(S): Enter the name(s) of author(s) as shown on or in the report. Enter last name, first name, middle initial. If military, show rank and branch of service. The name of the principal author is an absolute minimum requirement.

6. REPORT DATE: Enter the date of the report as day, month, year; or month, year. If more than one date appears on the report, use date of publication.

7*a*. TOTAL NUMBER OF PAGES: The total page count should follow normal pagination procedures, i.e., enter the number of pages containing information.

7*b*. NUMBER OF REFERENCES: Enter the total number of references cited in the report.

8*a*. CONTRACT OR GRANT NUMBER: If appropriate, enter the applicable number of the contract or grant under which the report was written.

8*b*, 8*c*, & 8*d*. PROJECT NUMBER: Enter the appropriate military department identification, such as project number, subproject number, system numbers, task number, etc.

9*a*. ORIGINATOR'S REPORT NUMBER(S): Enter the official report number by which the document will be identified and controlled by the originating activity. This number must be unique to this report.

9*b*. OTHER REPORT NUMBER(S): If the report has been assigned any other report numbers *(either by the originator or by the sponsor)*, also enter this number(s).

10. AVAILABILITY/LIMITATION NOTICES: Enter any limitations on further dissemination of the report, other than those imposed by security classification, using standard statements such as:

(1) "Qualified requesters may obtain copies of this report from DDC."

(2) "Foreign announcement and dissemination of this report by DDC is not authorized."

(3) "U. S. Government agencies may obtain copies of this report directly from DDC. Other qualified DDC users shall request through

_____."

(4) "U. S. military agencies may obtain copies of this report directly from DDC. Other qualified users shall request through

_____."

(5) "All distribution of this report is controlled. Qualified DDC users shall request through

_____."

If the report has been furnished to the Office of Technical Services, Department of Commerce, for sale to the public, indicate this fact and enter the price, if known.

11. SUPPLEMENTARY NOTES: Use for additional explanatory notes.

12. SPONSORING MILITARY ACTIVITY: Enter the name of the departmental project office or laboratory sponsoring *(paying for)* the research and development. Include address.

13. ABSTRACT: Enter an abstract giving a brief and factual summary of the document indicative of the report, even though it may also appear elsewhere in the body of the technical report. If additional space is required, a continuation sheet shall be attached.

It is highly desirable that the abstract of classified reports be unclassified. Each paragraph of the abstract shall end with an indication of the military security classification of the information in the paragraph, represented as *(TS)*, *(S)*, *(C)*, or *(U)*.

There is no limitation on the length of the abstract. However, the suggested length is from 150 to 225 words.

14. KEY WORDS: Key words are technically meaningful terms or short phrases that characterize a report and may be used as index entries for cataloging the report. Key words must be selected so that no security classification is required. Identifiers, such as equipment model designation, trade name, military project code name, geographic location, may be used as key words but will be followed by an indication of technical context. The assignment of links, rules, and weights is optional.

UNCLASSIFIED

Security Classification